Alternative Fuels and Chemicals From Synthesis Gas

Quarterly Report
April 1 - June 30, 1995

Work Performed Under Contract No.: DE-FC22-95PC93052

For
U.S. Department of Energy
Office of Fossil Energy
Federal Energy Technology Center
P.O. Box 880
Morgantown, West Virginia 26507-0880

By
Air Products and Chemicals, Inc.
7201 Hamilton Boulevard
Allentown, Pennsylvania 18195-1501

MASTER

Disclaimer

DISCLAIMER

Portions of this document may be illegible in electronic image products. Images are produced from the best available original document.

Alternative Fuels and Chemicals from Synthesis Gas

Quarterly Technical Progress Report

1 April- 30 June 1995

Contract Objectives

The overall objectives of this program are to investigate potential technologies for the conversion of synthesis gas to oxygenated and hydrocarbon fuels and industrial chemicals, and to demonstrate the most promising technologies at DOE's LaPorte, Texas, Slurry Phase Alternative Fuels Development Unit (AFDU). The program will involve a continuation of the work performed under the Alternative Fuels from Coal-Derived Synthesis Gas Program and will draw upon information and technologies generated in parallel current and future DOE-funded contracts.

Summary of Activity

- A Hydrodynamic study was successfully completed in the LaPorte 18" bubble column during June. Significant information on fluid dynamics was gathered during three weeks of liquid phase methanol operations. In addition to the usual nuclear density gauge and temperature measurements, differential pressure measurements (DP) were made to better understand the hydrodynamics of the system. The DP measurements worked very well mechanically, without the anticipated plugging problems, throughout the run. Gas holdup estimates based on DP measurements followed the same trends as those indicated by NDG readings. However, there appeared to be a systematic difference between gas holdup estimates from the two methods. Calibration of the DP readings by filling the reactor with a known-density fluid is planned to increase their accuracy. Interesting DP data that could provide insight on bubble size distribution were collected using Sandia's high speed data acquisition system. Responses to radioactive pulses were studied for both gas and liquid phase at three different operating conditions to evaluate the mixing in the reactor. A large effort will be required to understand and interpret the hydrodynamic data collected during this run.

- High velocity conditions were demonstrated during the Hydrodynamic run. Operation with a linear velocity of 1.2 ft/sec was achieved with stable bubble column and catalyst performance. The magnitude of the velocity was limited only by the recycle compressor capacity, as the plant was designed for 1 ft/sec maximum velocity. Acceptable oil carry-over from the reactor was observed at this velocity.

- Improvements included in the Kingsport design for catalyst activation were also demonstrated in the June operation. Successful activations were achieved using dilute CO as reductant, a quicker temperature ramp, and smaller gas flow, compared to previous "standard" activation procedures. An alternate catalyst was demonstrated for the LPMEOH™ process. Expected catalyst activity, by-product formation, and stability were obtained with

the Alternate catalyst. Overall, the catalyst appeared very comparable to the baseline LPMEOH™ catalyst. Stable performance was obtained at both high and very low (turndown) velocity.

- In addition, dephlegmator testing was conducted at various conditions during the run. During the carbonyl burnout period, testing was conducted with the two-phase system to eliminate fouling considerations. While detailed analysis is pending, it appeared that heat transfer performance of the dephlegmator was satisfactory. However, there was significant oil carry-over. Although flooding was ruled out, variability in oil capture was still apparent throughout the run. A large amount of data requires analysis before a final decision is made on inclusion in commercial flowsheets.

- Approximately 64,300 gallons of methanol were produced during the June demonstration, which will be used for testing in fuel and chemical (MTBE) applications.

- A meeting was held with Shell personnel on May 22 to discuss a proprietary run with Shell at LaPorte. Shell proposed a two month campaign with its own cobalt catalyst for October-November 1996. This schedule is significant, as the start-up date for Kingsport is December 1996, and this run is expected to monopolize resources for 4-6 months. Confidentiality, funding, and technical issues must be worked out before the project is kicked off.

- Deactivation of the DME catalyst systems is associated with some physical features of a slurry phase reactor, since both methanol and dehydration catalysts do not suffer long term deactivation in the LPDME run with Robinson-Mahoney basket internals and pelletized catalysts. Most likely, the intimate contact between the two catalysts is necessary for catalyst deactivation of our two component system. This suggests new directions in our future research to better understand the deactivation mechanism and develop solutions.

- A repeat of the LPDME run in the Robinson-Mahoney reactor confirmed the result that the methanol catalyst does not age significantly when only a small amount of physical contact is allowed by the catalysts. In addition, the long term deactivation of the dehydration catalyst is eliminated. The only deactivation of this catalyst was the initial drop discussed last month.

- Si modification of the alumina catalyst surface again reduced the initial steep deactivation seen in LPDME synthesis. However, the deactivation rate was still relatively high due to long term deactivation. In another LPDME approach, a Si-based dispersion aid gave the desired dispersion of the mixed catalysts in the slurry reactor, but the material polymerized during the run. More stable dispersants will be tried. A Si-modified Catapal B g-alumina sample with a very high SiO_2 content (35 wt%) was prepared using a polymeric Si-containing material. However, the modification resulted in little improvement in the long-term stability of the methanol catalyst.

- In LPDME studies BASF S3-86 methanol catalyst exhibited a better long-term stability when used with a potassium (k) doped Catapal B g-alumina. This is the first time that an improved **long-term** stability has been observed. However, the dehydration activity of this alumina was low due to high K loading. K-doped alumina samples of lower loading, and therefore higher dehydration activity, will be tested in the coming month to see if a similar stability can still be obtained.

- A *one-component* catalyst was made according to a Shell patent by impregnating Catapal B g-alumina with zinc and copper. This catalyst performs both methanol synthesis and dehydration functions. However, it has very low activity and poor stability. A recheck may be in order.

- At Lehigh, a Cu-free ZnO/Cr_2O_3 catalyst was doped with Cs and tested at 405°C and 7.6 MPa with $H_2/CO = 0.75$ at two different GHSV. At a GHSV of 5450 l/kg cat./hr., the space time yields (g/kg cat./hr.) for the major products were 52.8, 39.5, 51.6 and 11.1 for methanol, isobutanol, C_7+ oxygenates and C_2-C_4 hydrocarbons, respectively, at 8.1% CO conversion.

- A two step route to isobutanol was tested at Lehigh University, where a double bed catalyst configuration was operated with two different catalysts, each at different temperatures. The 3% Cs/Cu, ZnO, Cr_2O_3 (325°C) bed was followed by a 4% Cs/Zn, Cr_2O_3 (405°C) bed, and this configuration improved the isobutanol/methanol molar ratio from 1/11.8 (single $Cs/Cu/ZnO/Cr_2O_3$) to 1/1.7.

- The capability of producing a high isobutanol yield catalyst has been demonstrated (414 g/l-hr @ 20000 GHSV, 441°C, 25 KPa). Results show higher methanol production than previously measured by Falter. The big improvement was that five-fold reduction in methane formation has been achieved. Catalyst preparation continues to concentrate on the alkalinity of the catalyst surface using the sol gel technique.

- Professor Foley at Delaware reports continued work on testing of alkali-doped catalysts. He has determined that catalysts precipitated with lithium nitrate are more active than those precipitated with lithium hydroxide. A variable study showed that the catalyst activity is still far from the target, even at optimized conditions.

- Cobalt enhances the catalyst activity to produce alcohols at high temperature. Thus far, trials at the University of Delaware using IR and Rh as dopants have shown little improvement.

- Thermodynamic calculation of model syngas to alcohol reactions suggests that CO_2 rejection should be considered as a favored mode of oxygen rejection for maximizing isobutanol concentration.

- In previous months catalytic tests converting DME to ethylidene diacetate (EDDA) were restricted to 45 min. In order to improve yield of EDDA, the reaction time was increased to 180 min. Though the yield of EDDA was observed to improve up to the 100 min mark, it was found to decrease slowly thereafter due to hydrogenation to produce ethyl acetate and

acetic acid. It was also found that the product distribution was different for two different runs using the same batch of catalyst. Based on the results obtained thus far, it appears that in a reactor, partial conversion with recycle is better than complete conversion.

- A single batch of a rhodium complex supported on a Reillex polymer was tested in three consecutive catalytic runs using fresh charges of DME, methy iodide and acetic acid. The catalytic activity for the conversion of DME to ethylidene diacetate did not decrease from run to run, showing that the catalyst was not leaching out. An elemental analysis of the catalyst revealed a 23% decrease in rhodium content, and we feel that this decrease is due to the increase in the weight of polymer from methyl iodide incorporation.

- During June, several new catalysts were prepared in APCI Corporate laboratories. One was an alumina (methanol dehydration catalyst) that was treated with t-butyldiphenylchlorosilane in order to provide a sterically hindered blocking group. It is hoped that this treatment will mitigate the stability problems experienced in the liquid phase DME process. In addition, two other rhodium containing materials were prepared for testing as catalysts for the conversion of DME to EDDA.

- In screening catalysts for the cracking of ethylidene diacetate (EDDA), temperature studies indicate that at temperatures of 200°C and above, EDDA is unstable and leads to a polymeric decomposition product and plugging of sample lines. Several catalysts were examined, but at too high a temperature. VAM and acetic acid were observed prior to plugging.

- Initial design of the mobile Catalyst Poisons Test Lab was completed. The trailer has been selected, and reactor plans and the control system have been reviewed. This project is still on time and within budget. The trailer is being modified to separate the office from the lab area, and add insulation and steps. It is expected to be on site and ready for internals installation by the end of July.

- In the new Hydrodynamics Program, statements of work from both Ohio State University and Washington University were received, reviewed, and accepted. Work on the subcontracts is almost completed.

- B. Bhatt presented a paper entitled "Productivity Improvements for Fischer-Tropsch Synthesis" at the 14th North American Meeting of the Catalysis Society. The paper, which was co-authored by Shell and DOE personnel, was well received.

RESULTS AND DISCUSSION

TASK 1: ENGINEERING AND MODIFICATIONS

1.1 Liquid Phase Methanol/Hydrodynamic Run

Changes were incorporated into the AFDU process flow diagrams to reflect the ongoing modifications. A hazards review was conducted on April 10 to review Facility Change Notices (FCNs) for AFDU modifications. FCNs on reactor differential pressure (DP) taps, flow totalizers, local hand-operated valves, trailer pad/sump and trailer overfill protection were approved.

Final preparations were completed during May for the June run. The DEC workstation data acquisition system was set up on-site, and modifications were included. The analytical system was set up for methanol synthesis. Both the Baseline and Alternate methanol catalyst lots were received. A stronger source (8 curie - Cs) for the nuclear density gauge (NDG) was installed for the high-pressure reactor to achieve better resolution, and the NDG was calibrated with N_2.

1.2 Liquid Phase Fischer-Tropsch Demonstration

A meeting was held with Shell personnel on May 22 to discuss a Fischer-Tropsch run with Shell's participation at LaPorte. Shell proposed a two month campaign with their own cobalt catalyst for October-November 1996. This schedule is significant, as the start-up date for Kingsport is December 1996, and the Kingsport demonstration start-up is expected to utilize resources for 4-6 months. Confidentiality, funding, and technical issues must be worked out before the project can be kicked off.

1.3 Fischer-Tropsch Support

No progress to report this quarter.

1.4 AFDU R&D Support

1.4.1 Laboratory Testing of Alternate Methanol Catalyst

Establishment of a tested, alternate catalyst supply is part of any process development. For the LPMEOH™ process, demonstration must be made at the LaPorte scale. One of the objectives of the methanol/hydrodynamics run in the AFDU at LaPorte is to demonstrate the performance of an alternate catalyst.

After initial testing of old samples of this catalyst showed good performance, a new sample was obtained for LaPorte. The laboratory life data for this Alternate P (P for powder) catalyst is compared to the LPMEOH Baseline catalyst in Figure 1.4.1. The catalyst performed well, showing slightly higher activity than the Baseline catalyst. The Alternate catalyst aged slightly faster, but the activity of the Alternate catalyst was always higher than that of the LPMEOH Baseline catalyst.

5

Figure 1.4.1 Life Test Results
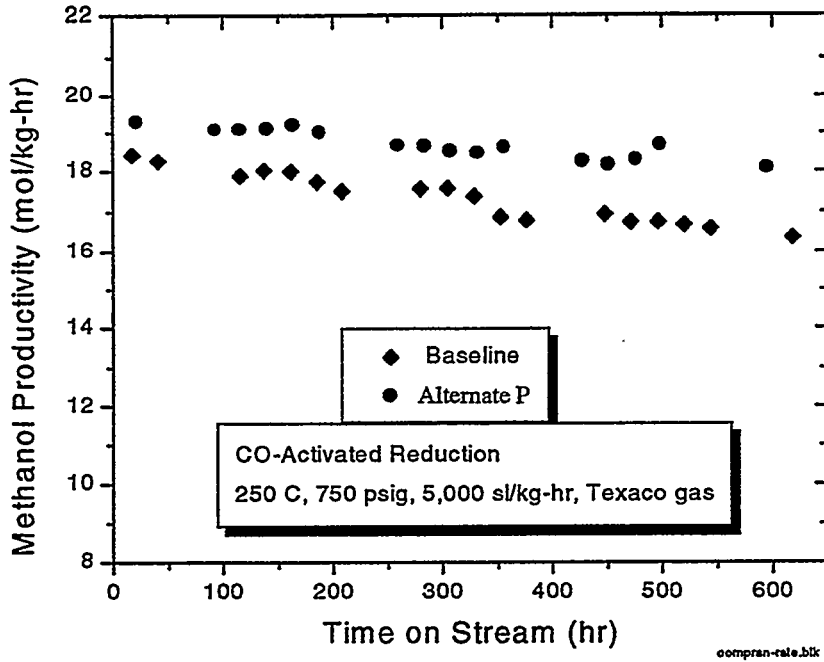
Reduction of the catalyst was accomplished by the new CO reduction procedure discussed in the last quarterly report. The reduction temperature profile is shown in Figure 1.4.2, and the off-gas profiles for the catalyst are shown in Figure 1.4.3. (NOTE: "Baseline" is the name of a catalyst type. The two lines are repeat runs for a catalyst type to show reproducibility. Also, all reductions were done at a lower flow rate.)

Figure 1.4.2 Reduction Temperature Profiles

Figure showing Temperature (°C) vs Time (hr). Inset text boxes:
4% CO/balance N₂
SV: 1,500-1600sl/kg-hr
Cut the flowrate by 25%
Switch from N₂ to 4%CO/N₂
Legend: Alternate P, Baseline, Baseline
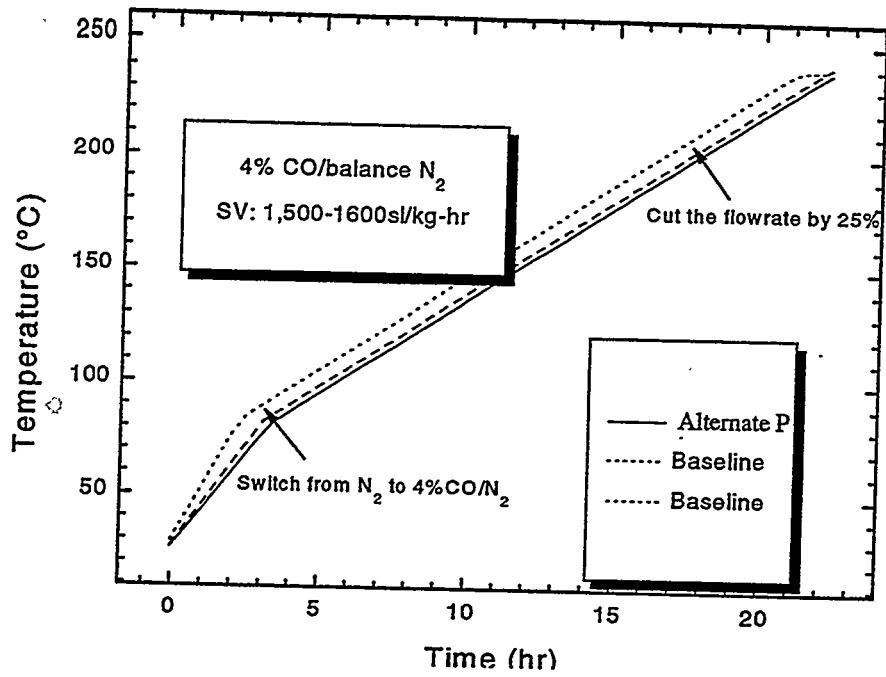
Figure 1.4.3 Off-Gas Profiles for Two Catalysts

Figure showing Reactor Exit Conc. (mol%) vs Temperature (°C).
Reduction Gas Feed: 4% CO/balance N₂
Legend: CO mol%, Baseline; CO₂ mol%, Baseline; CO mol% Baseline; CO₂ mol % Baseline; CO mol % Alternate P; CO₂ mol % Alternate P
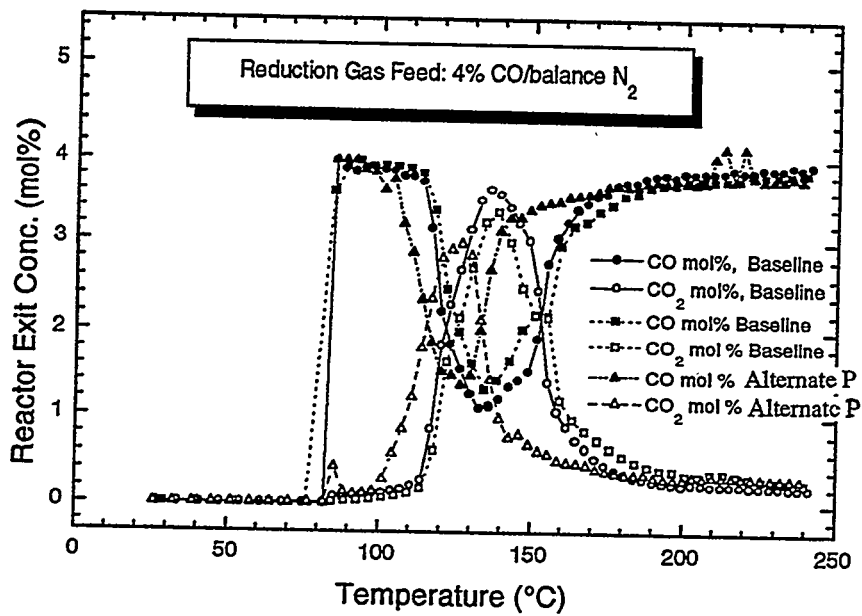
In addition to activity and life considerations, a candidate catalyst must pass the previously developed slurrification test, which indicates the suitability of a catalyst for use in a slurry bubble-column reactor. The rate of settling of the catalyst is compared to settling rates of standard catalysts. In this case the settling characteristics of the previous sample of Alternate catalyst, as well as the one representative of the current production, were tested and are compared to the results from the standard (see Figure 1.4.5). The candidate catalyst showed a satisfactory settling rate, and should perform well in the slurry reactor.

1.4.2 Summary and Recommendation

All recent data on the activation of the Baseline and Alternate catalysts are summarized in Table 1.4.1 and compared to historic data. The data are presented as the value of the specific rate constant for the methanol formation reaction and the productivity of the catalyst.

Based on the productivity of the initial two runs (14045-8 and 13458-90), we concluded that the CO activation leads to a catalyst with the same activity as does the standard activation procedure with hydrogen.

The life runs show some periodic difficulty in analytical measurement as described in the footnote to Table 1.4.1. However, as there is only a small difference in results, the CO activation is considered to be essentially the same as the standard. In addition, based on this run, catalyst life is adequate.

The Alternate catalyst exhibits at least as good an initial activity as the Baseline catalyst. Deactivation is a little higher, but even after 600 hours, the activity of the Alternate catalyst is higher than that of the Baseline catalyst.

The variation in the calculated value of the rate constant is interesting. We calculate rate constant from the concentration data. There may be a difference in water-gas shift activity for CO activated catalysts and, perhaps, between the various catalysts.

The Alternate catalyst showed adequate activity, life and slurriability in the laboratory tests and was considered suitable for testing in the AFDU in the upcoming trial.
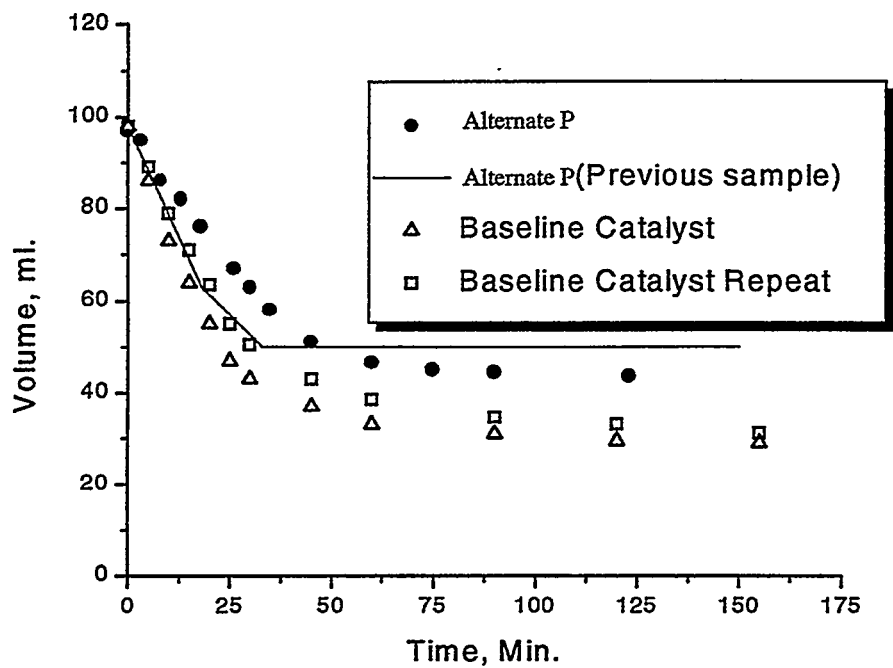
Figure 1.4.5 Results of Slurrification Test

9

Table 1.4.1 Catalyst Activation on Texaco Gas

Catalyst	$K(R=K\,f_{H_2}^{2/3}f_{CO}^{1/3})$ [1-appr] gmol/hr/atm		Productivity (5,000 GHSV, 250°C) gmol/kg cat/hr	
Source	Alcohols*	Bulk**	Alcohols	Bulk
Process Model for Baseline	2.86		17.4	
Historic Data (Hsuing)			17.4	
Plant Run-E-7 (after 7 days)	2.32			
Baseline, CO Activated				
Run 14045-8	2.29		17.2	
13458-90	2.55		17.3	
14191-62	2.18	2.8	16.5	18.4
Alternate, H_2, Activated	3.02	3.67	17.5	19.3
Alternate, CO Activated	2.87	4.29	17.5	19.7

*, **   Data after Run 62 are shown for both Alcohols and Bulk GC. This is indicative of our analytical problem. The Bulk GC data gives good material balances and shows low variation with time. The Bulk GC is the method that has been used to gather historical data.

Halfway into Run 62 the Alcohol GC calibration factor changed significantly and the day to day variability of the results became less steady. It is suspected that there is a leak that we have not yet been able to find.

Complicating the issue is that our calibration mixtures have only 5% MEOH, while MEOH concentrations in the reaction product are as high as 9%. We suspect the Bulk GC is not linear. We will soon receive a new calibration standard, at which time, the linearity of both GCs will be checked and we will use CRSD analytical help to find the GC stability problem in the Alcohols GC.

TASK 2: AFDU SHAKEDOWN, OPERATIONS, DEACTIVATION AND DISPOSAL

2.1 Liquid Phase Methanol/Hydrodynamic Run

2.1.1 Carbonyl Burnout

The reactor was loaded with Drakeol-10 oil and heated up on 30 May to start normal carbonyl burnout and, in parallel, the two-phase dephlegmator testing. Carbonyl levels were extremely low during the entire burnout: 2-10 ppb iron carbonyl and undetectable (< 10 ppb) nickel carbonyl. A summary of the carbonyl data is shown in Table 2.1.

The carbonyl burnout was completed at 19:00 on 2 June. At the end of the burnout, with sufficient data to permit a thorough analysis of the dephlegmator problem, the plant was cooled and drained in preparation for catalyst loading and reduction.

2.1.2 LPMEOH with Baseline Catalyst

Slurry Preparation

A 40 wt% oxide catalyst slurry was mixed in the 28.30 Prep Tank, which was charged with 1767 lbs of Drakeol-10 oil at 09:00 on 2 June and 1179 lbs of Baseline methanol catalyst at 08:00 on 3 June. Catalyst was taken from four drums of lot # 94/15730. The slurry was heated and agitated in the Prep Tank for two hours before it was transferred to the reactor.

11

Table 2.1 Metal Carbonyl Analysis Results

Nickel Tetracarbonyl: not detected in any samples (lower detection limit is 10 ppbv).

Iron Pentacarbonyl (ppbv): Averages of 2 injections

Reactor Temp = 482°F Reactor Pressure = 750 psig	Sample Point 3A Economizer Product Outlet	Sample Point 4 Combined Fresh Feed + Recycle	Sample Point 15 Inlet to Reactor
5/31/95 16:30-17:30 Once-through syngas (12 KSCFH)	4	8	8
5/31/95 21:30-22:30 Once-through syngas (12 KSCFH)	2	3	3
6/1/95 08:30-09:30 Once-through syngas (12 KSCFH)	3	2	3
6/1/95 11:30-12:00 Recycle syngas (84 KSCFH)	4	3	5
6/1/95 15:30-16:00 Recycle syngas (84 KSCFH)	6	4	7
6/1/95 20:30-21:00 Recycle syngas (84 KSCFH)	7	6	8
6/2/95 08:30-09:00 Recycle syngas (132 KSCFH)	9	7	10
6/2/95 11:30-12:00 Recycle syngas (132 KSCFH)	10	6	10

Catalyst Reduction

Catalyst reduction began at 14:30 on 3 June. The reduction gas (4% CO in N_2) was set at 12,500 scfh with the reactor pressure at 67 psig (Run # A9). The heat up commenced at 15:45 and proceeded from 197°F to 464°F at a rate of 15°F/hr, as shown in Figure 2.1. The temperature ramp was significantly faster than the previous "standard" ramp as this, in lab tests, had successfully saved time in the activation procedure.

The reduction under CO was quite rapid, as shown in Figure 2.2, and the total uptake peaked very close to the theoretical maximum value of 2.82 scf/lb oxide. This condition was obtained by about 360°F or 12-13 hours on-stream, which is an encouraging result for the Kingsport project. Reduction in the bubble column was faster than in the autoclave. Despite the rapid uptake, the 27.20 internal heat exchanger was easily able to control temperature, and the ramp rate proceeded on schedule with no evidence of an exotherm. At 392°F, the reduction gas flow was reduced to 9,375 scfh as planned to reduce oil loss from the reactor and conserve on nitrogen usage. Gas holdup during the reduction was close to expected: 27-30 vol% at 12,500 scfh and 24 vol% at 9375 scfh. The catalyst concentration was in the 39-41 wt% range.

Process Variable / Hydrodynamic Study

Reduction was completed at 10:00 hours on 4 June, and synthesis gas was brought into the reactor at 11:45. A run plan table corresponding to actual operating conditions during the campaign is given in Table 2.2. The initial data indicated typical hyperactivity of the catalyst. Problems were experienced with analytical communication boxes during the evening of 4 June. The problems were resolved and data were collected at the conditions of Run No. AF-R13.1 (Texaco gas, 7100 sl/hr-kg, 750 psig, 482°F, 0.85 ft/sec). A production rate of 12.1 TPD methanol was achieved which was close to expected for fresh catalyst. Mass balance around the plant was excellent. Liquid analysis showed typical methanol product composition. Nuclear density gauge readings indicated a gas holdup of 50.5 vol%, higher than the expected holdup of 43 vol%. The catalyst concentration was estimated at 45.8 wt%. Data were taken for an additional mass balance period to examine initial catalyst aging. Steady operations continued, and conversion to methanol showed an expected drop from 16.5% to 15.5%. Nuclear density gauge readings indicated a gas holdup of 54.7 vol% and a catalyst concentration of 48.2 wt%. These results were very steady during this period, in contrast to the previous data period when both showed measurable increases throughout the operation.

A high speed data acquisition system installed by Sandia National Laboratories personnel to monitor differential pressures on the reactor column was started up. Initial results indicated that a sampling rate of 1 hertz (1 sample/second) was optimum (see Figure 2.3). Also, the fluctuations being recorded were much above the noise in the signal.

Conditions were changed to Run No. AF-R13.2 (Kingsport gas, 4000 sl/hr-kg, 735 psig, 482°F, 0.49 ft/sec) shortly after noon on 6 June. The plant operated very steadily for three days at expected performance. CO conversion of 49.6% and methanol production of 9.9 TPD were achieved. Liquid analysis showed stable methanol product composition comparable to last year's Kingsport test period. Nuclear density gauge readings indicated a gas holdup of 42.7 vol% and a catalyst concentration of 41.9 wt%. During the operation at this condition, some methanol

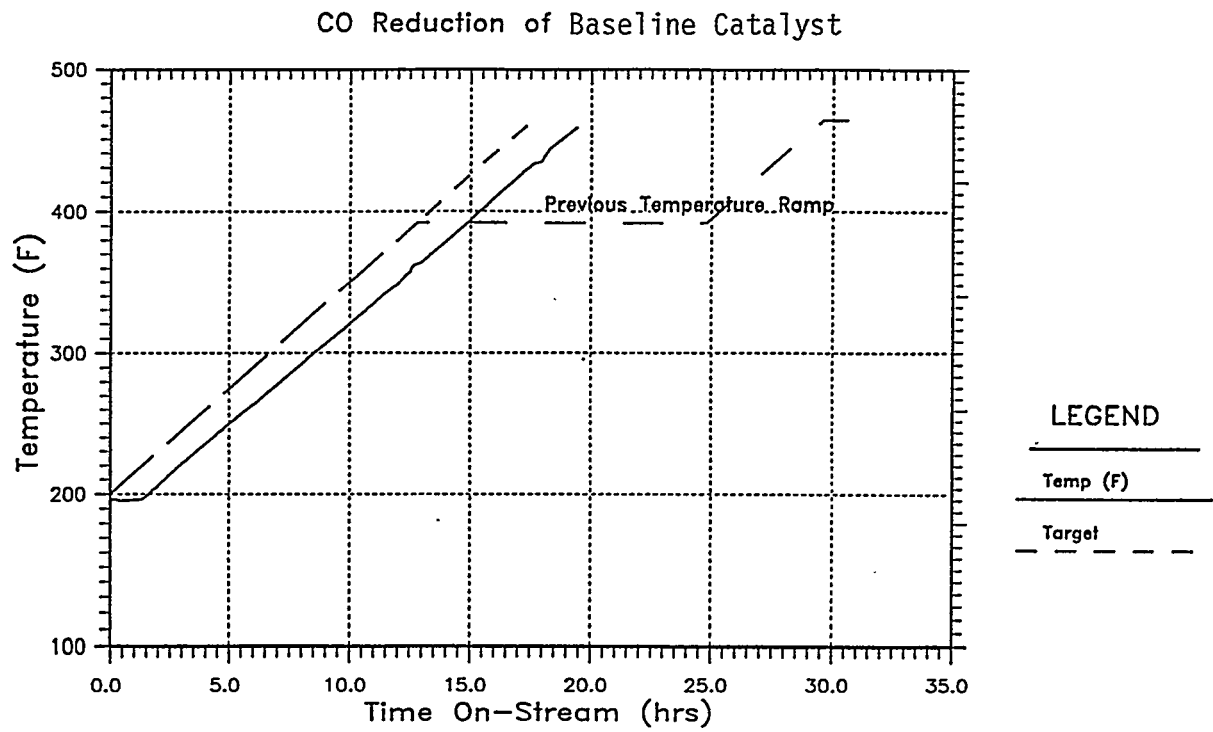**Figure 2.1 Hydrodynamic Run at LaPorte**

CO Reduction of Baseline Catalyst

LEGEND

Temp (F)

Target

Figure 2.2 Hydrodynamic Run at LaPorte

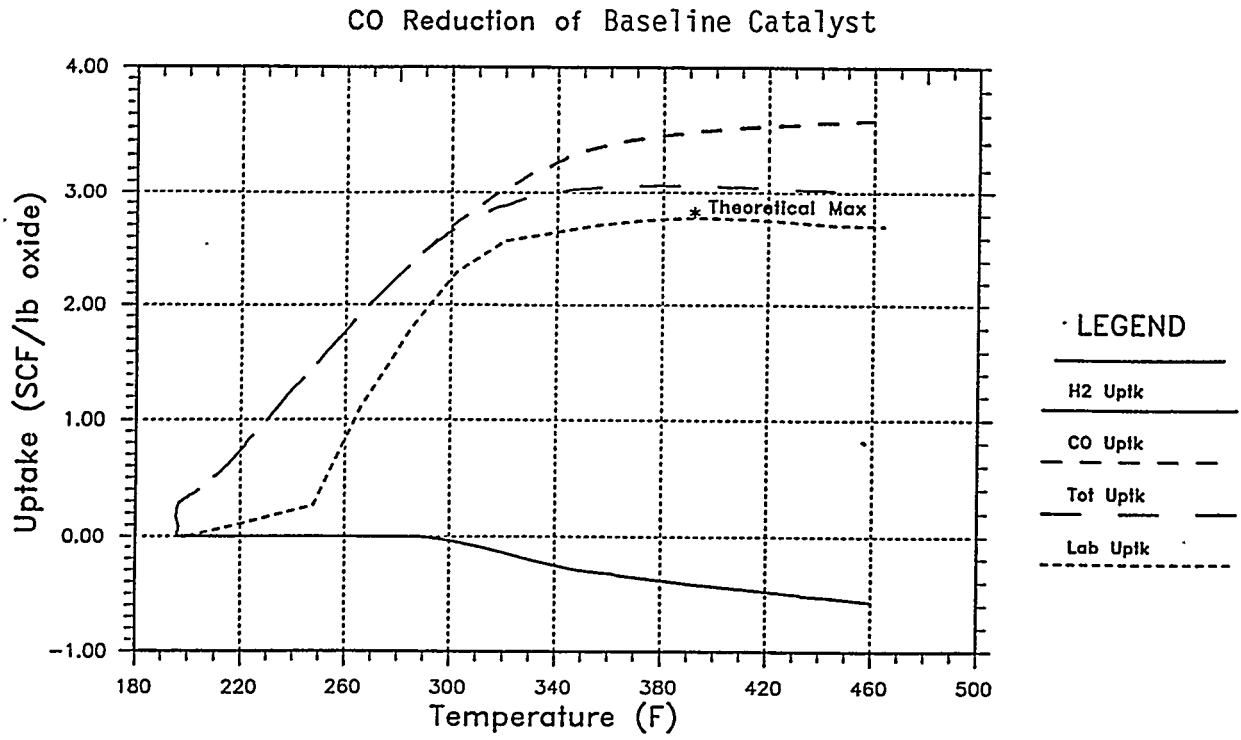CO Reduction of Baseline Catalyst

15

Table 2.2 LaPorte AFDU LPMEOH/Hydrodynamics Run - June 1995

Run No.	No. of Days	Comment	Gas Type	Reactor Pressure psia	Reactor Temp. deg F	Space Vel. sL/kg-hr	React. Fd. lbmol/hr	Inlet Sup. Vel. ft/sec	Slurry wt% oxide
NEW REACTOR (27.20) / BASELINE CATALYST									
	3	Dephlegmator Testing, Carbonyl Burnout	Nitrogen, Texaco						
AF-A9	1	Kingsport Reduction	4% CO in N2	67		615	32.3	0.62	40
AF-R13.1	2	Base Case	Texaco	765	482	7100	375	0.85	46
AF-R13.2	3	Kingsport Design	Kingsport	750	482	4000	210	0.49	41
AF-R13.3	2	High Velocity	Kingsport	735	482	9100	480	1.13	48
Subtotal	11								
NEW REACTOR (27.20) / ALTERNATE CATALYST									
AF-A10	1	Kingsport Reduction	4% CO in N2	67		615	32.3	0.62	40
AF-R14.1	2	Base Case	Texaco	765	482	7200	370	0.84	44
AF-R14.2	3	Kingsport Design	Kingsport	750	482	4000	210	0.48	39
AF-R14.3	1.5	High Velocity	Kingsport	535	482	7100	365	1.18	44
AF-R14.4	1.5		Texaco	765	482	4100	210	0.47	41
AF-R14.5	1	Base Case	Texaco	765	482	7200	370	0.83	45
AF-R14.6	0.8	Tracer Study	Texaco	765	482	7200	370	0.83	45
AF-R14.7	1	Tracer Study	Texaco	765	482	4100	210	0.47	41
AF-R14.8	1	Tracer Study	Kingsport	535	482	7100	365	1.18	44
AF-R14.9	0.2	Turn-down	Kingsport	765	482	1300	67	0.15	44
Subtotal	13								
GRAND TOTAL	24								

16

Figure 2.3 Pressure Signal versus Time for Different Sampling Rates

17
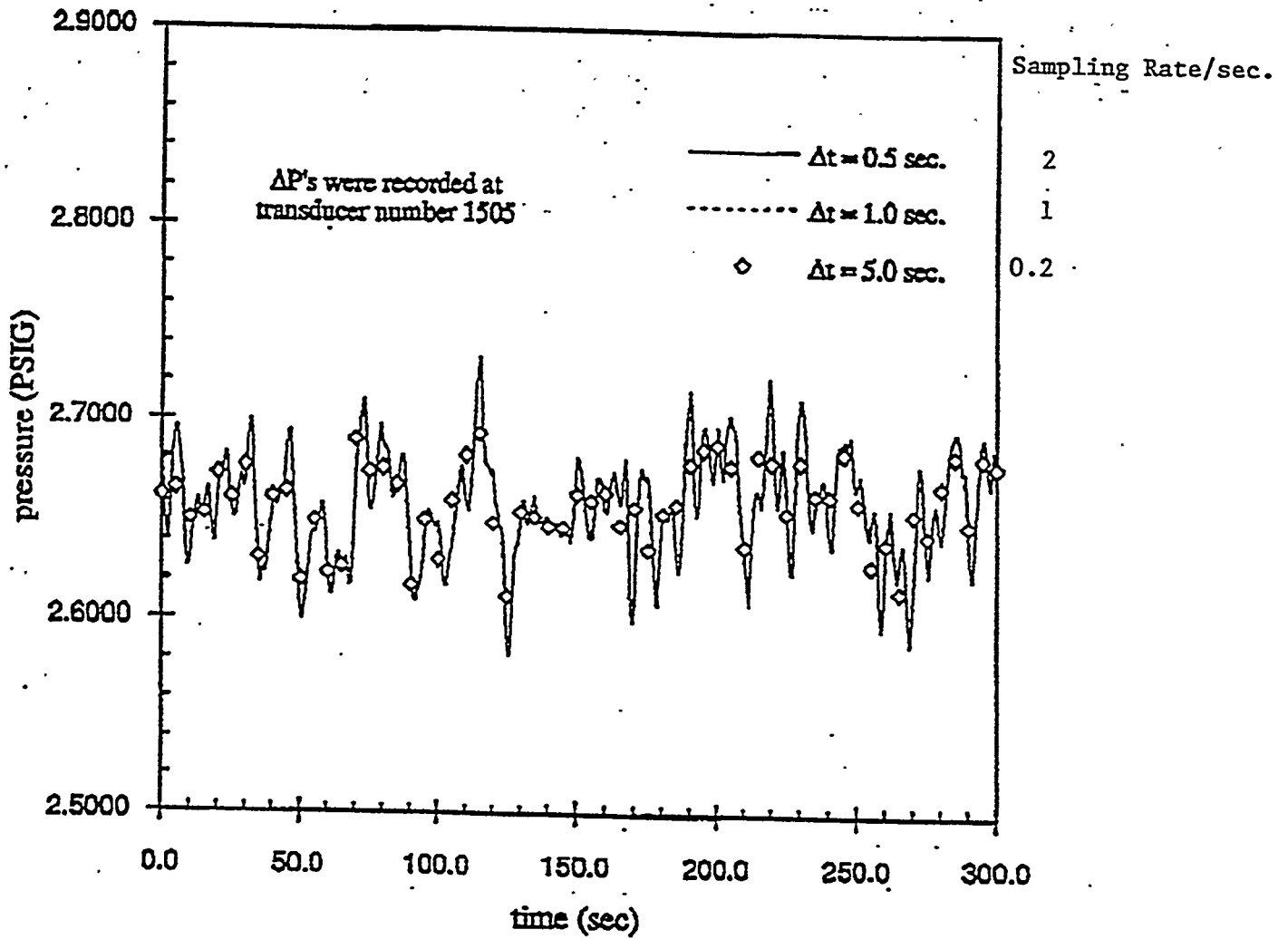
condensation was observed in the 27.14 oil separator. With almost 17 mole% methanol in the reactor effluent, the methanol dew point was 268°F. Hence, the temperature of the 27.14 was increased from 280 to 295°F to avoid methanol condensation.

The differential pressure (DP) measurements appeared to be working well. The DP measurement locations on the reactor are shown in Figure 2.4. Preliminary estimates of gas holdups from the DP readings indicated holdups showing similar trends, but lower in magnitude than those derived from nuclear density readings:

Run No.	Gas Holdup from DP vol%	Gas Holdup from NDG vol%
13.1A	43.8	50.5
13.1B	48.0	54.7
13.2A	36.3	42.3
13.2B	36.5	43.1

As observed with the NDG measurements, a holdup profile was also observed along the length of the reactor with the DP measurements. DP and gas holdups for different sections of the reactor are shown below for Run No. 13.2A. Holdup was higher at the top.

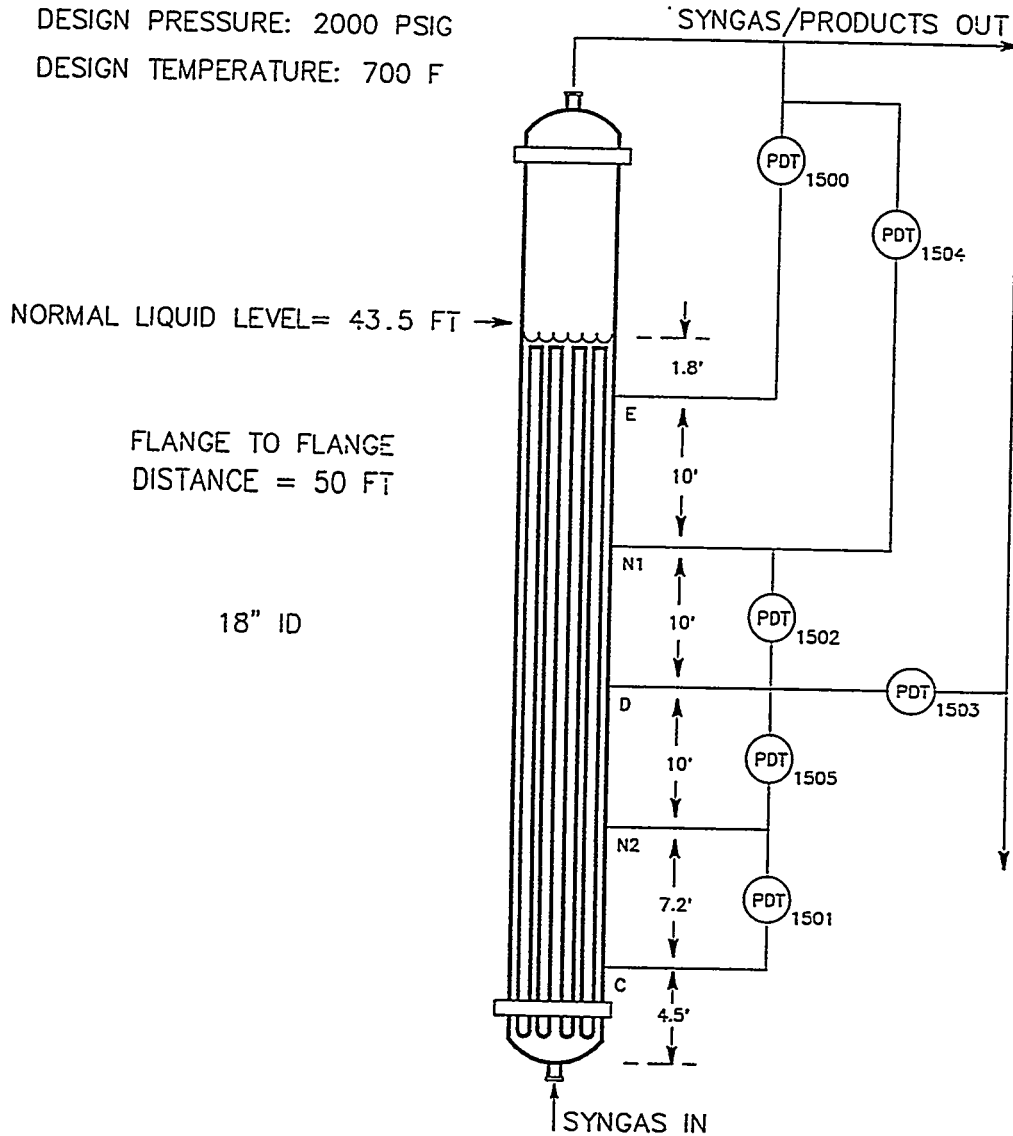| Nozzles	Transmitters PDT	Differential Pressure, psi	Gas Holdup, vol%
C-N2	1501	1.95	37.4
N2-D	1505	2.96	31.2
D-N1	1502	2.84	34.0
N1-E	1504 - 1500	2.49	42.5

A shutdown test was conducted at the end of Run AF-R13.2 to obtain a more accurate holdup estimate. Based on liquid level measurement with flow shutdown, gas holdup was calculated at 32.9 vol%. This compares with an estimate of 43.1 vol% based on NDG measurements and 36.5 vol% based on DP measurements. An attempt was made to measure the rate of drop of liquid level immediately after the gas was shut down using the NDG. However, this drop was too fast compared to the response of the NDG as well as the speed at which the NDG can be moved. DP data were collected during the shutdown test with the Sandia data acquisition system. These data may help sort out distribution of large bubbles vs. small bubbles. Kim Shollenberger (Sandia) conducted a preliminary analysis of the data. Smooth curves were obtained when gas holdup was plotted as a function of time during the shutdown test (Figure 2.5), indicating only a single normal bubble size distribution in the column. Further analysis is ongoing.

18

Figure 2.4 LaPorte AFDU Oxygenates High Pressure Reactor

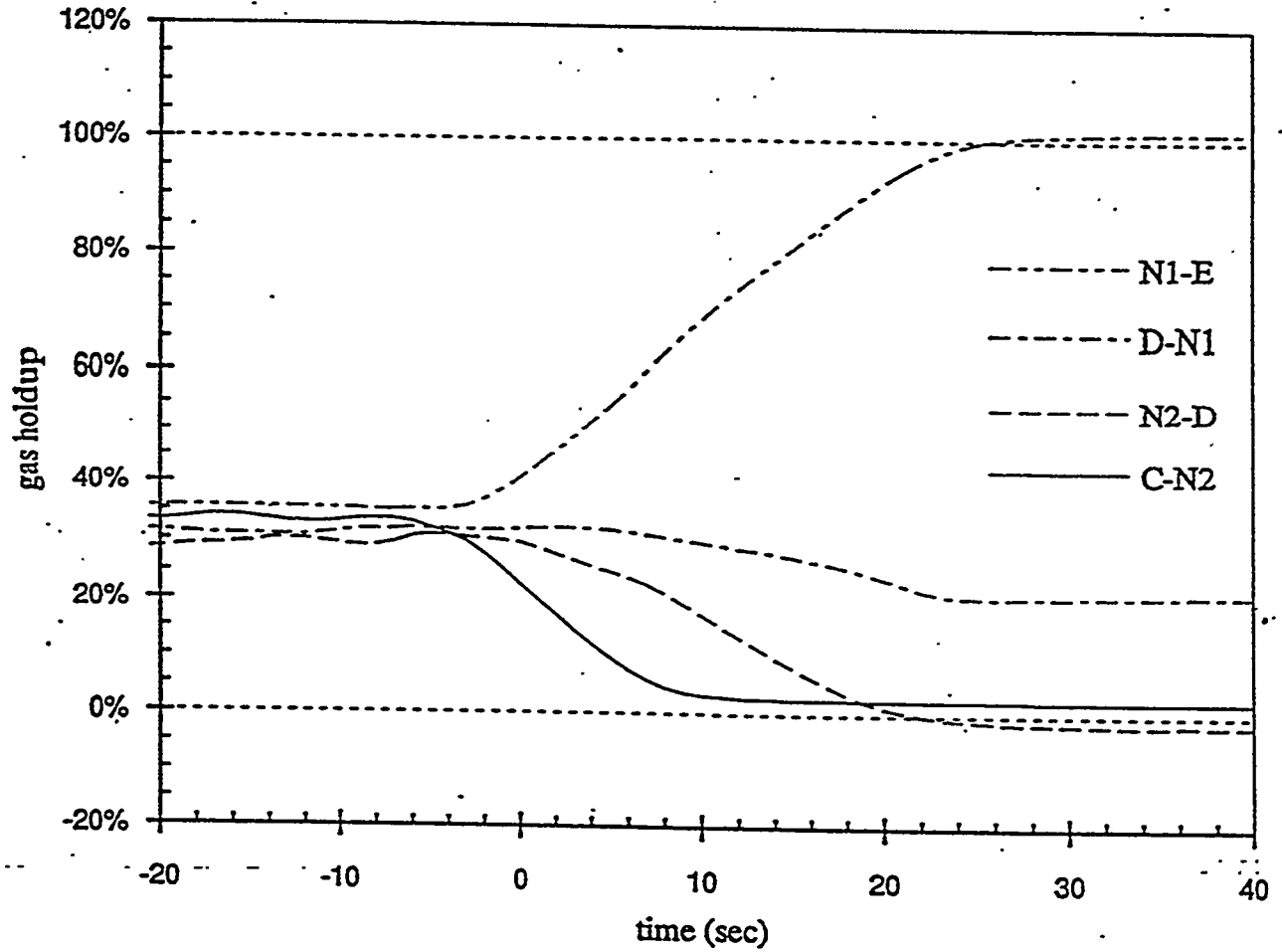DIFFERENTIAL PRESSURE TRANSMITTER POSITIONS

DESIGN PRESSURE: 2000 PSIG
DESIGN TEMPERATURE: 700 F

SYNGAS/PRODUCTS OUT

PDT 1500

PDT 1504

NORMAL LIQUID LEVEL= 43.5 FT →

1.8'

E

FLANGE TO FLANGE
DISTANCE = 50 FT

10'

N1

10'

18" ID

PDT 1502

D

PDT 1503

10'

PDT 1505

N2

7.2'

PDT 1501

C

4.5'

SYNGAS IN

DPT2720.SKD

BL3   9/20/95

19

Figure 2.5 Run No. R13.2B
Gas Holdup During Shutdown

After the shutdown test, the unit was brought on-stream with Texaco gas in an attempt to reach the conditions of Run AF-R13.3: 10,000 sl/hr-kg, 750 psig, 482°F, 1.2 ft/sec gas inlet velocity. With Texaco gas, the 01.20 recycle compressor reached its limit at 0.95 ft/sec. Operating at lower pressure helped little as pressure drop through the plant increased. In order to achieve higher gas velocity, the feed composition was changed from Texaco gas to Kingsport gas. Higher methanol production was expected with Kingsport gas, which would lower the pressure drop in the back end. A linear velocity of 1.13 ft/sec was achieved with this gas, and stable operation was obtained at this condition. Reactor performance was stable with a production rate of about 18 TPD. The NDG readings showed higher fluctuations compared to those typically observed at lower velocities. A gas holdup of 55.8 vol% with a catalyst concentration of 48.7 wt% was estimated from the NDG readings. The DP measurements indicated a holdup of 44.9 vol% and a catalyst concentration of 39.2 wt%. Oil loss rate from the reactor was measured at this velocity. A modest loss rate of about 10 gph was estimated from level rises in vessels downstream of the reactor (21.11 & 27.14).

At 00:45 hours on 11 June, the plant experienced a shutdown due to loss of compression. Belts on the motor for the two compressors broke, shutting down the plant 6 hours earlier than scheduled. Since there were enough data at this last condition with the Baseline catalyst, it was decided to cool down the reactor in preparation for a turnaround to the Alternate catalyst run. The slurry was drained directly from the reactor.

2.2 LPMEOH with Alternate Catalyst

2.2.1 Slurry Preparation
A 40 wt% oxide catalyst slurry was mixed in the 28.30 Prep Tank. The Prep Tank was charged with 1766 lbs of Drakeol-10 oil at 08:00 on 10 June and 1178 lbs of Alternate catalyst at 08:00 on 12 June. Catalyst was taken from eleven drums of lot # 022811. The slurry was heated and agitated in the Prep Tank for two hours prior to transfer to the reactor.

2.2.2 Catalyst Reduction
Catalyst reduction began at 14:30 on 12 June. The reduction gas (4% CO in N_2) was set at 12,500 scfh with the reactor pressure at 67 psig (Run # A10). The heat up commenced at 14:45 and proceeded from 193°F to 464°F at a rate of 15°F/hr.

Initially, the Alternate catalyst reduction seemed a little slower than the previous Baseline catalyst reduction. The reduction rate increased later, and most of the uptake was complete by about 360°F (12-13 hours on-stream, same as Baseline). The total uptake peaked out close to the theoretical maximum value of 2.68 SCF/lb oxide (see Figure 2.6). Reduction in the bubble column was a little slower compared to that in the autoclave. The 27.20 internal heat exchanger was easily able to control temperature, and the ramp rate proceeded on schedule with no evidence of an exotherm. At 392°F, the reduction gas flow was reduced to 9,375 scfh as planned to reduce oil loss from the reactor and conserve on nitrogen usage. When the flow was reduced, the slow adjustment of CO concentration in the reduction gas caused the calculated uptake value to drift. Gas holdup during the reduction was slightly higher than expected: 29-34 vol% at 12,500 scfh. Catalyst concentration was in the 41-42 wt% range.

Figure 2.6 Hydrodynamic Run at LaPorte

CO Reduction of Haldor-Topsoe   Alternate P

LEGEND

H2 Uplk
CO Uplk
Tot Uplk.
Lab Uplk

22
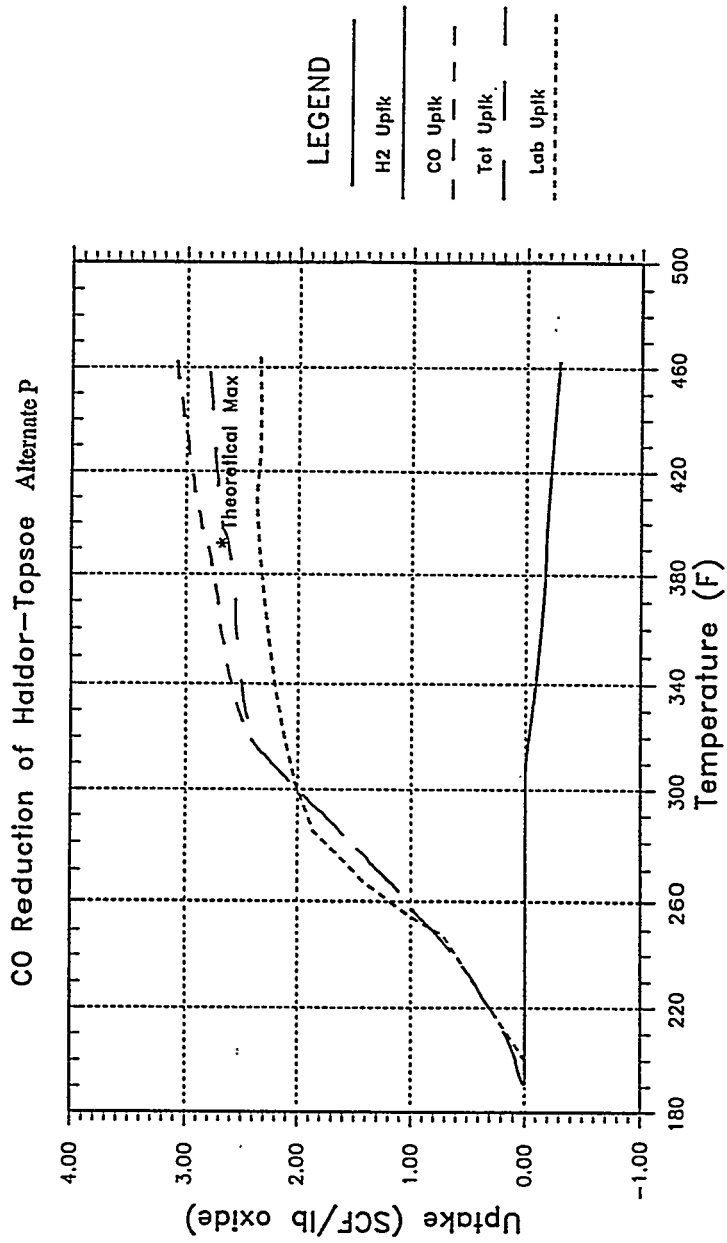
2.2.3 Process Variable/Hydrodynamic Study

Syngas flow to the reactor began at 11:00 on 13 June. The unit was fully lined out at the conditions of Run No. AF-R14.1 (Texaco gas, 7200 sl/hr-kg, 750 psig, 482°F, 0.84 ft/sec) by 18:00. The initial data indicated typical hyperactivity of the catalyst. The operational results were very similar to those seen previously during AF-R13.1 with the Baseline catalyst. The production rate was 12.0 TPD of methanol, and the CO conversion was 16.4%. The mass balance around the plant was excellent. Liquid analysis showed typical methanol product composition with some very slight variations in the impurity mix. Nuclear density gauge readings indicated a gas holdup of 49.6 vol%, and a catalyst concentration estimated at 45.4 wt%. Steady operations continued for another day at conditions of Run No. AF-R14.1. Compared to the Baseline catalyst, the Alternate catalyst showed even less decline in activity over its initial 24 hours of operation. The production rate decreased to 11.7 TPD of methanol, and the CO conversion dropped to 16.2%. Nuclear density gauge readings were identical to the previous data period. A shutdown test immediately following this run indicated 38.9 vol% gas holdup.

Conditions were changed to Run No. AF-R14.2 (Kingsport gas, 4000 sl/hr-kg, 735 psig, 482°F, 0.48 ft/sec) shortly after noon on 15 June. The plant ran smoothly at this condition for three days with stable catalyst performance. The Alternate catalyst continued to perform very similarly to the Baseline catalyst. The production rate was about 10 TPD methanol. Nuclear density gauge readings indicated a gas holdup of 37.8 vol%, and catalyst concentration was estimated at 39.6 wt%.

Due to the lack of an adequate CO supply, the originally planned condition of Run No. 14.3 (Kingsport gas, 10,000 sl/hr-kg, 735 psig, 482°F, 1.2 ft/sec inlet gas velocity) could not be achieved. Instead, it was decided to operate at another high velocity condition that would consume less CO. Conditions were changed to 7,100 sl/hr-kg, 520 psig, 482°F and 1.18 ft/sec inlet gas velocity with Kingsport gas. The plant performed steadily at this condition. Catalyst performance was close to expected. CO conversion was about 33% compared to a modeled 2-CSTR expectation of 32.5%. Nuclear density readings had some fluctuations similar to those observed with the Baseline catalyst at high velocity. A gas holdup of 50.4 vol% and catalyst concentration of 45.6 wt% were estimated based on the nuclear density readings. DP measurements on the reactor indicated a holdup of 36.6 vol%. A shutdown test was conducted at the end of the mass balance period. Gas holdup of 36.6 vol% was measured during the shutdown test.

After the shutdown test, the unit was brought to conditions of Run 14.4 (Texaco gas, 4,100 sl/hr-kg, 750 psig, 482°F, and 0.47 ft/sec inlet gas velocity). The plant performed steadily at this condition. Catalyst activity was close to expected. CO conversion was 17.5% compared to the modeled 2-CSTR expectation of 17.7%. Increased levels of higher alcohols, methyl formate and methyl acetate were observed at this low space velocity condition. Nuclear density readings had no fluctuations, as the linear velocity at this condition was low as well. A gas holdup of 42.9 vol% and catalyst concentration of 42.2 wt% were estimated based on the nuclear density readings. DP measurements on the reactor indicated a holdup of 33.3 vol%.

The operating conditions of the unit were changed to baseline conditions (Run No. AF-R14.5: Texaco gas, 7,200 sl/hr-kg, 750 psig, 482°F, and 0.83 ft/sec inlet gas velocity) on the morning of 21 June. The plant performed steadily at this condition. Catalyst activity was very close to that observed initially at the same condition (Run No. AF-R14.1). CO conversion dropped only slightly from 16.2% to 15.9%, and by-product formation was down to the same level as Run 14.1 A gas holdup of 50.8 vol% and catalyst concentration of 46.5 wt% were estimated based on the nuclear density readings.

Further measurements were made on the 21.11 dephlegmator at the baseline condition. Although flooding was ruled out as a reason for less-than-design performance, variability in oil capture was still apparent. A large amount of AFDU data is in need of analysis before a final decision is made on possible inclusion of dephlegmators in commercial flowsheets.

2.2.4 Catalyst Performance Comparison

The Alternate catalyst performance is compared with the Baseline catalyst performance in Table 2.3. The comparison can be made at two different conditions. Very similar CO conversion and methanol production rates are evident. Lower gas holdup was obtained with the Alternate catalyst. Results obtained with the two catalysts at high velocity are presented in Table 2.4. A direct comparison cannot be made because the two conditions were different. However, some similarities are notable. During both runs, the NDG readings had high fluctuations but a stable average. Also, the oil loss rate from the reactor was moderate. CO conversion obtained with both catalysts at different conditions is shown in Figure 2.7. In addition to the similarity of the two catalysts, the plot shows stable operation with the Alternate catalyst, when conversion for R14.5 is compared with that for R14.1.

By-product data were analyzed more closely because increased levels of higher alcohols, methyl formate and methyl acetate were observed with the Alternate catalyst at low space velocity condition (Run No. AF-R14.4). The Baseline catalyst was not operated at this condition in the previous run; however, comparison of the two catalysts is available at two other conditions: Run Nos. 13.1/14.1 and 13.2/14.2 (see Table 2.5). By-product formation was very similar for the two catalysts at these conditions.

2.2.5 Reactor Tracer Study

On 21 June, ICI Tracerco personnel started preparing for a 3-day tracer study of the reactor unit. The study was started on 22 June at the baseline conditions (Run AF-R14.6: 0.83 ft/sec inlet velocity, 7200 sl/hr-kg, 750 psig, 482°F, Texaco gas). Detectors were set up at various locations outside the reactor as shown in Figure 2.8. Sets of four detectors at 90° angles were set up at seven different heights. In addition, detectors were installed at the reactor inlet, reactor outlet, vapor space near the reactor top and recycle feed line. During the liquid injection, the detector at the reactor inlet was moved to the liquid injection nozzle.

Table 2.3 Catalyst Performance Comparison for LPMEOH

Catalyst Run No.	Baseline AF-R13.1B	Alternate AF-R14.1B	Baseline AF-R13.2B	Alternate AF-R14.2B
Syngas Composition	Texaco	Texaco	Kingsport	Kingsport
Space Vel., sL/hr-kg	7130	7200	4000	4030
Pressure, psig	751	754	735	735
Temperature, deg. F	484	482	483	483
Inlet Linear Velocity (ft/s)	0.85	0.84	0.49	0.48
CO Conversion to MEOH (%)	15.5	16.2	49.6	48.6
Methanol Production (TPD)	11.6	11.7	9.9	9.8
Slurry Concentration Based on NDG (wt %)	48.2	45.3	42	39.7
Gas Holdup Based on NDG (Vol %)	54.7	49.9	43.1	38.1

Table 2.4 LPMEOH Results at High Velocity

Catalyst	Baseline	Alternate
Run No.	AF-R13.3B	AF-R14.3
Syngas Composition	Kingsport	Kingsport
Space Vel., sL/hr-kg	9110	7090
Pressure, psig	720	521
Temperature, deg. F	482	482
Inlet Linear Velocity (ft/s)	1.13	1.18
CO Conversion to MEOH (%)	39.9	33
Methanol Production (TPD)	18.3	11.1
Slurry Concentration (wt %)	48.9	45.6
Gas Holdup (vol. %)	55.8	50.4
Limitation	Recycle Compressor	CO Supply
NDG Readings	High Fluctuations Stable Average	High Fluctuations Stable Average
Oil Loss Rate from Reactor	Moderate	Moderate
Reactor Design Basis	Kingsport:	0.64 ft/sec
	Recent Commercial Designs:	0.80-0.85 ft/sec
	New Commercial Design:	~1.0 ft/sec

Figure 2.7 Hydrodynamic/Methanol Run at LaPorte
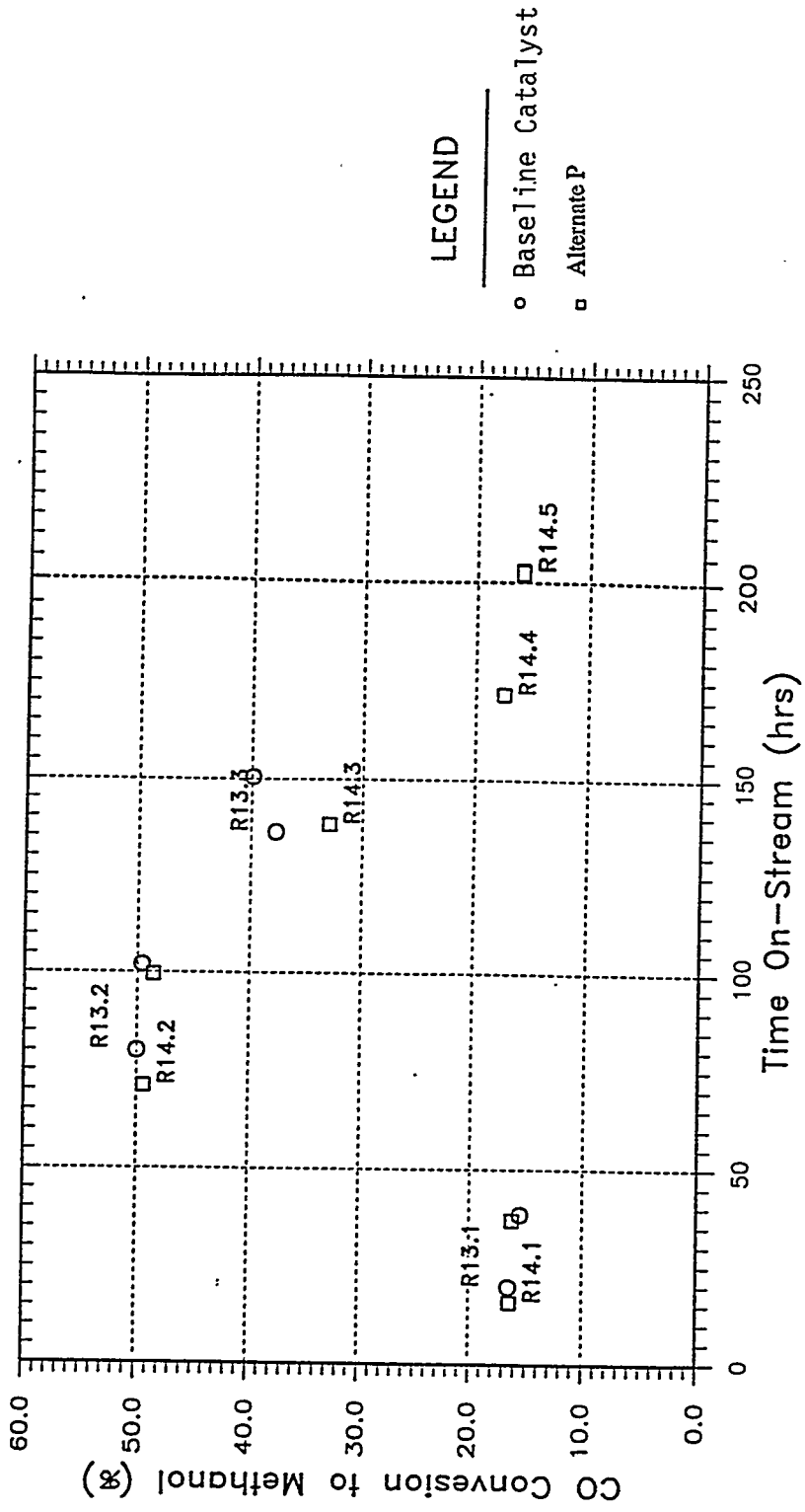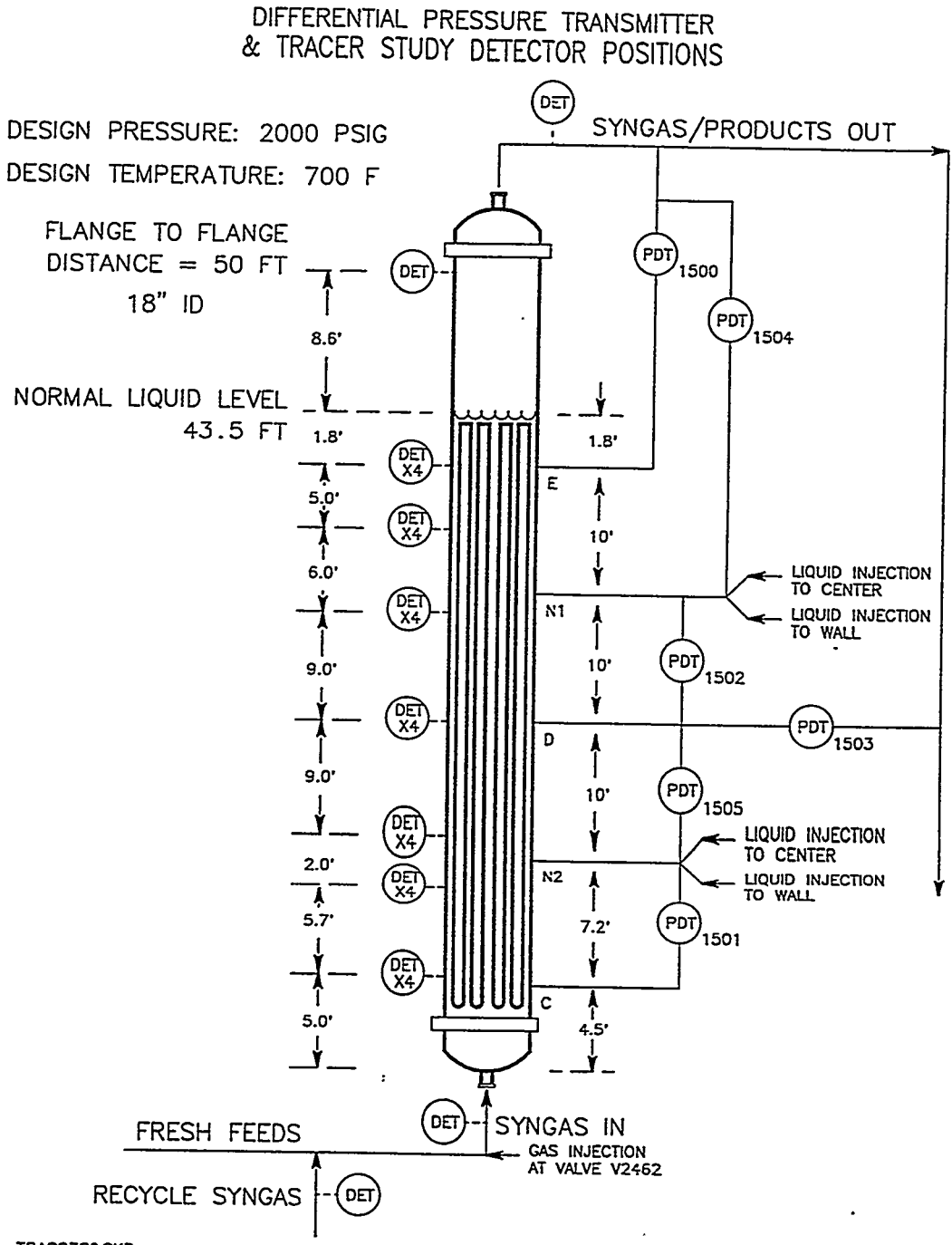
Table 2.5 By-Product Analysis Comparison for LPMEOH

Catalyst Run No.	Baseline AF-R13.1B	Alternate AF-R14.1B	Baseline AF-R13.2B	Alternate AF-R14.2B
Syngas Composition	Texaco	Texaco	Kingsport	Kingsport
Space Vel., sL/hr-kg	7000	7000	4000	4000
Pressure, psig	750	750	735	735
Temperature, deg. F	482	482	482	482
Product Analysis, wt %				
Methanol	96.72	96.73	97.31	97.42
Ethanol	0.89	0.91	0.32	0.35
1-propanol	0.25	0.26	0.08	0.10
isopropanol	0.02	0.02	0.01	0.00
1-butanol	0.17	0.17	0.09	0.08
2-butanol	0.06	0.05	0.03	0.03
isobutanol	0.06	0.05	0.01	0.02
2-Methyl 1-Buoh	0.00	0.00	0.00	0.00
1-pentanol	0.08	0.08	0.03	0.03
2-Methyl 1-Peoh	0.00	0.00	0.00	0.00
1-hexanol	0.04	0.04	0.00	0.00
2-Methyl 1-Isobutyrate	0.00	0.00	0.00	0.00
meAc	0.20	0.22	0.06	0.07
etAc	0.00	0.00	0.00	0.00
meFm	0.91	0.99	0.42	0.44
DME	0.00	0.00	0.00	0.00
CO2	0.00	0.00	0.00	0.00
Water	0.43	0.42	1.46	1.30
Oil	0.19	0.06	0.19	0.16
Total	100.00	100.00	100.00	100.00

28

Figure 2.8 LaPorte AFDU Oxygenates High Pressure Reactor

DIFFERENTIAL PRESSURE TRANSMITTER
& TRACER STUDY DETECTOR POSITIONS

DESIGN PRESSURE: 2000 PSIG

DESIGN TEMPERATURE: 700 F

FLANGE TO FLANGE
DISTANCE = 50 FT
18" ID

8.6'

NORMAL LIQUID LEVEL
43.5 FT   1.8'

5.0'

6.0'

9.0'

9.0'

2.0'

5.7'

5.0'

SYNGAS/PRODUCTS OUT

PDT 1500

PDT 1504

1.8'

E

10'

N1

LIQUID INJECTION
TO CENTER

LIQUID INJECTION
TO WALL

10'

PDT 1502

D

PDT 1503

9.0'

PDT 1505

10'

LIQUID INJECTION
TO CENTER

LIQUID INJECTION
TO WALL

N2

7.2'

PDT 1501

C

4.5'

FRESH FEEDS

SYNGAS IN
GAS INJECTION
AT VALVE V2462

RECYCLE SYNGAS

DET

TRAC2720.SKD

BLB 9/20/95

29

A vapor residence time distribution study was initiated by injecting Argon-41 into the inlet gas line and monitoring its progress through the reactor. Excellent pulses were obtained at the inlet and sharp responses were observed at other locations. It appeared that the pulse moved through the reactor at a velocity equivalent to the superficial gas velocity. This was in contrast to the previous study during the 1993 isobutylene run when the pulse appeared to move up more slowly.

Four injections of radioactive manganese oxide (Mn_2O_3) were made in the reactor slurry to study liquid phase mixing. Portions of radioactive Mn_2O_3 mixed in Drakeol-10 were injected at: (1) nozzle N2-4.5" from wall, (2) nozzle N2-wall, (3) nozzle N1-4.5" from wall, and (4) nozzle N1-wall. The data showed some of the tracer flowing in both an upward as well as downward direction. There appeared to be more downward movement at the wall.

Both gas and liquid injections were made at the two other conditions: low velocity condition (Run AF-R14.7: 0.47 ft/sec, 4100 sl/hr-kg, 750 psig, 482°F, Texaco gas) and high velocity condition (Run AF-R14.8: 1.18 ft/sec, 7100 sl/hr-kg, 520 psig, 482°F, Kingsport gas). Detailed analysis on data collected is necessary before any conclusions can be made on the mixing in the reactor. The data will take several months for workup.

Following the tracer study, a very low velocity condition (Run No. AF-R14.9: 0.15 ft/sec, 1270 sl/hr-kg, 750 psig, 482°F, Texaco gas) was operated briefly to evaluate the bed stability at the expected minimum velocity. Hydrodynamic information was gathered at this condition to ensure the same turndown capability with this catalyst as with the Baseline catalyst. All hydrodynamic data such as nuclear density readings, differential pressure readings and reactor temperature appeared uniform and extremely stable, suggesting acceptable turndown capability. Following this test, the unit was shut down at 23:10 hours on 24 June. The plant was cooled overnight and liquid drained on 25 June.

2.3 Summary and Future Work
The hydrodynamic study was successfully completed in the bubble column reactor at pilot scale. Significant hydrodynamic information was gathered during three weeks of liquid phase methanol operations. In addition to the usual nuclear density gauge and temperature measurements, differential pressure measurements (DP) were made to better understand the hydrodynamics of the system. The DP measurements worked very well mechanically, without the anticipated plugging problems, throughout the run. Gas holdup estimates based on DP measurements followed the same trends as those indicated by NDG readings. Interesting DP data were collected using Sandia's high speed data acquisition system, which could provide insight on bubble size distribution. Responses to radioactive pulses were studied for both the gas and liquid phase at three different operating conditions to evaluate mixing in the reactor. A large effort will be required to understand and interpret the hydrodynamic data collected during this run. Help from Washington University in St. Louis and Ohio State University is expected for this analysis.

High gas velocity conditions were demonstrated during this run. Operation with a linear velocity of 1.2 ft/sec was achieved with stable hydrodynamics and catalyst performance. The magnitude of the velocity was limited only by the recycle compressor capacity as the plant was designed for 1 ft/sec maximum velocity). Acceptable (i.e., low) oil carry-over from the reactor was observed at this velocity.

Improvements included in the Kingsport design for catalyst activation were also demonstrated. Successful catalyst activations were achieved using dilute CO as reductant, a faster temperature ramp, and smaller gas flow, compared to previous "standard" activation procedures.

An Alternate catalyst was demonstrated for the LPMEOH™ process. Expected catalyst activity, by-product formation, and stability were obtained with the Alternate catalyst. Overall, the catalyst appeared very comparable to the Baseline catalyst. Stable performance was obtained at both high and very low (turndown) velocity.

Dephlegmator testing was conducted at various conditions during the run. During the carbonyl burnout period, testing was conducted with a two-phase system to eliminate fouling considerations. While detailed analysis is pending, it appeared that heat transfer performance of the dephlegmator was satisfactory. However, there was significant oil carry-over. Although flooding was ruled out, variability in oil capture was still apparent throughout the run. A large amount of data requires analysis before a final decision is made on possible inclusion in commercial flowsheets.

Approximately 64,300 gallons of methanol were produced during this demonstration which will be used for product testing both in support of the Kingsport demonstration and other independent DOE studies.

TASK 3: RESEARCH AND DEVELOPMENT

3.1 New Processes for DME

3.1.1 DME Catalyst Activity and Maintenance
The progress made in this quarter features more advanced understanding of the mechanism of catalyst deactivation under LPDME conditions. This understanding was obtained by analyzing the results from 1) screening runs using different dehydration catalysts, and 2) the experiments using Robinson-Mahoney basket internals and pelletized catalysts. This understanding provides new directions in solving the catalyst stability problem. The details of the analysis and the work conducted based on the new understanding are given below.

Analysis of the Trends in Catalyst Deactivation
We have reported previously that an interaction between the methanol synthesis and dehydration catalysts is responsible for catalyst deactivation under LPDME conditions. Since then, we have been screening for alternative dehydration catalysts that could be compatible with a standard methanol catalyst (e.g., BASF S3-86). One need for efficient screening is an idea of the properties required in a dehydration catalyst. Part of the answer to this question has been

31

obtained by analyzing the results from the previous screening runs, including 14 samples described in the last two quarterly reports.

One of the key ideas developed during this analysis is that the catalyst deactivation is divided into four modes: the initial and long term deactivation of the methanol catalyst, and the initial and long term deactivation of the dehydration catalysts.

Major conclusions so far include:

1. The initial deactivation of the methanol catalyst is caused by the strong acid sites on the dehydration catalyst.

2. The initial deactivation of the dehydration catalyst is related to the type as well as the strength of the acid sites. Both strong acid sites and sites of Bronsted acid nature appear to deactivate rapidly.

3. The long term deactivation of both methanol and dehydration catalysts is not directly correlated to the acidity (e.g., the dehydration activity) of dehydration catalysts. Most dual catalyst systems show a similar rate of long term deactivation for the methanol catalyst. This rate is about a factor of 2 greater than that of the methanol catalyst-only system.

The following are the details of the analysis.

a. Observations of Deactivation of the Methanol Catalyst
Observations were made according to groups consisting of different dehydration catalysts. All systems used BASF S3-86 methanol catalyst as the other catalyst in the dual system.

Catalyst systems based on Catapal B g-alumina. Figures 3.1.1 and 3.1.2 display the activity of methanol catalyst and dehydration catalyst, respectively, as a function of time on stream for Catapal B-based catalyst systems, namely S3-86 plus virgin Catapal B or Catapal B modified by Si, WO_3, and ZnO. (Activity is measured by the rate constants of the methanol synthesis and dehydration reactions. The rate expressions for these rate constants and the adjustment performed to make the comparison between the different catalysts possible are given in the Appendix.) All data were obtained under standard conditions (i.e., 250°C, 750 psig, 6000 GHSV, Shell gas, and a methanol-to-dehydration catalyst ratio of 80:20).

As shown in Figure 3.1.1, the deactivation of the methanol catalyst can be divided into two stages: an *initial*, fast deactivation followed by a stage of slower but continuous, *long-term* deactivation. The division between the initial and long-term deactivation is the point at which the deactivation starts to slow down and the deactivation rate becomes almost constant. For example, for the catalyst system containing virgin alumina, the initial deactivation period stops at ca. 80 hr on stream. For the system containing ZnO-modified alumina, it stops at ca. 40 hr. The first observation from these two figures is that *the methanol catalyst deactivates at a similar rate in the second stage, regardless of the activity of the dehydration catalysts*. The deactivation in this stage is referred to as *long-term deactivation* hereafter.

32

Figure 3.1.1 "Normalized" Methanol Synthesis Rate Constant as a Function of Time on Stream for Different Catalyst Systems
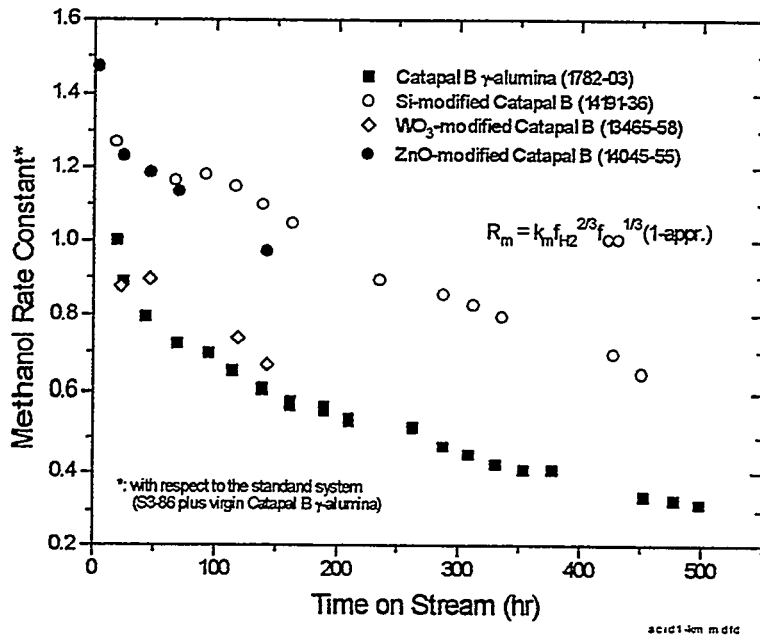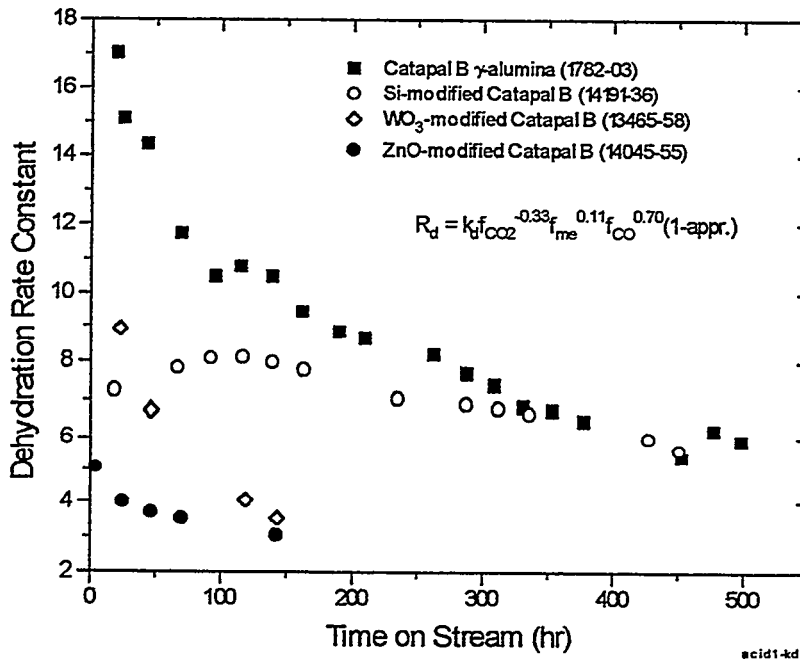

Legend:
■ Catapal B γ-alumina (1782-03)
○ Si-modified Catapal B (14191-36)
◇ WO₃-modified Catapal B (13465-58)
● ZnO-modified Catapal B (14045-55)

$$R_m = k_m f_{H2}^{2/3} f_{CO}^{1/3} (1\text{-appr.})$$

*: with respect to the standard system
(S3-86 plus virgin Catapal B γ-alumina)

Y-axis: Methanol Rate Constant*
X-axis: Time on Stream (hr)

acid1-km m dtc

Figure 3.1.2 Dehydration Rate Constant as a Function of Time on Stream for Different Catalysts

Legend:
■ Catapal B γ-alumina (1782-03)
○ Si-modified Catapal B (14191-36)
◇ WO₃-modified Catapal B (13465-58)
● ZnO-modified Catapal B (14045-55)

$$R_d = k_d f_{CO2}^{-0.33} f_{me}^{0.11} f_{CO}^{0.70} (1\text{-appr.})$$

Y-axis: Dehydration Rate Constant
X-axis: Time on Stream (hr)

acid1-kd

33

The second observation is that *deactivation of the methanol catalyst can occur during reduction*, as suggested by the different initial activities of the same methanol catalysts in different catalyst systems. Rapid deactivation continues into the early period when the system is switched to syngas. The deactivation in this stage is referred to as *initial deactivation,* hereafter. In the standard catalyst system (S3-86 plus virgin Catapal B alumina), the methanol catalyst loses 20-30% of its activity in the initial stage.

Systems of other traditional solid acids. The deactivation patterns of the catalyst systems consisting of S3-86 and silica alumina or zeolites are shown in Figures 3.1.3 and 3.1.4, along with that of the standard catalyst system. Again, all the data were collected under the standard reaction conditions. The two observations mentioned above hold true for these four additional systems, that is, the rate of the long-term deactivation of the methanol catalyst is similar among different systems, and the initial deactivation of the methanol catalyst varies from one system to another.

Systems of inert materials. A number of metal oxides we have tested, including silica gel, titania, zirconia, and, zirconia-doped silica gel, exhibited nil or negligibly small dehydration activity. The most important observation from these runs, as shown in Figure 3.1.5, is that *there is no significant initial deactivation of the methanol catalyst when the dehydration component is inert.* The system containing the silica gel shows a long-term methanol catalyst deactivation similar to that of S3-86 in a LPMEOH run (no dehydration catalyst). The experiments using other systems are too short to establish a trend in the long-term deactivation.

Figure 3.1.3 "Normalized" Methanol Synthesis Rate Constant as a Function of Time On-Stream for Different Catalyst Systems
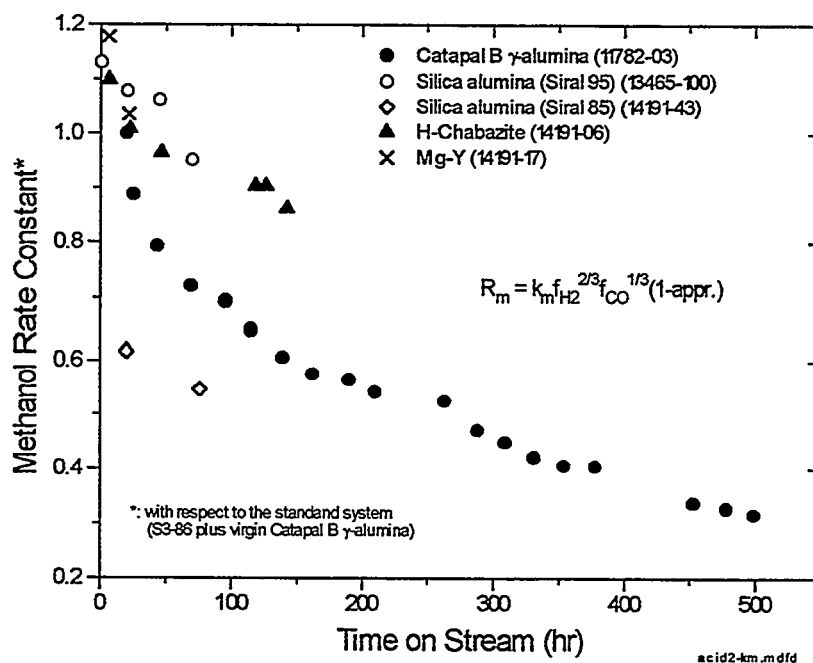

34

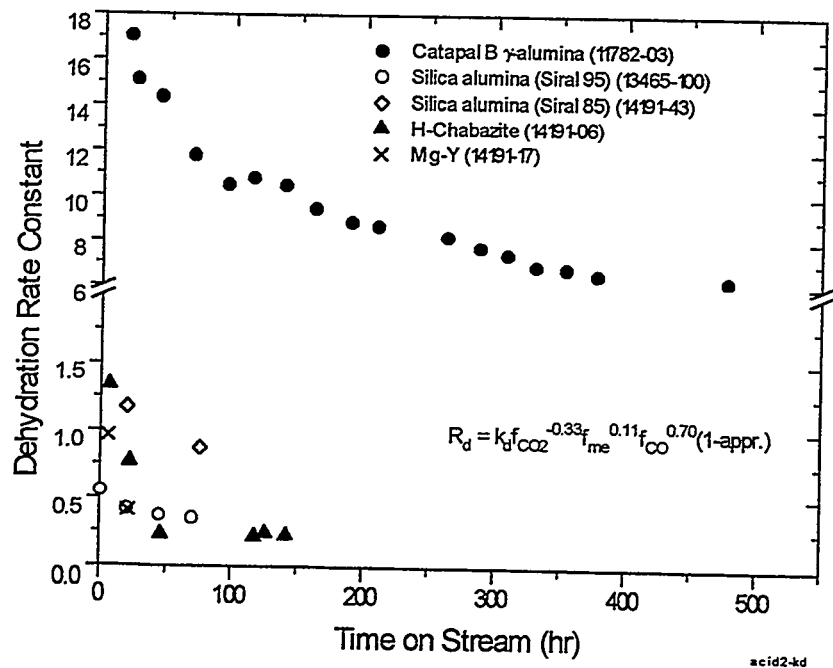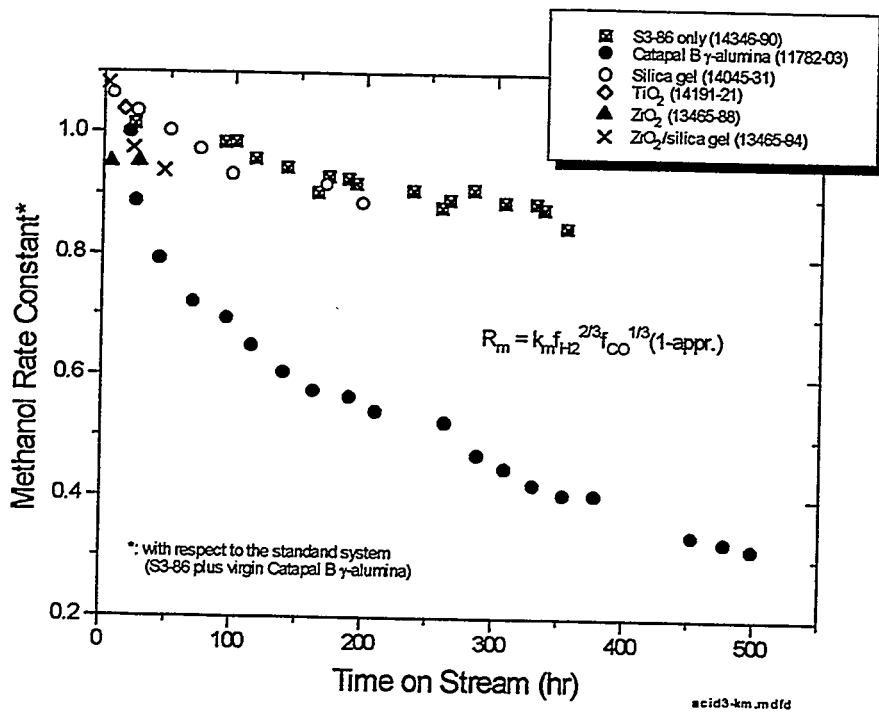## Figure 3.1.4 Dehydration Rate Constant as a Function of Time On-Stream for Different Catalysts

Legend:
- ● Catapal B γ-alumina (11782-03)
- ○ Silica alumina (Siral 95) (13465-100)
- ◇ Silica alumina (Siral 85) (14191-43)
- ▲ H-Chabazite (14191-06)
- ✕ Mg-Y (14191-17)

$$R_d = k_d f_{CO2}^{-0.33} f_{me}^{0.11} f_{CO}^{0.70}(1\text{-appr.})$$

acid2-kd

Figure 3.1.5 "Normalized" Methanol Synthesis Rate Constant as a Function of Time On-Stream for Different Catalyst Systems

Legend:
- ⊠ S3-86 only (14346-90)
- ● Catapal B γ-alumina (11782-03)
- ○ Silica gel (14045-31)
- ◇ TiO₂ (14191-21)
- ▲ ZrO₂ (13465-88)
- ✕ ZrO₂/silica gel (13465-94)

$$R_m = k_m f_{H2}^{2/3} f_{CO}^{1/3}(1\text{-appr.})$$

*: with respect to the standard system
(S3-86 plus virgin Catapal B γ-alumina)

acid3-km.mdfd

35

b. Trends in Deactivation of the Methanol Catalyst

With the exception of the system containing silica gel, *long-term deactivation* of the methanol catalyst is observed in all dual systems, and does not depend on the activity of dehydration catalysts. The methanol catalyst deactivates at a rate of ~ 0.082% hr^{-1}, which is about a factor of 2 greater than that of the S3-86-only system (0.045% hr^{-1}).

It is not straightforward to correlate the initial deactivation of the methanol catalyst to the activity of dehydration catalysts, because the dehydration catalysts may also have deactivated during reduction. Thus, the dehydration activity shown by the first data point in Figures 3.1.2 and 3.1.4 may not be a fair indication of the initial or intrinsic activity of a dehydration catalyst. The best way to determine the activity of a dehydration catalyst is to conduct a measurement using only the dehydration catalyst with methanol as feed gas. Since few measurements have been made in this regard, we have to use literature and general principles to estimate the initial dehydration activity.

Figure 3.1.6 displays the *initial deactivation* of the methanol catalyst against different dehydration catalysts. Dehydration catalysts are arranged in increasing dehydration activity order with the least active catalyst at the bottom. The initial deactivation of the methanol catalyst is measured approximately by methanol synthesis activity at 80 hours on syngas stream. Although we do not have direct measurements of the initial or intrinsic activity of these dehydration catalysts as mentioned above, a correlation can be established based on the following discussion.

First, silylation (i.e., Si-modification) has been known in the literature as a means to passivate strong acid sites on metal oxides. Modification of Catapal B by ZnO was also aimed at passivating the catalyst through acid-base reaction between ZnO (a base) and acid sites on Catapal B. Therefore, these two catalysts should have less dehydration activity than virgin Catapal B g-alumina. Second, WO_3 has been reported in the literature to have greater or similar dehydration activity compared to g-alumina. Third, silica alumina is generally more acidic than g-alumina. Siral 85, a silica alumina containing 85 wt % of SiO_2, has shown higher isobutanol dehydration activity in this lab than a g-alumina comparable to Catapal B. While the dehydration activity of the Chabazite and Siral 95 samples remains to be determined, the available data indicate that the initial deactivation of the methanol catalyst is correlated to the activity of dehydration catalysts. The greater the dehydration activity is, the larger is the initial deactivation of the methanol catalyst.

Figure 3.1.6 Correlation Between the Initial Deactivation of the Methanol Catalyst and the Activity of Dehydration Catalysts

Methanol Synthesis Activity of S3-86 at 80 hr on Syngas Stream
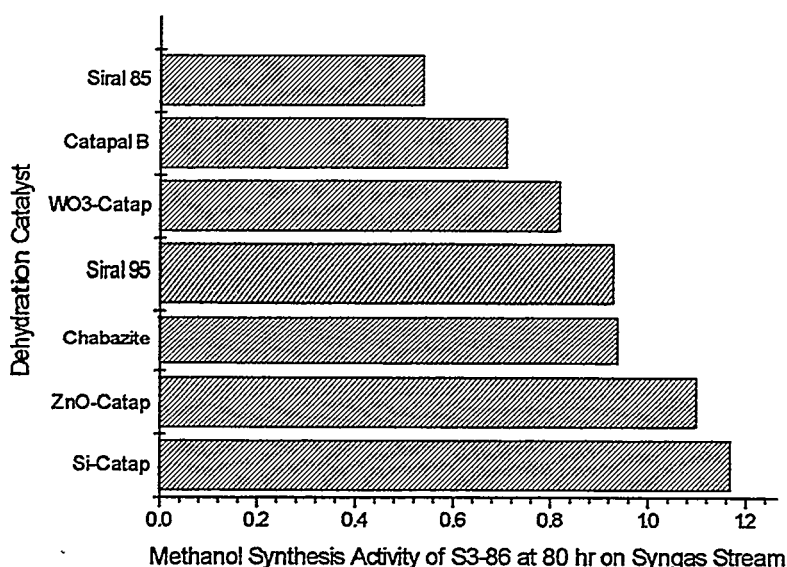
acid4-plot1

c. Patterns in the Deactivation of Dehydration Catalysts

There are several different patterns in the deactivation of different dehydration catalysts. The first pattern includes MgY, Chabazite, Siral 85, and WO$_3$-Catapal. This group of catalysts is characterized by rapid initial deactivation to a small residual activity. Significant deactivation occurs during reduction. For example, although Siral 85 has a known higher dehydration activity than g-alumina, its measured initial activity is much lower than that of Catapal B (1.2 vs. 17 mol/kg-hr, see Fig. 3.1.4). The Chabazite and MgY samples were expected to have activities comparable to g-alumina, but their measured initial activities were much lower than expected (Fig. 3.1.4). This rapid deactivation continued when the system was switched to syngas, and the dehydration activity dropped to a residual level within 100 hr on syngas stream.

Si-modified Catapal B g-alumina represents another extreme. No significant initial deactivation was observed. Instead, there was only a slow, long-term deactivation (Fig. 3.1.2).

Catapal B g-alumina undergoes a two-stage deactivation: an initial rapid deactivation (~ 40% loss in its activity) followed by a slower but continuous deactivation. ZnO-modified Catapal also falls into this pattern.

The rapid initial deactivation of dehydration catalysts may depend on the type as well as the strength of acid sites on the catalysts. MgY and Chabazite are typical Bronsted acids. Their fast deactivation may be indicative of the extra vulnerability of the Bronsted acid under LPDME conditions. Siral 85 and Catapal B should contain both Bronsted and Lewis acid sites according to conventional knowledge. Without solid evidence, it is assumed for the time being that the fast deactivation of Siral 85 and of Catapal B in the initial stage is due to the acid sites of great strength and/or Bronsted nature. This assumption is supported by the following observation.

37

The initial fast deactivation of Catapal B can be eliminated by modifying the surface with silica (Si-modified Catapal B), a process called silylation, and known for eliminating strong and Bronsted acid sites. It may not be just a coincidence that this passivated catalyst starts with an activity similar to that of the virgin Catapal B alumina after the first stage of deactivation.

The long-term deactivation of dehydration catalysts does not follow any clear pattern. The deactivation varies from one system to another. The higher dehydration activity (i.e., greater acidity) does not necessarily result in faster deactivation of the dehydration catalyst, or vice versa. This is clearly illustrated by the results from the Si- and WO_3-modified Catapal B samples shown in Figure 3.1.2.

d. Deactivation of the Methanol Catalyst vs. That of Dehydration Catalysts

In the standard catalyst system the initial deactivation of the methanol catalyst is accompanied by a corresponding deactivation of Catapal B alumina (Figs. 3.1.1 and 3.1.2). Relatively stable Si-Catapal B and ZnO-Catapal B correspond to smaller initial deactivation of the methanol catalyst. However, the almost complete deactivation of Chabazite and MgY samples is not accompanied by significant initial deactivation of the methanol catalyst (Figs. 3.1.3 and 3.1.4). And the initial loss in the methanol activity is totally outweighed by that of the dehydration activity in the case of Siral 85.

This lack of correlation between the deactivation of the methanol catalyst and the deactivation of dehydration catalysts can be further illustrated. Figures 3.1.7A and 3.1.7B plot the ratio of the methanol synthesis rate constant to the dehydration rate constant, both normalized by their initial values, for different catalyst systems. This serves as a measurement of the relative deactivation rates of two catalysts in a given catalyst system. It can be seen that the ratio is about 1 for the standard catalyst system, the systems containing silica alumina (Siral 85 and 95), and ZnO-modified Catapal B. In the case of Si-modified Catapal, the dehydration catalyst deactivates more slowly than the methanol catalyst. For the rest of the catalyst systems, the dehydration catalyst deactivates much faster than the methanol catalyst. This variation suggests that the deactivation of methanol and dehydration catalysts does not have to be a concerted process. Furthermore, different deactivation mechanisms may be operational for different catalyst systems.

38

Figure 3.1.7A The Deactivation Rate of the Methanol Catalyst Relative to that of Dehydration Catalysts in Different Catalyst Systems
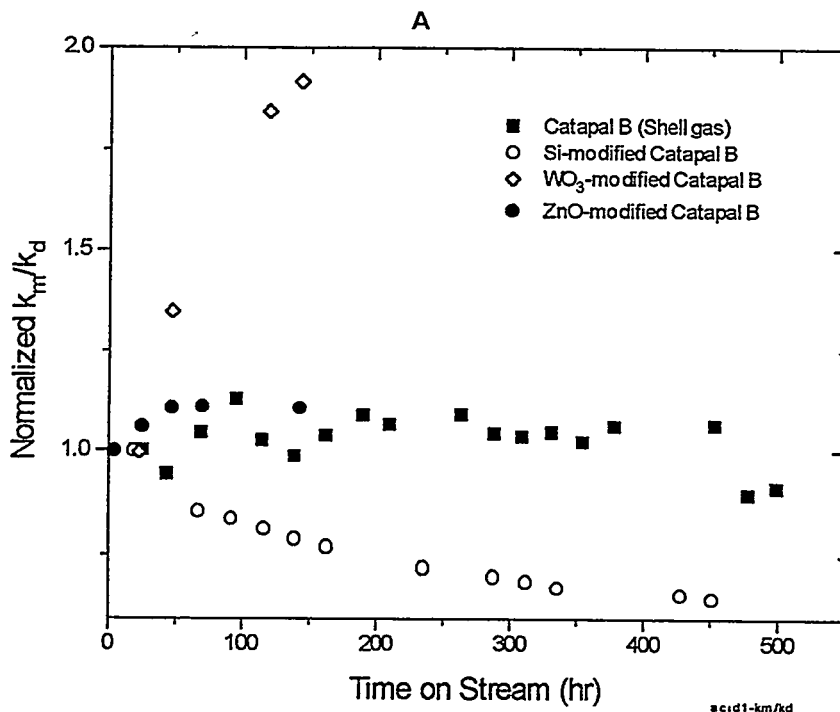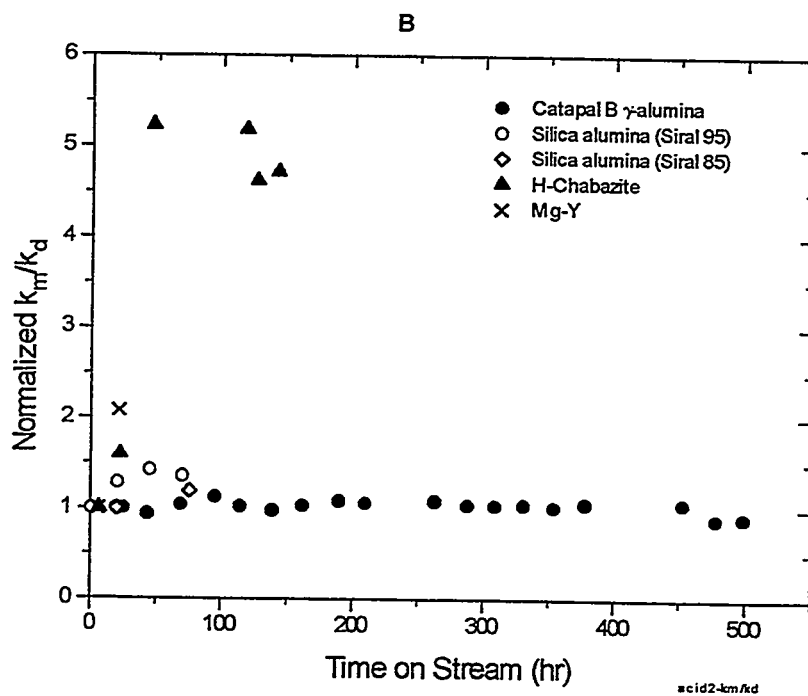

A

Legend:
- ■ Catapal B (Shell gas)
- ○ Si-modified Catapal B
- ◇ WO₃-modified Catapal B
- ● ZnO-modified Catapal B

Normalized k_m/k_d vs Time on Stream (hr)

acid1-km/kd

Figure 3.1.7B The Deactivation Rate of the Methanol Catalyst Relative to that of Dehydration Catalysts in Different Catalyst Systems

B

Legend:
- ● Catapal B γ-alumina
- ○ Silica alumina (Siral 95)
- ◇ Silica alumina (Siral 85)
- ▲ H-Chabazite
- ✕ Mg-Y

Normalized k_m/k_d vs Time on Stream (hr)

acid2-km/kd

39

e. Mechanistic Considerations

The initial deactivation of the methanol catalyst is possibly *driven by the acid-base interaction* between the two catalysts, since it correlates with the dehydration activity (Fig. 3.1.6). Among the possible mechanisms are the inter-catalyst mass transfer and inter-catalyst solid state reaction. For instance, ion exchange could take place between Cu- and Zn-containing species from the methanol catalyst and the protons on the dehydration catalyst. Or the deactivation could be due to a reaction between ZnO (a base) in the methanol catalyst and the acid sites on a dehydration catalyst. The same acid-base interaction may also be responsible for the initial deactivation of dehydration catalysts.

Surprisingly, the initial deactivation of the methanol catalyst is not correlated to the initial deactivation of dehydration catalysts, considering that both may be due to the acid-base interaction. However, this lack of correlation can be understood if acid sites of different natures (Bronsted or Lewis) undergo deactivation through different routes. Furthermore, we still have not ruled out the possibility that coke formation deactivates, as a parallel route, dehydration catalysts. If it is, certainly it will complicate the pattern of the deactivation of dehydration catalysts.

The mechanism for the long-term deactivation of both methanol and dehydration catalysts is not clear. For one thing, it is not directly related to the dehydration activity. The long-term deactivation may still be due to inter-catalyst mass transfer or solid state reactions, but is not likely acid-base in nature. For example, the migration of Zn- and Cu-containing species from the methanol catalyst to dehydration catalysts can be *driven by the concentration gradient* of these species between the methanol catalyst and dehydration catalysts. Note that most of the metal oxides tested as dehydration catalysts are also good catalyst supports with dispersing capability for metal, metal oxides, and salts, and the dispersing capability is not necessarily related to the acidity of the materials.

3.1.2 What We Learned from the Experiments using Robinson-Mahoney Basket Internals

3.1.2.1 A Repeated Run Using Robinson-Mahoney Basket Internals

A second LPDME run using Robinson-Mahoney (R-M) basket internals was conducted this quarter. The goal of this experiment was twofold: first, to confirm the results from the first experiment using the basket internals because of their important implication for future work, and second, to determine when the deactivation of the dehydration catalyst occurs under this setup.

The current run (14045-69) was carried out at the same conditions as the first one (Shell gas, 750 psig, 250°C). Two different space velocities and stirrer speeds were used in the previous R-M run: 6,000 GHSV and 1600 rpm vs. 1500 GHSV and 2000 rpm. The second set of conditions was used in the current run, which was also shorter, 121 hr compared to 500 hr for the earlier run. As for the first experiment, due to the mass transfer limitations under the R-M setup, the activity of the catalysts could only be checked in a subsequent run using the normal LPDME setup and the powdered catalyst mixture made from the spent pellets. The previous experiment showed that the powders from the R-M experiment were reduced (i.e., hydrogen uptake of the

powder was minimal). Therefore, the system was brought to the reaction conditions without reduction in the run of activity measurement.

Table 3.1.1 lists the activity results of the catalysts from both R-M runs, along with those from a standard LPDME life run (powder mixture, 11782-3). There are some differences between the two R-M runs; mainly, the second run exhibits higher methanol activity and lower dehydration activity. This difference is likely due to the experimental variability. As mentioned previously, the spent pellets were ground into powders, then reloaded into the autoclave to check activity. In both runs, only a portion (1/4 in the first and 1/2 in the second run) of the catalyst mixture was ground, saving the other portion for analytical purposes. Since the pellet mixture might not have been perfectly mixed, the ratio of the two catalysts in the ground samples may have been different from the nominal values, resulting in the uncertainty in data analysis.

Given the experimental variability, the same conclusion can be drawn from the two R-M runs. Judging by the rate constant, the spent methanol catalysts from the R-M runs have almost the same activity as the fresh methanol catalyst in the standard run, and much higher activity than the methanol catalyst at a similar time on stream in the standard run. Therefore, both runs indicate that the methanol catalyst is stable under the R-M setup. The dehydration catalyst deactivated in the R-M runs by 37-59%. Since the longer time on stream in the initial experiment did not result in greater deactivation in the dehydration activity, it can be concluded that the deactivation of the dehydration catalyst occurred only in the earlier stage of the run (< 127 hr). That is, there is no long-term deactivation of the dehydration catalyst under the R-M setup.

Table 3.1.1 Activity of the Catalysts Used in the LPDME Runs Using Robinson-Mahoney Basket Internals
Reaction conditions: 250°C, 750 psig, Shell gas.

Run	Catalyst	Time On-Stream	MEOH Equiv. Prod.	Concentration (%)		Rate Constant	
	S3-86:A1203	(hr)	(mol/kg-hr)	MEOH	DME	$k_m{}^a$	$k_d{}^b$
1st R-M (14045-52)	82.2:17.8	508	28.1	1.59	6.13	2.7	10.7
2nd R-M (14045-75)	**80:20**	**127**	**27.1**	**2.74**	**4.87**	**3.1**	**7.0**
Standard (11782-3)	81.3:18.7	20	30.7	1.01	6.95	3.0	17.0
		115	23.6	0.83	4.89	19	10.8
		499	30.37	0.49	2.67	1.0	5.9

a: Methanol synthesis rate constant calculated from $R_m = k_m f_{H_2}^{2/3} f_{CO}^{1/3}$ (1-*appr.*), based on methanol catalyst weight.

b: ethanol dehydration rate constant calculated from $R_d = k_d f_{CO_2}^{-0.33} f_{MEOH}^{0.11} f_{CO}^{0.70}$ (1-*appr.*), based on alumina weight.

3.1.2.2 The Role of Intimate Contact Between the Two Catalysts in Catalyst Deactivation
There are two important observations from the experiments using Robinson-Mahoney basket internals and pelletized catalysts. First, this system is free of methanol catalyst deactivation,

indicating that the presence of an active dehydration catalyst in the system does not necessarily cause the deactivation of the methanol catalyst. This is true for even the potential initial deactivation stage, a stage associated with dehydration activity. It also indicates that the slurry fluid does not participate in deactivation of the methanol catalyst.

Second, we did see initial deactivation of the dehydration catalyst under this setup. This deactivation may be due to either inter-catalyst mass transfer or coking. The analysis of the spent samples from this experiment will enable us to distinguish between these two mechanisms. If inter-catalyst mass transfer is the cause, the slurry fluid must have served as the mass transfer medium. And apparently the methanol catalyst has some "free" Zn- and/or Cu-containing species to spare before its activity starts to suffer. *In summary, among four modes of catalyst deactivation under the standard LPDME conditions, three of them do not occur under the Robinson-Mahoney setup.*

Why is the catalyst deactivation pattern so different between a normal slurry phase operation and the run using Robinson-Mahoney basket internals and pelletized catalysts? If one assumes that the inter-catalyst mass transfer or reaction causes the deactivation of both catalysts, this process requires a **driving force** and the **intimate contact** between two catalysts. The driving force, as discussed above, could be acid-base interaction between the methanol catalyst and dehydration catalysts (the initial deactivation of both catalysts), or simply the concentration gradient between the two catalysts and the dispersion capability of dehydration catalysts (the long-term deactivation of both catalysts). The driving force alone is not sufficient; intimate contact between the two catalysts is necessary to provide the time and area for the mass transfer or/and reaction to take place.

One can envision that the solid state reaction between the two catalysts can only occur when they touch each other and remain that way for a long enough time. Under the slurry phase operation conditions, this intimate contact can be provided by: 1) collision between the catalyst particles, 2) the attachment of small particles to the large ones, either on the outside surface or inside the pores, and 3) the agglomeration of small particles. Collision and attrition continuously generate particles of smaller and smaller size, resulting in large and fresh (therefore active) contact area.

3.1.3 Efforts in Developing Stable LPDME Catalysts
According to the above analysis, the stability of LPDME catalyst systems should be improved by eliminating or reducing either the driving force for the inter-catalyst mass transfer/reaction or the intimate physical contact between the two catalysts. In principle, these can be accomplished by using:

- Chemically modified alumina or methanol catalysts to reduce the driving force of the interaction between methanol and dehydration catalysts, such as removal of strong acid sites.

- Physically modified alumina or slurry system to eliminate the contact between the two catalysts.

- Alternative methanol catalysts such as one-component catalyst systems.

The following are the efforts we have made in these directions this past quarter.

3.1.3.1 Improvement in the Long-Term Stability of the Methanol Catalyst using K-Doped Alumina

A potassium-doped Catapal B g-alumina sample was prepared by impregnating Catapal B g-alumina with a KOH solution. This catalyst was used in a LPDME run along with S3-86 methanol catalyst (19045-85). As shown in Figure 3.1.8, the stability of this catalyst system is better than the standard system (S3-86 plus virgin Catapal B g-alumina). However, its productivity is lower due to the low dehydration activity of the K-doped alumina (Figure 3.1.9). This low activity apparently is due to the high K loading.

Figure 3.1.8 Productivity as a Function of Time
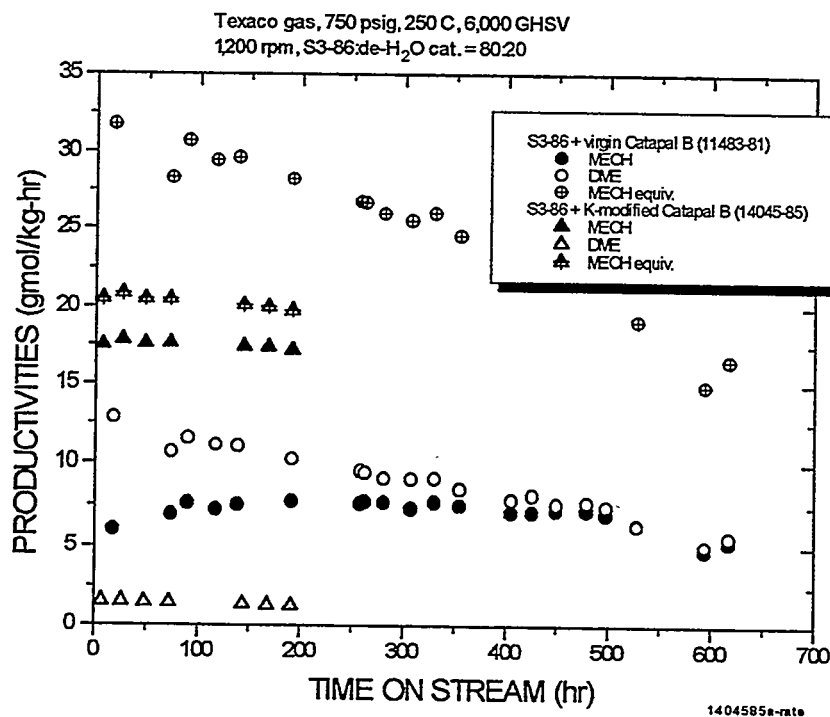
Figure 3.1.9 Dehydration Rate Constants of Different Catalyst Systems as a Function of Time
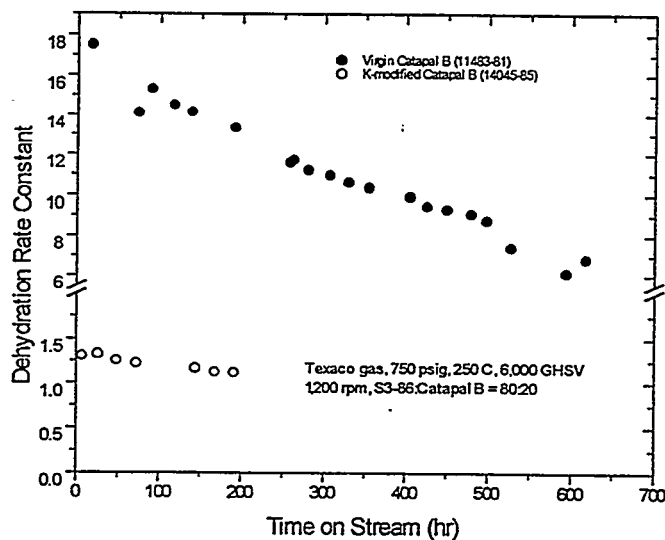
An important observation from this experiment is the improved stability of the methanol catalyst. As shown in Figure 3.1.10, the methanol catalyst has a higher initial activity (i.e., smaller initial deactivation) and slower long-term deactivation, compared to the standard system. Smaller initial deactivation of the methanol catalyst was observed previously whenever a dehydration catalyst without strong acidic sites was used. *However, this is the first time that improvement in the long-term stability of the methanol catalyst has been observed.* This improvement cannot be simply attributed to the low dehydration activity of the K-doped alumina. For example, H-Chabazite, Mg-Y, and two silica alumina catalysts (Siral 85 and 95) have a similar or lower dehydration activity than the K-doped alumina upon initial deactivation. However, little improvement in the long-term stability of the methanol catalyst was observed in these systems (Figs. 3.1.3 and 3.1.4).

We have tried to increase the productivity of the current catalyst system by adding more K-doped alumina into the system (from a ratio of 20:80 to 43:57). The productivity is still too low to be attractive. In the coming quarter K-doped alumina samples with lower loading, therefore, higher dehydration activity, will be tested to see if a similar stability can still be obtained.

Another observation from this experiment is that the production of high alcohols, e.g., isobutanol, from this catalyst system is not any higher than a typical LPMEOH run. This suggests that there is little migration of K from the K-doped alumina to the methanol catalyst.

Figure 3.1.10 Methanol Rate Constants of Different Catalyst Systems as a Function of Time

Figure 3.1.10 Methanol Rate Constants of Different Catalyst Systems as a Function of Time
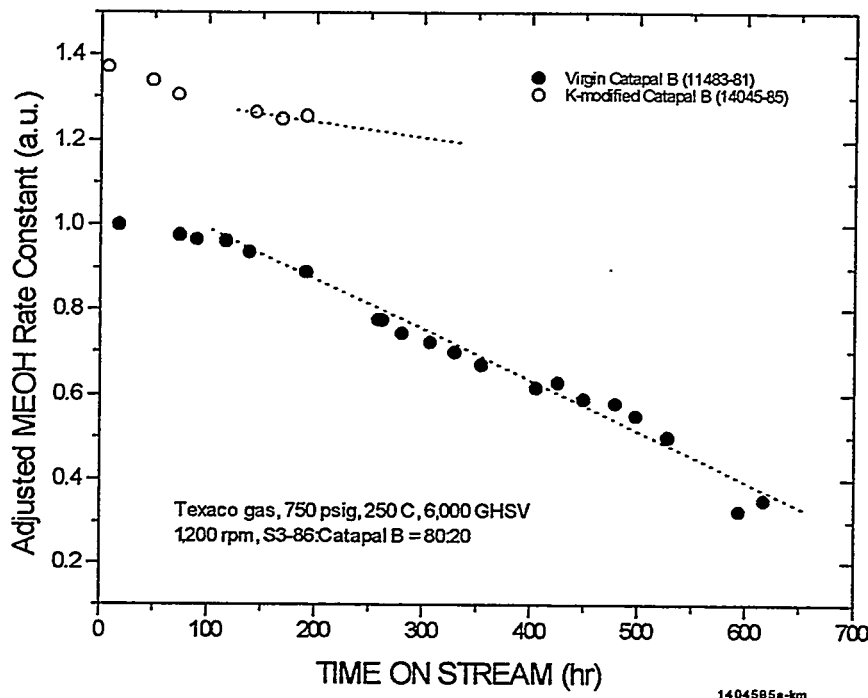
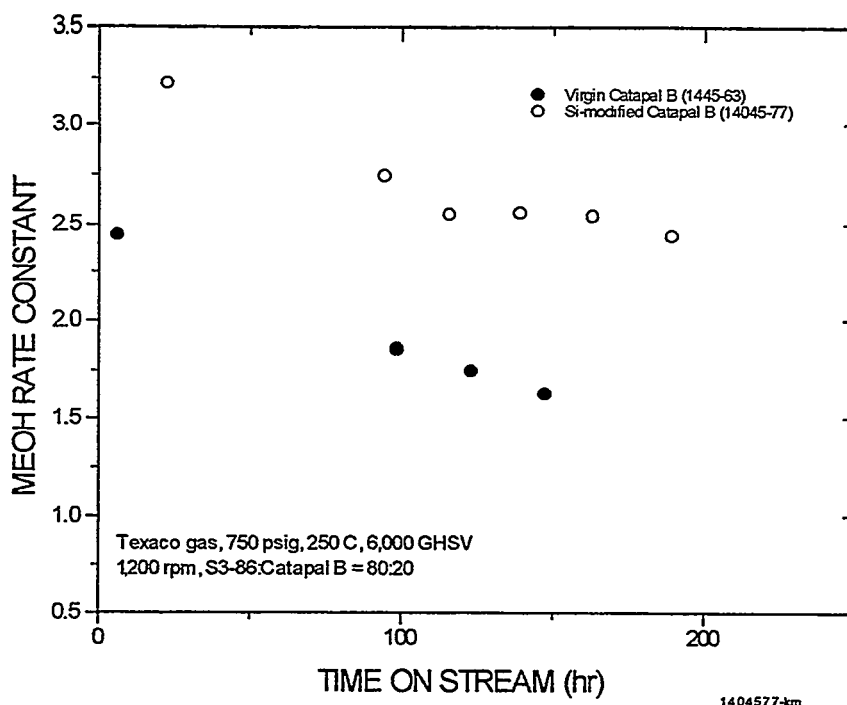### 3.1.3.2 Efforts in Passivating the Exterior of Catapal B g-Alumina Particles

A Si-modified Catapal B g-alumina (14191-104) was prepared using a polymeric siloxane precursor. Because of their large size, the siloxane molecules will most likely attach to the outer surface of the alumina. Therefore, when the siloxane is converted into silica upon calcination, only the outer surface of the alumina will be modified or passivated. (This is a technique mentioned in the literature to passivate the strong acid sites on the exterior of zeolites.) Only the outer surface of the alumina is concerned here, because that is where the deactivation of the methanol and dehydration catalysts probably occurs.

Figures 3.1.11a and b display the results of a LPDME run using sample 14045-77, along with samples of a virgin Catapal B g-alumina (14045-63). It can be seen that silica modification of the outer alumina surface results in smaller initial deactivation of the methanol catalyst, as indicated by the greater rate constant for the modified sample compared to that of the unmodified sample (Fig. 3.1.11a). This agrees with our theory that the initial deactivation of the methanol catalyst is due to the strong acid sites on the dehydration catalyst. Figure 3.1.11a shows that the long-term deactivation of the methanol catalyst is also improved somewhat.
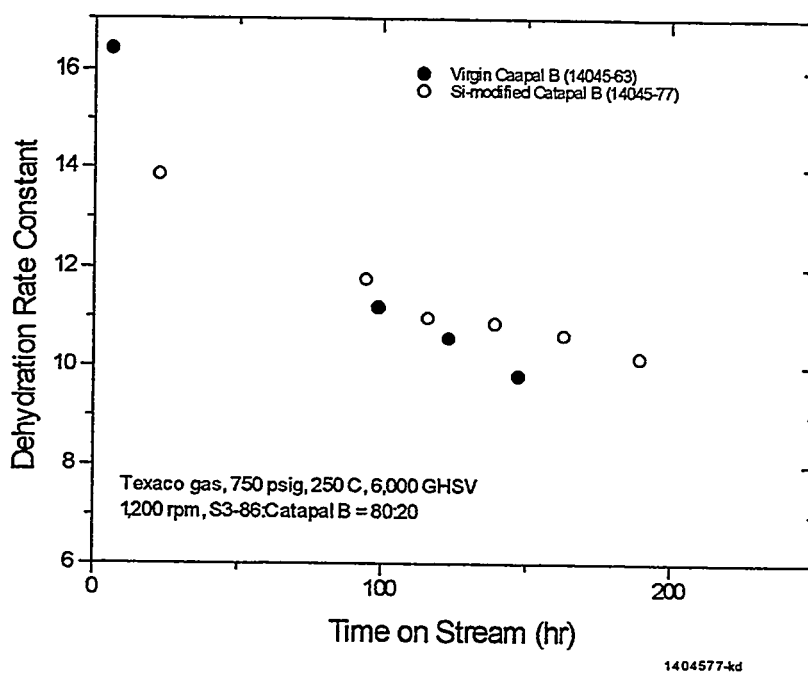
Figure 3.1.11b shows that the initial dehydration rate constant of the Si-modified sample is smaller than that of the virgin Catapal B g-alumina, apparently due to reduction in the number of acid sites by the passivation. The modified alumina, however, deactivates more slowly than the virgin one, and becomes more active after 100 hr on stream. In brief, the modification results in significant improvement in the stability of the catalyst system, but not enough as far as the long-term stability of the system is concerned.

45

Figure 3.1.11 Stability of LPDME Catalyst Systems: Si-Modified vs. Virgin Catapal B

a

Texaco gas, 750 psig, 250 C, 6,000 GHSV
1,200 rpm, S3-86:Catapal B = 80:20

1404577-km

b

Texaco gas, 750 psig, 250 C, 6,000 GHSV
1,200 rpm, S3-86:Catapal B = 80:20

1404577-kd

46

A second sample was prepared in a similar manner, but with much higher Si loading (35 wt % SiO_2). High loading was used so that alumina particles would not be only passivated on the outside surface, but hopefully encapsulated or embedded inside SiO_2. This in turn might reduce the contact between the methanol catalyst and alumina, therefore, improving the stability of the catalyst system. The sample was tested along with S3-86 methanol catalyst at the standard conditions using Texaco gas (14656-17). The dehydration activity of the sample was fairly low, about 19% of the activity of the virgin Catapal B g-alumina. No improvement in the long-term stability of the methanol catalyst was observed from this catalyst system. Note that the technique used in the preparation of this sample is best suited for silylation, but not for encapsulation and embedment.

3.1.3.3 A Single Particle DME Catalyst

A single particle DME catalyst was prepared by impregnating Catapal B g-alumina with zinc and copper (14656-9). The preparation was based on a Shell patent (US 4,375,424, 1983) for a syngas-to-DME catalyst. The catalyst is claimed to perform both methanol synthesis and dehydration functions, and is therefore referred to as single particle catalyst to distinguish it from the dual catalyst mixture in our standard LPDME system.

The standard liquid phase reduction procedure was used to activate this catalyst using 2% H_2 in N_2. The activity of this catalyst was checked using Texaco syngas and standard reaction conditions (250°C, 750 psig, and 6,000 GHSV, run 14045-91). The methanol productivity of this catalyst was found to be an order of magnitude lower than that of our standard dual catalyst system (S3-86 plus Catapal B g-alumina). It is not straightforward to compare this catalyst with the ones reported in Shell's patent, because their test reaction was run at 280°C and 1700 psig. However, catalyst stability is that which is of greatest concern. Figure 3.1.12 depicts the normalized methanol equivalent productivity of this catalyst in comparison with that of our standard dual catalyst system. It can be seen that the rate of deactivation of this one component catalyst is greater than that of our standard dual catalyst system. In the coming months, other one-component catalysts will be examined.

Figure 3.1.12 Stability of the Cu and Zn Doped Alumina Catalyst

47
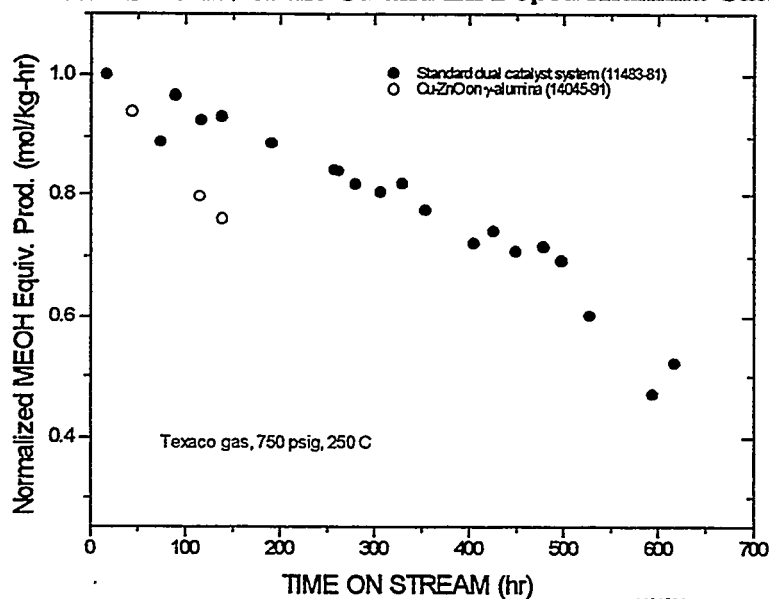
Appendix 3.1.1 The Scheme for Quantification of Catalyst Deactivation

Quantitative description of catalyst deactivation calls for good kinetic models, which are currently not available. What is available are two power law rate expressions as shown below:

$$R_m = k_m f_{H_2}^{2/3} f_{CO}^{1/3} \ (1\text{-}appr.) \tag{1}$$

$$R_d = k_d f_{CO_2}^{-0.33} f_{MEOH}^{0.11} f_{CO}^{0.70} \ (1\text{-}appr.) \tag{2}$$

where Eq. (1) is the methanol synthesis reaction, Eq. (2) is the methanol dehydration reaction, and *appr.* denotes approach to equilibrium. Both rate expressions have been examined previously (Quarterly Report, April-June 1994). Although both of them have limitations as shown below, they can be used as a semi-quantitative tool to provide the correct ranking in activity among different catalyst systems.

The rate expression for methanol synthesis (Eq. 1) correlates the data from LPDME runs fairly well (14.4% of relative mean deviation in the rate constant, k_m), especially for Shell and Texaco gas under the standard conditions (250°C, 750 psig, 6,000 GHSV), because most of the data used in the regression were obtained in the vicinity of these conditions. However, this rate expression yields rate constants of smaller values when the reaction conditions shift from LPDME to LPMEOH. Figure 3.1.13 illustrates this change as a function of the deviation from the LPDME conditions in terms of DME productivity (RDME). All the data are from freshly reduced catalyst systems (S3-86 plus Catapal B g-alumina, < 25 hr on stream). The variation in DME productivity was achieved by using different ratios of methanol to dehydration catalyst. Equation (1) plus the plots in Figure 3.1.13 provide a scheme to compare the methanol catalyst activity in any catalyst system (S3-86 plus a dehydration catalyst) with that in the standard catalyst system (S3-86 plus virgin Catapal B). That is, the methanol synthesis rate constant of a catalyst system, k_m, is calculated from Eq. (1). This rate constant can then be compared with k_m of the standard catalyst system at a similar dehydration activity (RDME) using Figure 3.1.13. In other words, if we normalize k_m from any catalyst system with that obtained from Figure 3.1.13, we can rank, on a semi-quantitative but consistent basis, the activity of the methanol catalyst in different catalyst systems.

Equation (2) correlates the dehydration data of the standard catalyst system around the standard conditions (250°C, 750 psig, 6,000 GHSV, Shell and Texaco gas) reasonably well (14.1% relative mean deviation in rate constant, k_d). However, poor correlations are observed when the reaction conditions deviate from the standard ones. In addition, there is no reason to believe that the rate expression obtained from Catapal B data should be applicable to other dehydration catalysts. In the absence of a better and universal kinetic model, the rate constant, k_d, from Eq. (2) is used to measure the activity of different dehydration catalysts in the above analysis. Hopefully, Eq. (2) gives us a semi-quantitative description of the activity of dehydration catalysts, that is, the right ranking among different catalysts.

Figure 3.1.13 Adjustment of the Methanol Synthesis Rate Constant as a Function of DME Productivity
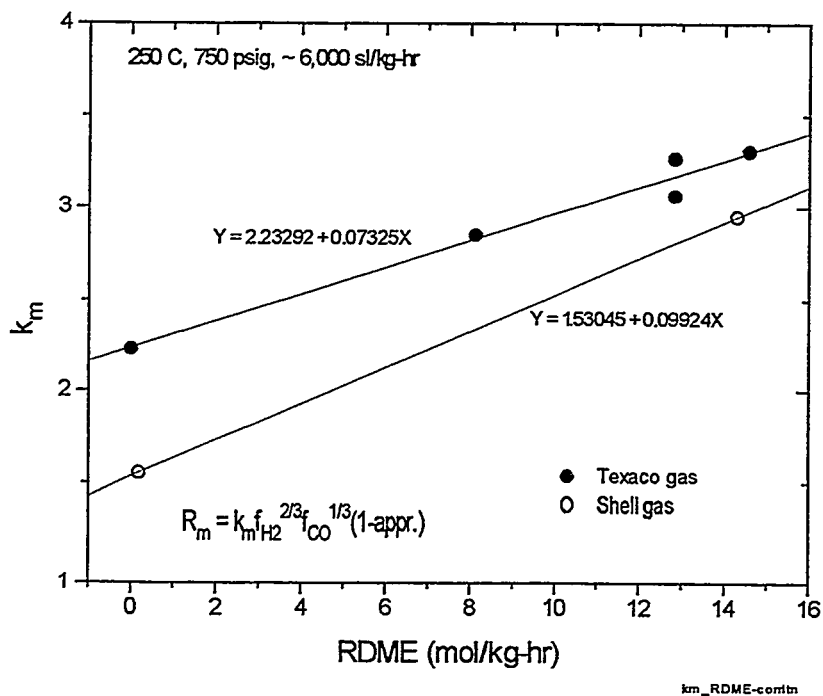
3.2 New Fuels from Dimethyl Ether (DME)

3.2.1 Overall 3 QFY95 Objectives

The following set of objectives appeared in Section III of the previous Quarterly Technical Progress Report No. 2:

- Continue to screen immobilized catalyst candidates for hydrocarbonylation of dimethyl ether to ethylidene diacetate.

- Determine the extent of any catalyst leaching from the best candidate.

- Initiate catalyst development on the cracking of ethylidene diacetate to vinyl acetate and acetic acid.

3.2.2 Chemistry and Catalyst Development

Dimethyl Ether to Ethylidene Diacetate (EDA)

The effort has focused on understanding the rhodium complexes anchored to the Reillex polymers for the catalytic conversion of DME to EDA. The goals were as follows:

- To compare catalytic runs where twice the amount of Reillex was used.

- To compare catalytic runs with different concentrations of rhodium.

- To perform three runs with the same catalyst to investigate loss in activity.

- To investigate the activity of a bimetallic Rh Pd on Reillex.

Catalytic Runs (45 minutes, 300 cc autoclave)

Experiment A

This catalytic run used 1.48g of Reillex polymer containing ~ 2.24%Rh, assuming that all the rhodium incorporated uniformly during impregnation. Samples were tested by GC at 5,10, 20, 30, and 45 minutes, respectively. As starting materials, this run contained 145.65g acetic acid, 9.1g methyl iodide and 9.96g DME.

Experiment B

This catalytic run used 3.34g of Reillex polymer containing ~5.10%Rh, assuming that all the rhodium incorporated uniformly during impregnation. Samples were tested by GC at 5, 10, 20, 30, and 45 minutes, respectively. As starting materials, this run contained 144.28g acetic acid, 9.0g methyl iodide and 10.17g DME.

Experiment C

This catalytic run used 3.35g of Reillex polymer containing ~2.24%Rh, assuming that all the rhodium incorporated uniformly during impregnation. Samples were tested by GC at 5, 10, 20, 30, and 45 minutes, respectively. As starting materials, this run contained 146.20g acetic acid, 9.0g methyl iodide and 9.88g DME.

Experiment D

This experiment was a repeat of Experiment C with a fresh charge of acetic acid, methyl iodide, and DME.

Experiment E

This experiment was a repeat of Experiment D with a fresh charge of acetic acid, methyl iodide, and DME.

Experiment F

This catalytic run used 1.56g of Reillex polymer containing ~2.24%Rh that was treated with an equivalent of palladium acetate. Samples were tested by GC at 5, 10, 20, 30, and 45 minutes, respectively. As starting materials, this run contained 146.30g acetic acid, 9.0g methyl iodide and 10.53g DME.

To compare the results, mass balances were initially calculated by the formula {2[EDA] + [DME] + [MeOAc] + [acetic anhydride]} 100/Total [DME] added and expressed as %. The 2[EDA] is required because one EDA requires two DME for synthesis. Both MeOAc and acetic anhydride require one DME. With this formula the mass balances were found to worsen with time. Better mass balances were obtained by taking into account the ethyl acetate concentrations from the reduction of EDA and the methane concentration from the reduction of DME found by head-space analysis. To compare the various runs the following terms were defined:

50

Yield = {2[EDA]} 100/[DME] added
Conversion = {[MeOAc]reacted} 100/[DME added]
Selectivity = {2[EDA]} 100/[MeOAc] reacted
Conversion x Selectivity = Yield

The assumption in defining these expressions is that all the DME reacts cleanly with acetic acid to give methyl acetate. The results at 45 minutes are tabulated in Table 3.2.1.

Table 3.2.1 Dimethyl Ether to Ethylidene Diacetate Material Balance

EXP.	MASS BAL%	YIELD%	CONV%	SEL%
A	91.6	10.1	42.3	24
B	95.5	22.8	76.5	29.8
C	92.6	18.4	60	30
D	93.3	35.5	69.5	51
E	86.9	24.3	65	37.4
F	92.8	8.4	41.6	20

Comparison of Various Samples
Experiment A versus Experiment F
Both samples showed similar yields and selectivities at 45 minutes. The only difference between these two samples was that Experiment F was treated with $Pd(OAc)_2$. An elemental analysis of Experiment F sample after the run showed 1.73% Pd, which indicated that there is significant Pd concentration. The fact that there is very little difference in the catalytic activity of both samples indicates that it is the rhodium concentration that decides the activity.

Experiment A versus Experiment C
The only difference in both these samples is that approximately two times the catalyst was used in the Experiment C run. The yield of EDA at 45 minutes increased from 10% to 18.4%, which is to be expected.

Experiment C versus Experiment D versus Experiment E
These consecutive runs with the same catalyst showed that rhodium did not leach out significantly from run to run since the catalytic activity would be expected to diminish were this to occur. In fact, catalytic activity appeared to increase, and Experiment D and E runs had higher yields and selectivity towards the product EDA (see Table 3.2.1). The Rh analysis after Experiment E was found to be 1.73% compared to the theoretical of 2.2%. The 23% difference was probably not due to loss of Rh from the Reillex polymer, but rather to an increase in the molecular weight of polymer via methyl iodide incorporation. Additional supporting evidence was reported in the previous quarterly when the Rh concentration decreased from 2% to 1.63% after one run. Since the same decrease occurred even after three runs, this indicated that no additional catalyst was being leached out.

Experiment C versus Experiment B

Both of these runs had the same amount of Reillex, but a sample from Experiment B had a higher Rh concentration (5.1% versus 2.2%). However, no great increase in EDA yield was seen (22.8% versus 18.4%). In fact Experiment B produced more methane and less acetic anhydride than did Experiment C. It appears that a higher concentration of catalyst is detrimental, in that methane is produced by another mechanism. We plan to investigate this. Elemental analysis of Experiment B after the run showed a 3.93% Rh content compared to a 5.1% value. This 23% loss was similar to that observed with all samples. As discussed above, this is probably due to an increase in polymer weight from methyl iodide incorporation.

*Background for Catalytic Runs (180 minutes, 300 cc autoclave)*

The research effort focused on longer test times with rhodium / Reillux polymer for the catalytic conversion of DME to EDA. The goals were as follows:

- Perform a catalytic run for 180 minutes and compare the results with the 45 minute run from above.

- Repeat the catalytic run for 180 minutes using a fresh charge of reactants.

Catalytic Runs (180 minutes, 300 cc autoclave)

The catalytic run in Experiment G used ~1.5g of catalyst containing ~2.24% Rh by weight. Samples were analyzed by GC at 30, 60, 90, 120, 150 and 180 minutes, respectively. As starting materials, this run contained 144.7g acetic acid, 9.4g methyl iodide and 8.4g DME. A 1:1 ratio of CO/H_2 was used at a pressure of 1500 psi and a temperature of 190°C. A graphical representation of the concentrations of some products versus time is shown in Figure 3.2.1.

Figure 3.2.1 300cc Autoclave Run
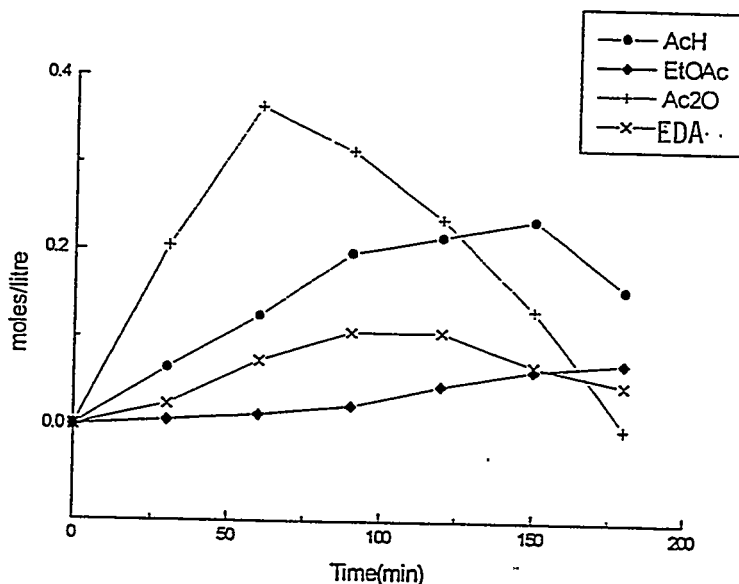
The graph shows that the EDA concentration continued to increase up to 90 minutes, after which it slowly decayed presumably by hydrogenation to give ethyl acetate and acetic acid. This reasoning is supported by the fact that the ethyl acetate concentration also began to increase after 90 minutes. The acetic anhydride concentration increased up to 60 minutes, after which it dropped rapidly. We have not yet characterized what the anhydride is converted to, but possibilities are acetic acid or acetone and carbon dioxide. The results also showed that the reaction between anhydride and acetaldehyde to give EDA was not rapid.

The catalytic run of Experiment H used the same catalyst as Experiment G with a fresh charge of starting materials. The results are shown in Figure 3.2.2.

Figure 3.2.2 300 cc Autoclave Run
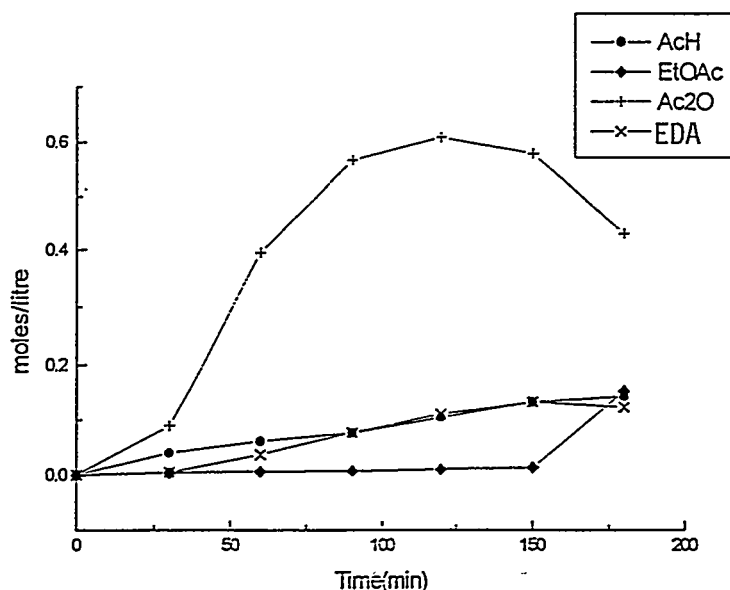
It can clearly be seen by a comparison with the results of Experiment G that the product distribution was different. The EDA concentration continued to rise slowly up to 150 minutes, after which it dropped slightly. The acetic anhydride increased to an appreciable concentration up to 150 minutes, after which it dropped steeply presumably via hydrogenation to give ethyl acetate, the concentration of which increased. It is interesting to note that both runs appeared to behave similarly up to 50 minutes. In order to numerically compare both the runs, the following equations are defined:

Yield = {2[EDA]} 100/[DME] added

Mass Balance = {2[EDA] + 2 [EtOAc] + [MeOAc] + [AcH] + [Ac2O] + [CH4]} 100/ {DME added]

53

Table 3.2.2 presents a comparison of yields and mass balances at various times during the reaction.

The mass balances in the Experiment G sample progressively worsened because the acetic anhydride was converted to other products not accounted for in the mass balance (see Figure 3.2.2). In contrast, the Experiment H sample had better mass balances because the acetic anhydride concentration was still appreciable at 180 minutes. It is also interesting to note that the yield of EDA at the 60 minute mark for Experiment G was 12.4%, which compares well with the 45 min. yield of 10.1% obtained with Experiment A in the first quarter report. The Experiment H sample showed only a 5.5% yield at 60 minutes, but with longer time the EDA concentration increased to 19.7%. This shows that after the 180 minute run, Exp G, the behavior of the catalyst has changed considerably from a fresh charge (Exp H). This result is different from that obtained for three consecutive runs (Exp C, Exp D, Exp E), when the yield of EDA at 45 minutes did not decrease. This indicates that the catalyst performs better for three 45 minutes runs than for a 180 minute run, implying that in a reactor, partial conversion with recycle is better than complete conversion.

Table 3.2.2 Dimethyl Ether to Ethylidene Diacetate Material Balance

EXP	TIME (min.)	EDA YIELD %	MASS BAL. %
G	30	4.0	88.7
G	60	12.4	90.8
G	90	17.9	78.7
G	120	17.9	68.8
G	150	11.5	55.1
G	180	8.0	42.6
H	30	0.7	82.8
H	60	5.5	87.2
H	90	11.4	90.3
H	120	16.4	87.7
H	150	19.7	85.1
H	180	18.4	93.2

## Catalytic Runs (180 minutes, 100 cc autoclave)

We attempted to commission a smaller scale batch reactor (100cc) for the DME to EDA conversion. The first reaction tried was the homogeneously catalyzed reaction for which we already had successful results in a 300 cc reactor. However, the reaction did not progress as expected for three consecutive attempts. In all three cases the reactions were run for 3 hours with samples being taken every 30 minutes. The results from the first run are shown in Figure 3.2.3.

Figure 3.2.3 100cc Autoclave Run
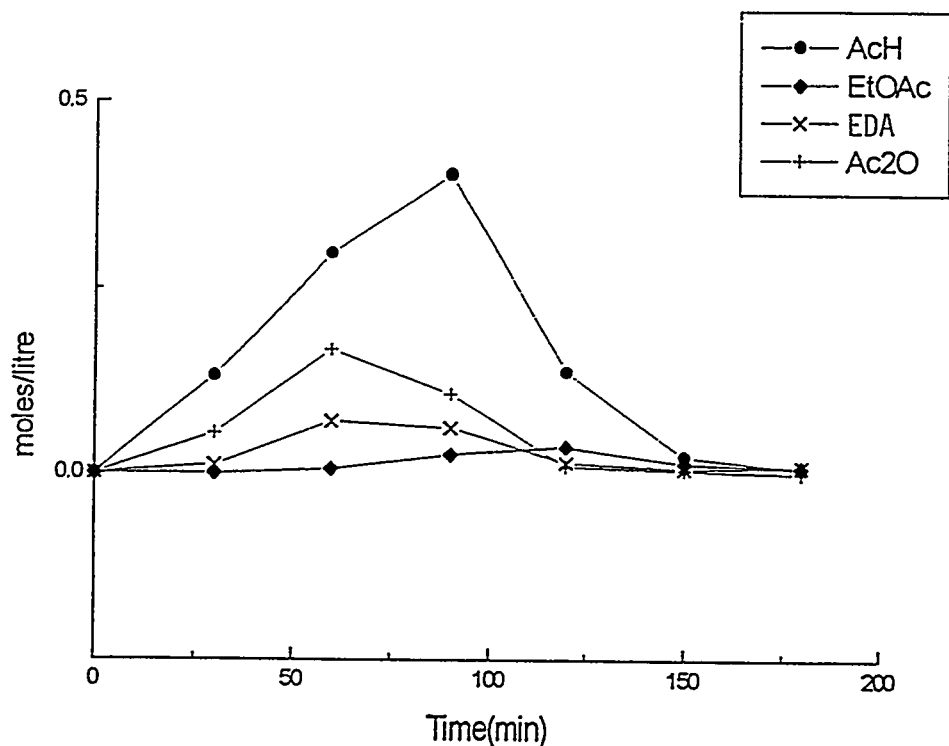
The graph shows that the major product until 90 minutes is acetaldehyde, after which it falls rapidly and is presumably converted to acetic acid. A low concentration of the desired product EDA is seen up to 60 minutes, after which it decays rapidly. However, no EDA was seen in the second and third runs (see Figure 3.2.4).

Figure 3.2.4 100 cc Autoclave Run
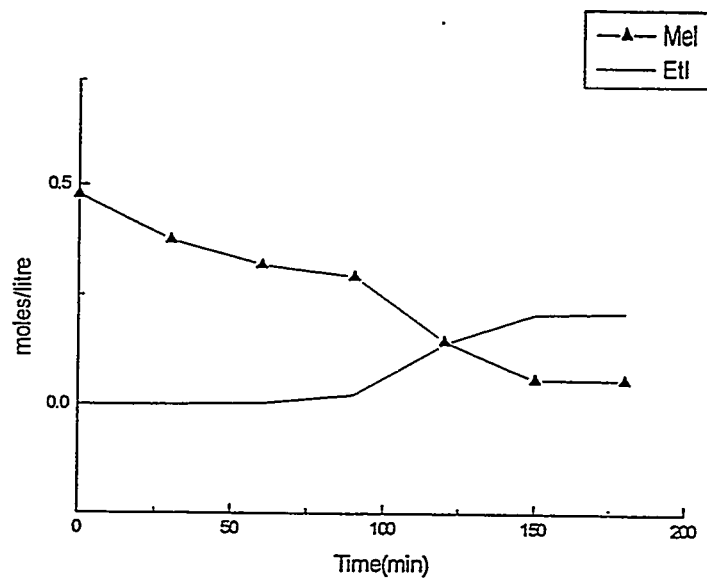
In all three runs the methyl iodide was converted to ethyl iodide (see Figure 3.2.5).

Figure 3.2.5 100 cc Autoclave Run
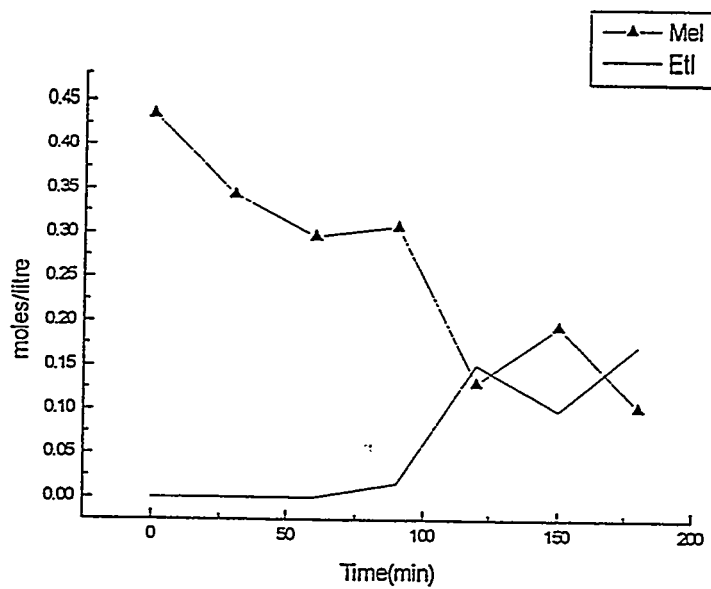
In contrast to these results, the earlier homogeneous catalytic reaction in the 300 cc reactor showed a different product profile. Figure 3.2.6 shows this different product profile over a period of 45 minutes. These results indicate that to get an adequate concentration of EDA in the reaction, the carbonylation reaction to form acetic anhydride must work well. For unknown reasons the 100 cc reactor experiment gives a different reaction pathway. Therefore, experiments in the 300cc reactor are planned.

Figure 3.2.6 300 cc Autoclave Run
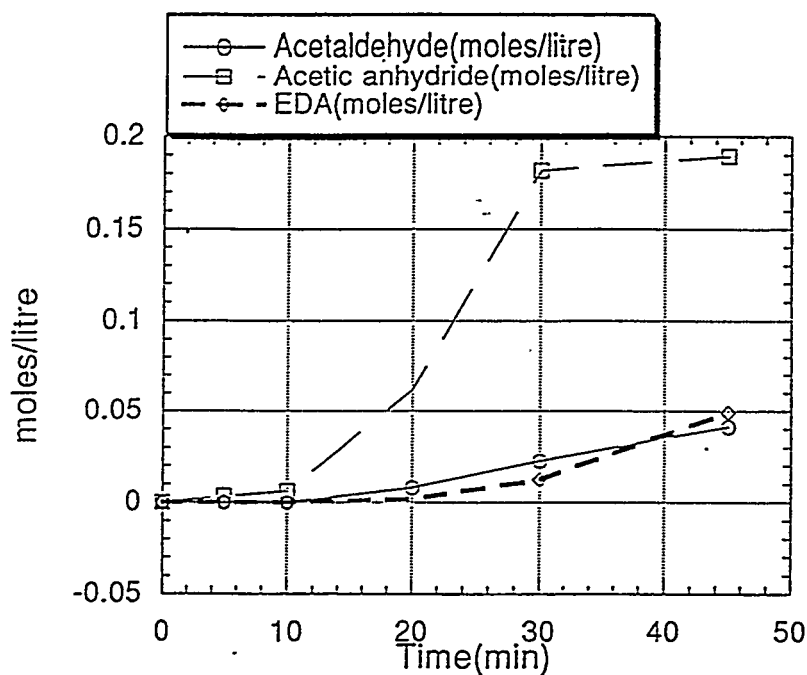
**Ethylidene Diacetate to Vinyl Acetate**
Background for EDA Cracking
The cracking of ethylidene diacetate (EDA) [$CH_3CH(O_2CCH_3)_2$] to vinyl acetate (VAM) [$CH_2=CHO_2CCH_3$] and acetic acid has been shown to proceed at about 170°C via benzenesulfonic acid catalysts in the liquid phase. Efforts to extend this catalysis to the gas phase are underway.

Temperature Effects
The desired cracking chemistry is as follows:

$$CH_3CH(O_2CCH_3)_2 \longrightarrow CH_2=CHO_2CCH_3 + CH_3CO_2H$$

　　　EDA　　　　　　　　　　VAM　　　　　　AcOH

57
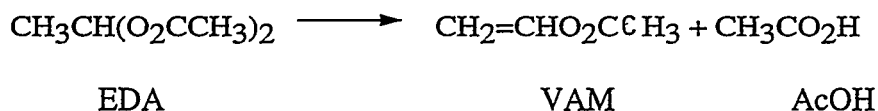
One potential unwanted reaction is the reverse synthesis reaction of EDA from acetic anhydride and acetaldehyde, as follows:

$$CH_3CH(O_2CCH_3)_2 \longrightarrow (CH_3CO)_2O + CH_3COH$$

EDA   Ac2O   AcH
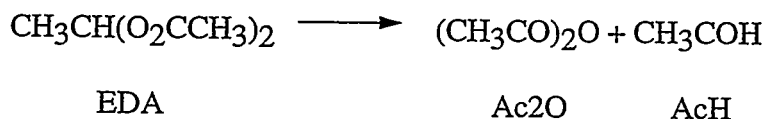
In order to determine how much back reaction existed, a blank tube was loaded in the reactor oven. A 0.2 ml/hr liquid feed of EDA with 10 cc/min of N_2 was fed to the reactor tube. This feed, once vaporized, was approximately 5 mol% EDA in N_2. At 180°C, the predominate peak observed was ethylidene diacetate. However, approximately 1% acetic anhydride and acetaldehyde from the reverse synthesis reaction was observed. These levels are sufficiently low as to pose no major problems with interpretation of results. As an alternative, the addition of acetic anhydride to the liquid feed should prevent this reaction.

At 200°C, the reactor system quickly plugged. It is presumed that at temperatures above 180°C, the ethylidene diacetate decomposes to VAM, which quickly polymerizes to polyvinyl acetate. This result sets temperature limits for the catalysis to under 200°C.

Catalytic Runs
Several catalysts were tested for the cracking of EDA to VAM and acetic acid. Unfortunately, these were examined at too high a temperature. Qualitative results are discussed below.

Sulfated Zirconia
Two grams of sulfated zirconia catalyst were loaded in a reactor tube and placed in the lab reactor system. A flow of 0.35 ml/hr EDA and 10 cc/min N_2 was initiated. The reactor was heated to 250°C. The reactor system plugged within several hours. However, several injections were obtained before plugging. In addition to unreacted EDA, the following materials were detected:

       VAM and Acetic Acid - from cracking
       Acetic anhydride and Acetaldehyde - from reverse synthesis
       C_2 and C_3 gases (ethylene/ethane/propylene/propane)
       Trace amounts of CO_2

Activity appeared to start high and drop off quickly. This may indicate deactivation of the catalyst or may be caused by the plugging.

C Coated w/NR50
Several carbons coated with NR50 (Nafion®) were examined. As mentioned previously, these were evaluated at temperatures above 200°C and were prematurely ended by plugging of sample lines.

Initial conversion of EDA was in excess of 90%, although selectivity to VAM and acetic acid was less than 25%. The predominant peak was acetic anhydride, suggesting that the same catalyst may effect not only the cracking, but also the dissociation of EDA. As mentioned previously, acetic anhydride may need to be added to the feed to suppress this reaction.
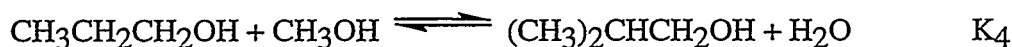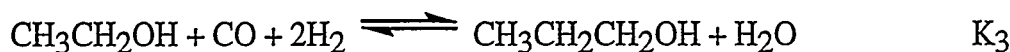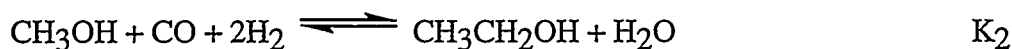
The product slate was very similar to that reported above for sulfated zirconia.

Syngas to Higher Alcohols
Equilibrium Concentration of Alcohols in Syngas to Higher Alcohols
A mol fraction vs temperature plot of the equilibrium concentrations of methanol, ethanol, n-propanol and isobutanol based on experimental (or estimated) thermodynamic values is needed to understand the conversion of syngas to higher alcohols. The existing thermodynamic parameters for all compounds involved are from Air Products' thermo database, CAPP.

The reactions to be considered are in Scheme 1 using H_2O rejection for oxygen removal. The temperature coordinate is 275, 325, 375, and 425°C. Mol fraction vs temperature plots were done at 1, 50 and 100 bar.

$$CO + 2H_2 \rightleftharpoons CH_3OH \qquad K_1$$

$$CH_3OH + CO + 2H_2 \rightleftharpoons CH_3CH_2OH + H_2O \qquad K_2$$

$$CH_3CH_2OH + CO + 2H_2 \rightleftharpoons CH_3CH_2CH_2OH + H_2O \qquad K_3$$

$$CH_3CH_2CH_2OH + CH_3OH \rightleftharpoons (CH_3)_2CHCH_2OH + H_2O \qquad K_4$$

Scheme 1. Higher alcohol synthesis with H_2O rejection
The first-pass results obtained are shown below by computing the equilibrium concentrations of alcohols obtained from converting 70 mol% CO and 30 mol% H_2. Plots for 1 and 100 bar are represented in Figures 3.2.7 and 3.2.8, respectively.

Figure 3.2.7 Plot of Mol Fraction of Alcohols vs Temperature at 1 Bar with H_2O Rejection

Figure 3.2.8 Plot of Mol Fraction of Alcohols vs Temperature at 100 Bar With H_2O Rejection

The same approach was applied toward the reactions in Scheme 2. Here, however, CO_2 is rejected instead of H_2O for oxygen removal.

$$CO + 2H_2 \rightleftharpoons CH_3OH \qquad\qquad K_1$$

$$CH_3OH + 2CO + H_2 \rightleftharpoons CH_3CH_2OH + CO_2 \qquad\qquad K_5$$

$$CH_3CH_2OH + 2CO + H_2 \rightleftharpoons CH_3CH_2CH_2OH + CO_2 \qquad\qquad K_6$$

$$CH_3CH_2CH_2OH + CH_3OH \rightleftharpoons (CH_3)_2CHCH_2OH + H_2O \qquad\qquad K_4$$
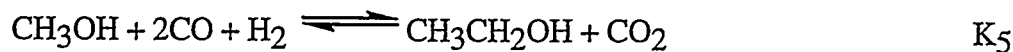
Scheme 2. Higher alcohol synthesis with CO_2 rejection

Plots for 1 and 100 bar are represented in Figures 3.2.9 and 3.2.10, respectively.

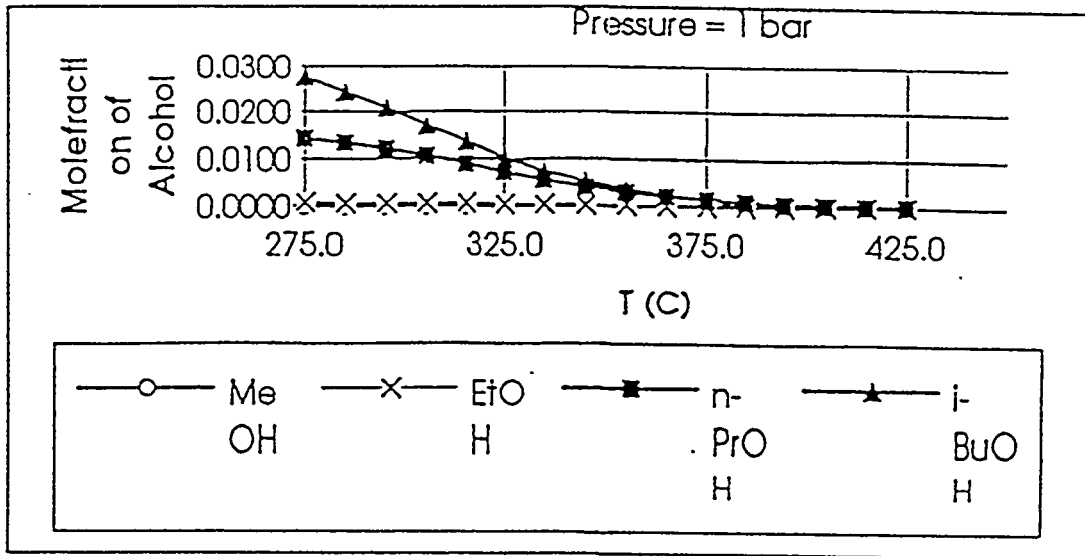**Figure 3.2.9 Plot of Mol Fraction of Alcohols vs Temperature at 1 Bar With CO_2 Rejection**
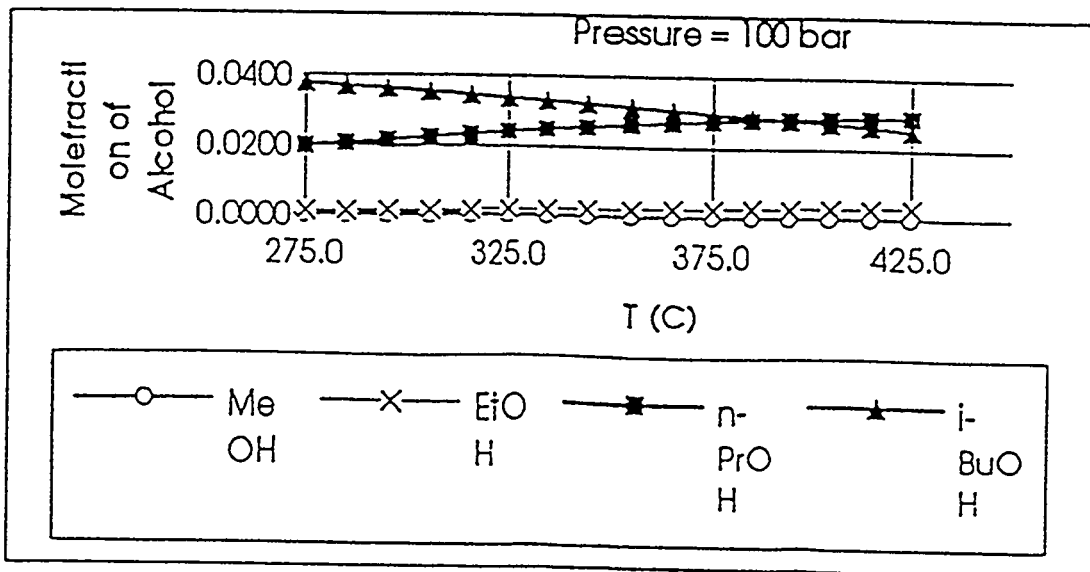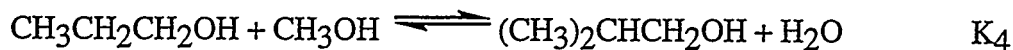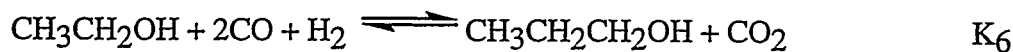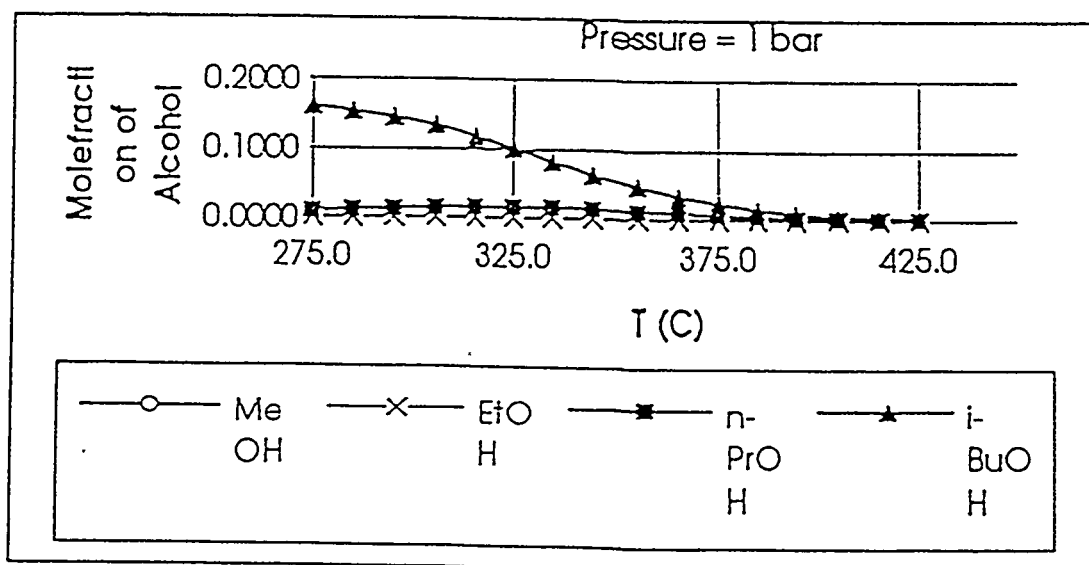
Figure 3.2.10 Plot of Mol Fraction of Alcohols vs Temperature at 100 Bar with CO_2 Rejection
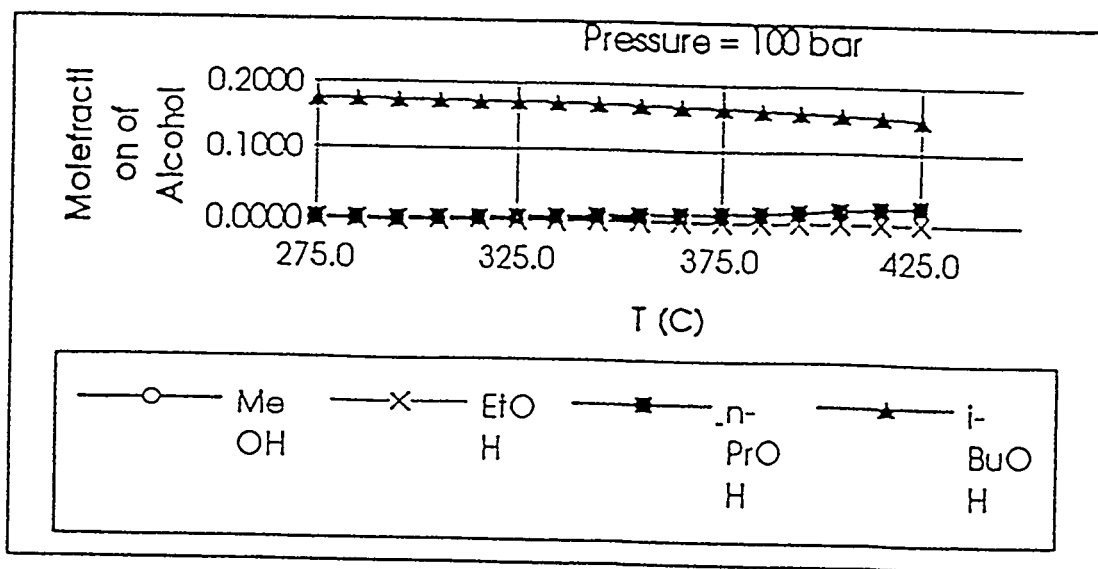
The plots are revealing, especially the difference between H_2O and CO_2 rejection. No methanol is observed in all cases, even at the higher pressures. The chemical pathways were fixed (see Scheme 1 and 2). In all the plots the remaining mol fractions are CO and H_2. In general it can be seen that the higher pressure favors a higher mol fraction of alcohols. Comparison of the 100 bar plot for H_2O and CO_2 rejections reveals a marked difference, that is, isobutanol is dramatically favored.

If these calculations resemble any approximation to the true thermodynamic picture, does this suggest that any catalyst for HAS should also have built in shift activity.

3.2.3 4Q FY95 Objectives

Future plans for Task 3.2 will focus on the following areas:

- continue to screen immobilized catalyst candidates for hydrocarbonylation of dimethyl ether to ethylidene diacetate.

- continue catalyst development work on the cracking of ethylidene diacetate to vinyl acetate and acetic acid.

Task 3.3 New Processes for Alcohols and Oxygenated Fuel Additives

3.3.1 Isobutanol Synthesis in a Three Phase System (RWTH Aachen)

Fixed Bed Reactor Design and Runs

The problem of methanization was solved. The activity toward methane was in the same low range W. Falter mentioned. His STY to isobutanol could be reproduced with an additional amount of methanol (Table 3.3.1).

Table 3.3.1 Comparison of Catalytic Results

Run	WF 77 /thesis p. 143	CH 51-10	CH 51-11
Temperature [°C] Pressure [MPa] GHSV [h^{-1}]	423 25 20000	415 25 20000	400 25 20000
Conversion CO [%]	22	33	31
Selectivity CO_2 [%]	46	24	20
STY [gl^{-1}h^{-1}] Methane Methanol Isobutanol	 40 340 355	 45 1095 414	 < 30* 1390 360

* below the minimum registration value
Catalyst: $ZrO_2/ZnO/MnO/K_2O$ (pH 9)

To obtain these results it was necessary to enlarge the volume of the filter filled with activated carbon and to change the arrangement of the catalyst in the fixed bed. It was optimal to mix the catalyst particles with only a few glass particles and to fill the remaining five centimeters of the tubular reactor with pure glass particles. This arrangement seemed to make catalyst poisons adsorb onto the surface of the glass particles instead of onto the active site of the catalysts.

Slurry Reactor Design and Runs

The results obtained in the slurry reactor clearly showed external parameter effects. The only intrinsic effect was observed by changing the temperature. The influence of reaction temperature on selectivity in slurry and fixed bed reactors was comparable in a qualitative way.

Decalin was used because of its resistance to hydrogenation and cracking, rendering it suitable for slurry runs. It does not hamper analytical measurements and will be used as inert oil until further notice. A disadvantage of decalin is the very high volatility, which could be compensated through refilling by a high pressure pump. If alternatives are found that show better properties relative to solubility and rate of diffusion of feedstock and products, they will be investigated further.

A temperature of about 160°C for the reflux condenser seems to be a useful compromise. At lower temperatures, the removal of products is hindered, and above 180°C, loss of decalin increases rapidly.

The slurry runs had a catalyst content of about 4 wt%. Two indications for mass transfer limitation were obtained as follows:

1. By increasing stirring speed, the STY to methanol and isobutanol increases remarkably. For example, doubling the stirring speed from 1000 to 2000 rpm increases the STY to methanol by 30%, while isobutanol is also synthesized in notable amounts.

2. STY to methanol and isobutanol is directly proportional to the applied mass flow of feed stock. Doubling GHSV doubles yield products as well. Selectivity and conversion are not affected. Catalyst capacity seems to be under-utilized. By increasing the mass flow, the concentration gradient across the boundary layer is increased, thereby increasing the diffusion rate.

The influence of reaction temperature mentioned earlier for the fixed bed reactor also holds qualitatively for the slurry reactor. In the range of 400°C, the STY of isobutanol and methane increase and decrease, respectively. Quantitatively, the activity for the slurry reactor is less than that for the fixed bed reactor (Table 3.3.2):

Table 3.3.2 Comparison of STY in Two Different Reactors

STY [g/(l*h)]	slurry reactor	fixed bed reactor
isobutanol	130	540
methanol	800	1500
isobutanol/methanol	0.16	0.36

At the same measured temperature in both reactors, the selectivity to isobutanol by the slurry reactor is lower. The following reasons for this behavior can be assumed:

1. By reducing the size of the catalyst particles as well as back mixing in the slurry reactor, heat transport is improved. The temperature rise at the active sites of the catalyst in the slurry is lower compared with the fixed bed. Thus, the temperature necessary for the synthesis of isobutanol is not reached.

2. The mass transfer limitation mentioned above may cause a shift of activity towards the different products.

Catalyst Preparation and Screening
Besides transferring the syngas conversion to isobutanol from a fixed bed into a slurry bed system--the main objective--the search for suitable catalysts under reproducible preparation conditions is ongoing. The latest results with alkaline promoted $ZrO_2/ZnO/MnO$- catalysts showed significant activity towards isobutanol and methanol. In the fixed bed as well as in the .

slurry bed system, the optimum reaction conditions for these catalysts are p > 200 bar, T > 400°C. Therefore the main objective of current research has to be understanding and optimizing this catalyst type and related ones in order to achieve milder reaction conditions.

Alkali Impregnation of Coprecipitated Catalysts

First results of this work have been presented in the last quarterly report. So far as the $ZrO_2/ZnO/MnO$- type catalysts precipitated at different pH- values have been investigated, the major difference is in the alkali content. As described in the last report, a large number of alkali free coprecipitated catalysts have been prepared and impregnated with defined amounts of potassium compounds. The following set of catalysts (Table 3.3.3) will be tested:

Table 3.3.3 Coprecipitated Catalysts of the $ZrO_2/ZnO/MnO$- Type

	Precipitation pH = 9	Precipitation pH = 11	Precipitation pH = 11 + 0.25 wt. % Pd
Potassium / wt. %	0.0	0.0	0.0
		0.5	0.5
	1.0	1.0	1.0
		2.0	2.0
	3.0	3.0	3.0
		4.0	4.0

calcination temperature = 450°C

This set of catalysts will clarify the influence of the pH of precipitation, the alkali content and the palladium impregnation. If these runs are successful, further catalysts will be prepared in order to investigate effects of different first and second main group bases and different transition metals like copper, platinum or rhodium.

Sol-Gel Based Catalysts

To elucidate the scope and limits of the $ZrO_2/ZnO/MnO$ system for isobutanol synthesis, different synthesis procedures are being investigated. Among others a relatively new and promising route is formed by the sol-gel method as was already pointed out in the last quarterly report. Sol-gel preparation initially involves the formation of a sol (ideally consisting of a viscous clear solution) followed by formation of a gel. Generally metal alkoxides are used as starting materials that form gels in which an oxide network is progressively built via inorganic polymerization reactions. Using this procedure one can obtain mesoporous zirconium oxide with high surface areas and narrow pore size distributions. The objective of the present work is the introduction of zinc and manganese precursors without sacrificing the beneficial properties of the zirconium oxide network.

Depending on the reaction conditions, the product of a sol-gel reaction may be a precipitate, a colloid, a sol or a gel. For clarity, a gel can be defined as a clear, three dimensional oxide network in which the solvent fills the pores.

Control of hydrolysis and condensation reaction rates can be influenced by the addition of complexing agents such as acetic acid or acetylacetone. In addition one can differentiate between acid and base catalyzed sol-gel reactions. Under acidic conditions, hydrolysis occurs at a faster rate than condensation, and the resulting gel is weakly branched. Condensation is accelerated relative to hydrolysis with increasing pH. Thus, a base-catalyzed gel is highly branched and contains colloidal aggregates. In this way the pore structure (surface area, pore volume and pore size distribution) can be tuned. The influence of the above described parameters on the formation of a multicomponent gel has been investigated. The wet gels were transformed into so-called aerogels via supercritical drying in an autoclave. These materials will be impregnated with defined amounts of potassium compounds, and tests will be performed in the near future. Future work will also include the preparation of different zirconia supports impregnated with zinc and manganese precursors.

Catalyst Screening

For catalyst screening a large number of test runs under reproducible reaction conditions are necessary. However, attempts to do this in a discontinuous way by using batch autoclaves failed. Catalysts that showed significant differences towards activity and selectivity in a continuous system behave nearly identically to each other in discontinuous runs.

In order to screen catalysts parallel to the comparison of the fixed bed and slurry reactions, a second isobutanol unit has been built. This unit is simpler than the existing one. An on-line analysis and process control system have been excluded, but the unit is capable of nearly the same reaction conditions as the first one, that is:

- pressure: 300 bar
- temperature: 500°C
- mass flow: 60 Nl/h.

The fixed bed reactor used in this unit is a U-tube with an outer diameter of 8 mm and an inner diameter of 5 mm. The length of each tube leg is less than 15 cm. The reactor is placed in an oven with a height of 20 cm and an inner diameter of 8 cm. This type of reactor has a very smooth inner surface and is, as well as the rest of the unit, built from stainless steel. The unit has been completed, and first calibration runs are estimated for the middle of July.

Appendix 3.3 Legend to the Flow Scheme

VR	back pressure valve
VH	stop valve
T	drier filled with activated carbon
F	sintered metal filter
VDM	pressure regulator
FIC	thermal mass flow meter
PI	manometer
BS	rapture disc
TIC	jacket thermocouples
Z	cyclone
VB	bubbler
KA-D	multiple coil condenser
GMA-D	gas probe

Flow scheme of the Second Continuous Isobutanol Unit
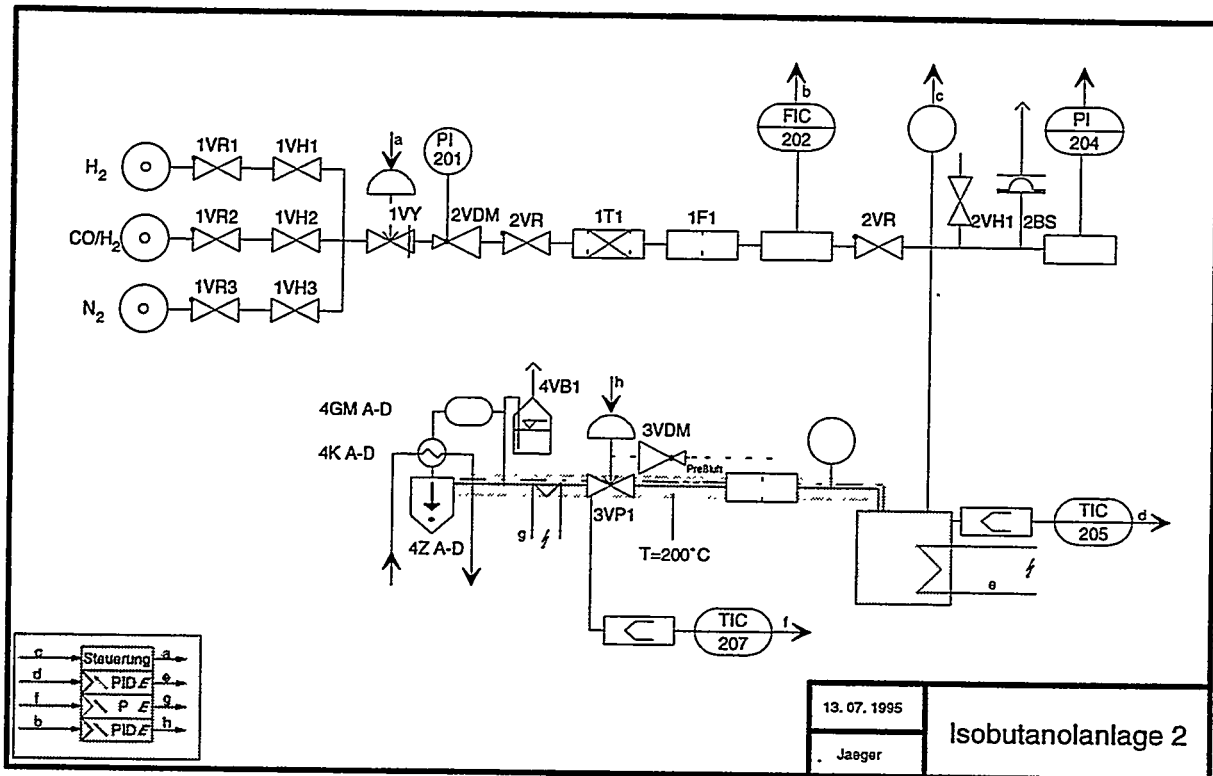
3.3.2 Oxygenates via Synthesis Gas (Lehigh University)

Overall 3QFY95 Objectives

(i) Continue studies of increasing the conversion of H_2/CO to higher alcohols by promotion of the $C_1 \rightarrow C_2$ carbon chain growth step over Cs-promoted $Cu/ZnO/Cr_2O_3$ and MoS_2 catalysts,

(ii) Enhance the $C_2 \rightarrow C_3 \rightarrow C_4$ carbon chain growth steps over $Cs/Cu/ZnO/Cr_2O_3$ catalysts, and

(iii) Prepare and test high surface area Cu/ZrO_2 catalysts, both Cs-doped and undoped, that are candidates for the synthesis of C_1-C_5 alcohols, in particular branched products such as isobutanol.

Results and Discussion
Double Bed Catalyst Studies
As documented in previous reports, the Cs-promoted ternary Cu-based catalyst has been the center of recent kinetic studies of higher alcohol synthesis (HAS), and it is characterized, under optimized HAS operating conditions, by high productivities toward the intermediate species (ethanol (EtOH) and propanol (PrOH)) that lead to isobutanol (2m-PrOH) formation. The $C_1 \rightarrow C_2$ step is the slow synthesis step, and the EtOH is rapidly converted to PrOH and subsequently to 2m-PrOH. With an increase in the reaction temperature to at least 340°C, enhanced levels of ethanol and propanol are converted to isobutanol (and other terminal branched products). However, at this high temperature, the Cu-based catalyst tends to deactivate within a short period (150 hr).

An alternative approach to the enhancement of ethanol and propanol conversion to isobutanol is represented by the coupling of the low temperature Cu-based catalyst to a high-temperature catalyst, that is, the commercial Cu-free ZnO/Cr_2O_3 catalyst. During this quarter, double-bed experiments were designed and performed using a series configurations in which the Cs-doped $Cu/ZnO/Cr_2O_3$ catalyst occupied the top layer in the downflow reactor and was kept at a temperature of ≤325°C, and a Cs-doped ZnO/Cr_2O_3 catalyst occupied the lower layer where the temperature was kept at ≥400°C. The reactor is described in greater detail later in this report.

Preparation of the Catalysts. A single sample of the commercial ZnO/Cr_2O_3 catalyst (Harshaw Zn-0311 T 1/4") was broken, sieved to 0.85-2.0 mm particles that were calcined under N_2 at 400°C for 4 hr, and doped with CsOOCH. The calcined catalyst was added to a N_2-purged aqueous solution of CsOOCH, which was then slowly evaporated under flowing N_2 at 50°C. The dried catalyst was recalcined at 350°C for 3 hr. The composition of the catalyst corresponded to 4 mol% $CsOOCH/ZnO/Cr_2O_3$, which was not determined to be an optimized level of the promoter. By X-ray powder diffraction (XRD), it was shown that the catalyst consisted of crystalline $ZnCr_2O_3$ with spinel-like structure and microcrystalline ZnO. Reduction of the catalyst was carried out at 450°C under a flowing $H_2/N_2 = 2/98$ vol% mixture (60 ml/min) at ambient pressure. The temperature was decreased and the reduction terminated when the quantity of

68

water generated by reduction of the catalyst, as monitored by gas chromatography (GC), decreased significantly.

The $Cs/Cu/ZnO/Cr_2O_3$ was prepared by using the same doping procedure with a $CuO/ZnO/Cr_2O_3$ = 30/45/25 mol% catalyst that was prepared by coprecipitation of a hydrotalcite-like precursor calcined using a step-wise procedure to 350°C, which was maintained for 3 hr. The composition of the doped catalyst corresponded to 3 mol% $CSOOCH/CuO/ZnO/Cr_2O_3$. Reduction was carried out at 250°C using the procedure described above.

Catalyst Testing. Catalyst testing was carried out in a tubular down-flow fixed-bed reactor. A schematic description of the catalyst testing system is provided in Figure 3.3.1. Special arrangements were made to minimize the formation of iron carbonyl formed by contact of CO with iron-containing surfaces. The deposition of iron from $Fe(CO)_5$ over the Cu-based catalyst sites is in fact known to cause irreversible deactivation. Charcoal and molecular sieve traps were employed for filtering the CO stream fed from high-pressure stainless steel tanks, an internally copper-lined stainless steel reactor and copper thermocouple wells for the reading of the catalyst temperature were adopted, and a water cooling system was used to keep the temperature of the stainless steel tubing upstream from the reactor below 65°C. Indeed, elemental analysis of tested catalysts (500 hr on stream) indicated iron content <60 ppm.

In the case of the single-bed experiments, 2.0 g of each catalyst was diluted with 0.5 mm Pyrex beads to a total volume of about 7.0 ml. The bed (about 7 cm long) was placed in the center of the reactor tube (1.9 cm I.D. and 55 cm long), using 3.0 mm Pyrex beads as packing material upstream and downstream. In the case of the double-bed experiments, 1.0 g of each catalyst was diluted with the Pyrex beads up to a 4.0 ml volume. As indicated in Figure 3.3.2, the $Cs/Cu/ZnO/Cr_2O_3$ bed was loaded in the top portion of the reactor, about 15 cm downstream from the reactor inlet section. The $Cs/Zn/Cr_2O_3$ bed was loaded in the bottom portion of the reactor at a distance of about 20 cm below the first bed. The temperatures of the beds were monitored by use of two independent thermocouples, a copper-thermocouple well being connected to each reactor end.

The catalyst pretreatments in the double-bed reactor required a step-wise procedure. Initially, the Cu-based catalyst was reduced by heating the top portion of the reactor at 250°C under flowing H_2/N_2 mixture, while the bottom portion of the reactor was kept unheated. When the reduction was completed, the first bed was cooled to room temperature under flowing N_2. Subsequently, the treatment of the zinc chromite catalyst was carried out by heating the bottom portion of the reactor to 450°C under a flowing H_2/N_2 mixture. During this phase, in order to "protect" the Cu-based catalyst from possible Cu sintering or over-reduction, the temperature of the first bed was kept below 70°C by means of an external water circulating system.

The gas stream fed to the synthesis reactor consisted of a mixture of H_2, CO, and N_2, where separate lines for H_2 and CO allowed for easily varying the H_2/CO molar ratio (N_2/CO = 5/95 mol% in each experiment). Nitrogen behaved as an inert in the reacting system and provided an

Figure 3.3.1 Schematic of the Catalyst Testing Unit

70
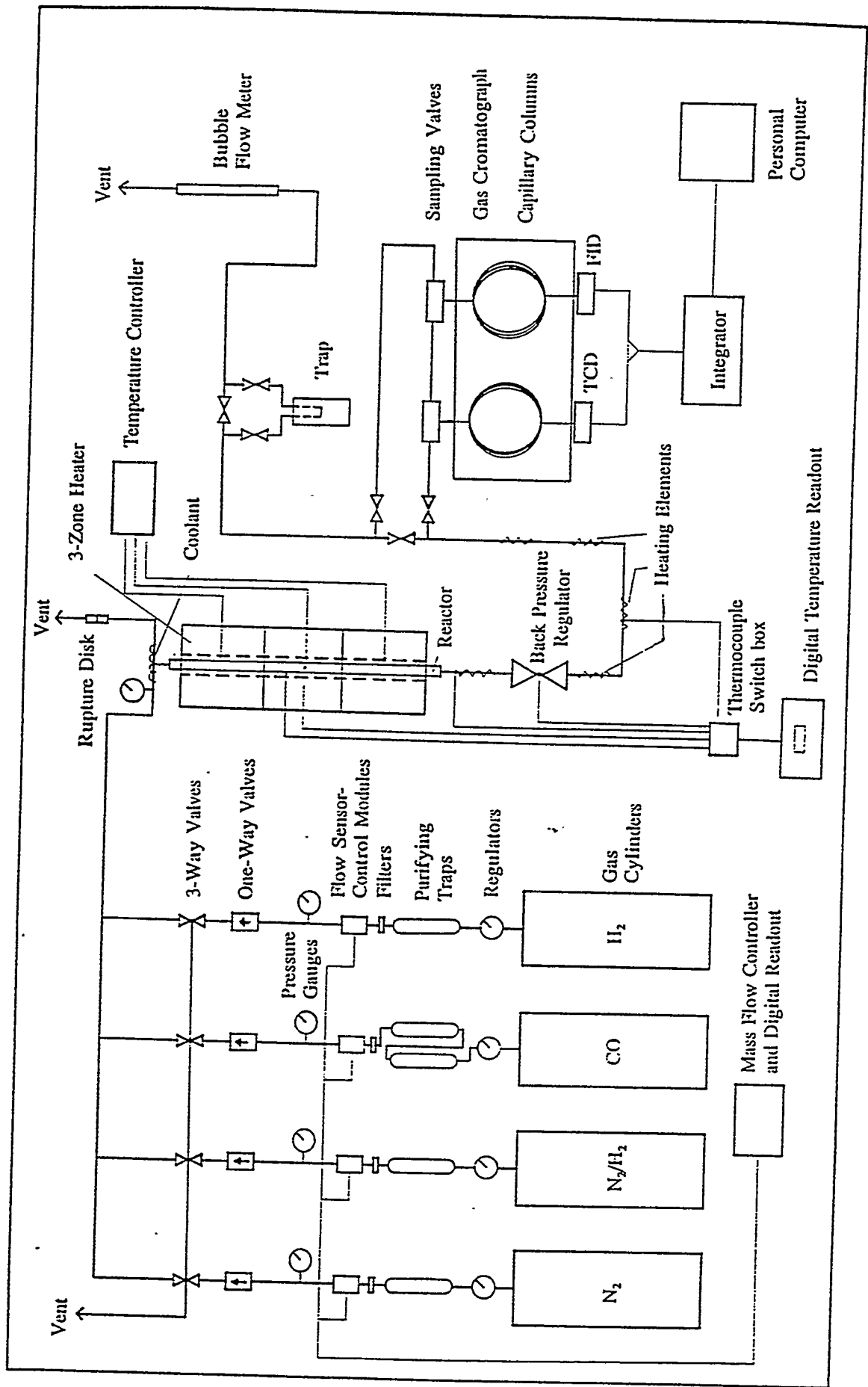
Figure 3.3.2 Scaled Drawing of the Copper-Lined Synthesis Reactor used in the Double-Bed Experiments. Note that the water circulating system was employed during the catalyst reduction treatments, but it was removed during the activity testing experiments. The same cooling system was used during the testing of the single bed 3 mol % $Cs/Cu/ZnO/Cr_2O_3$ catalyst to maintain the temperature of the stainless steel tubing upstream from the reactor below 65°C.

Cu Thermocouple Well, o.d. 3.2 mm

INLET

Rupture Disk / Vent

Stainless-steel
Swagelock Fittings

H_2O Circulating System:
Cu tube, o.d. 3.2 mm

Furnace

Heater 1

140 mm

Quartz wool

3% $Cs/Cu/ZnO/Cr_2O_3$
+ 0.5 mm Pyrex beads

40 mm

220 mm

Heater 2

12 mm

4% $Cs/ZnO/Cr_2O_3$
+ 0.5 mm Pyrex beads

40 mm

520 mm

Heater 3

3 mm Pyrex beads

OUTLET

Reactor:
SS tube, o. d. 19 mm, i. d. 14 mm
+ 1 mm internal Cu lining

Cu Thermocouple Well, o.d. 3.2 mm
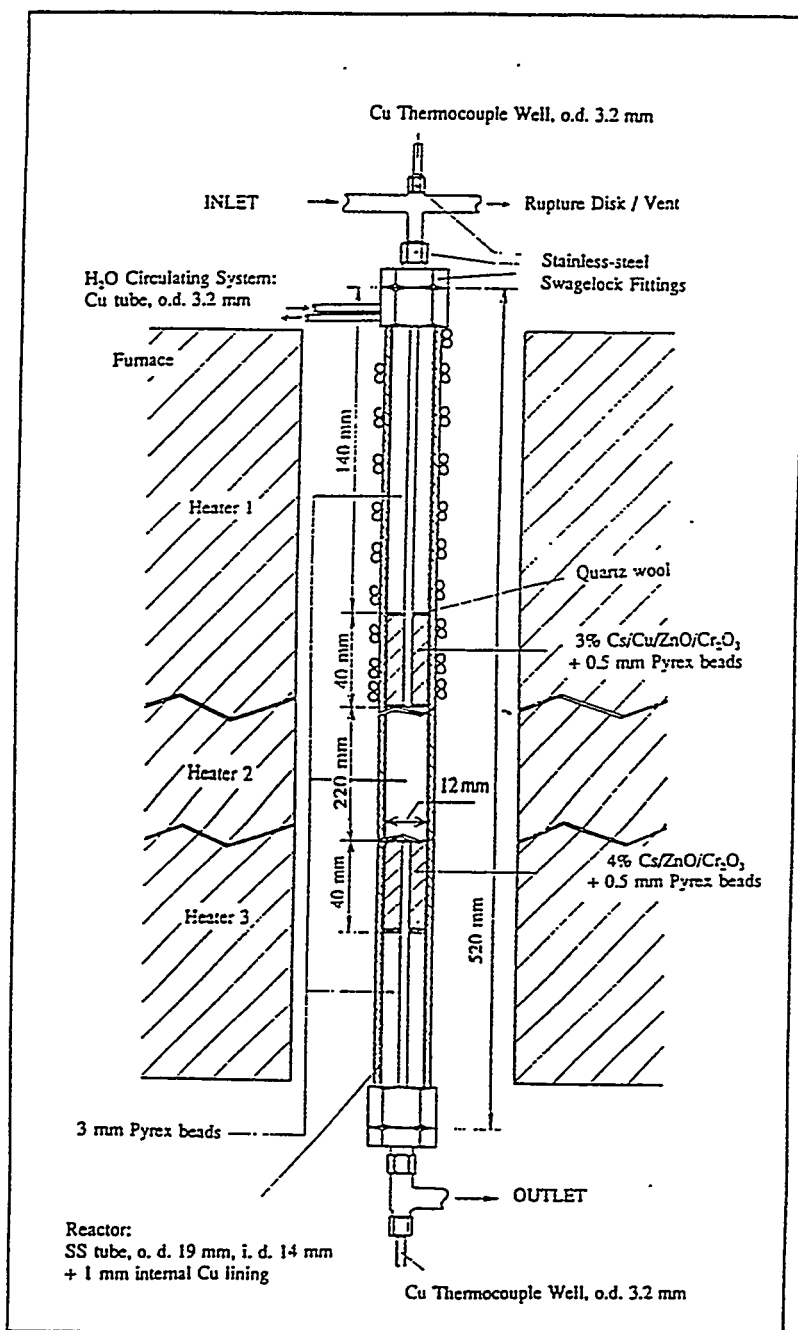
internal standard for the evaluation of the product yields. The kinetic runs carried out over the Cs/Cu/ZnO/Cr$_2$O$_3$ catalyst ranged over the following windows of operating variables: T = 310-340°C, P = 6.5-7.6 MPa, H$_2$/CO = 0.45-3.5, gas hourly space velocity (GHSV) = 3,300-18,375 l(STP)/kg cat/hr. The activity tests over the Cs/ZnO/Cr$_2$O$_3$ catalyst and the double-bed experiments were carried out at constant pressure (7.6 MPa) and synthesis gas composition (H$_2$/CO = 0.75), while the GHSV was varied in the range of 5,450-18,375 l(STP)/kg cat/hr. Over the zinc chromite catalyst, a constant temperature of 405°C was maintained. In the double-bed experiments, the first and second beds were kept at 325 and 405°C, respectively. In each experiment, the set of conditions was maintained for a period of 24 hr.

Quantitative Product Analysis. The reactor outlet stream was sampled every 20-60 min using an on-line automated heated sampling valve and analyzed by a Hewlett-Packard 5390 gas chromatograph. The analyses were quantified and averaged for evaluation of product yields and selectivities after a steady-state activity was reached (about 6 hr from the initial setting of the operating conditions). A Molsieve capillary column was used to separate N$_2$, CH$_4$ and CO. The column was connected to a thermal conductivity detector (TCD). The CO/N$_2$ and CH$_4$/N$_2$ molar ratios were applied as follows to evaluate CO conversion and methane production:

$$\%CO \text{ conversion} = 1 - (CO/N_2)_{outlet}/(CO/N_2)_{inlet}$$
$$CH_4 \text{ productivity} = CH_4/N_2 * N_2 \text{ Molar Flow} * MW_{CH4} \quad (g/kg \text{ cat/h})$$

Knowledge of methane productivity provided for the quantification of the oxygenates and hydrocarbons separated in a capillary CP13 column and analyzed by a flame ionization detector (FID). The same column was temporarily connected to the TCD to determine CO$_2$ and H$_2$O yields. The FID response factors were determined by a thorough calibration of the instrument, resulting in significant deviations from the literature data. The identification of products was based on comparison of the retention times with those of known standards and on fragmentation patterns obtained from analyses of liquid samples by a Hewlett-Packard gas chromatograph/mass spectrometer. Carbon balances were calculated in each experiment by comparing the overall amount of carbon detected in the outlet product mixture with the measure of CO conversion; relative errors were always lower than 10%.

Experimental Results. The catalysts were systematically tested at three different GHSV conditions while the other reaction parameters were maintained constant. Comparisons of the CO conversions and product space time yields of the double bed catalyst system with the single bed catalysts are given in Tables 3.3.4 and 3.3.5 for GHSV = 5450 and 18,375 l/kg cat/hr, respectively. The mol% CO conversion is expressed as the total quantity of CO converted to products, including CO$_2$.

Comparisons of the data in Table 3.3.4 (GHSV = 5450 l/kg cat/hr) show that:

- While the 3 mol% Cs-promoted Cu/ZnO/Cr$_2$O$_3$ catalyst provided high productivities to methanol, ethanol, and propanol, the 4 mol% Cs-doped commercial high-temperature ZnO/Cr$_2$O$_3$ catalyst exhibited a low selectivity to methanol (due to the chemical equilibrium

of methanol synthesis) and very low productivities to ethanol and propanol, which are efficiently converted to isobutanol (due to the higher reaction temperature).

- In the coupled double-bed configuration, a synergism between the two catalysts was obtained. This synergism resulted in enhanced productivities to isobutanol (47% incremental increase with respect to the single low temperature Cu-based catalyst and 94% incremental increase with respect to the single high-temperature catalyst). As expected, the coupling allowed the efficient conversion of ethanol and propanol "intermediates" formed over the top Cu-based catalyst to form the terminal isobutanol over the bottom layer of Cu-free high temperature catalyst.

- Due to the increased reactor exit temperature, the productivity of methanol over the double-bed catalyst system was much lower than that over the single Cu-based catalyst. This consequently resulted in a much improved isobutanol/methanol molar ratio (1.0/11.8 for the single $Cs/Cu/ZnO/Cr_2O_3$ catalyst and 1.0/1.7 for the double-bed catalyst configuration). The lower quantity of methanol produced in the double-bed system resulted from partial decomposition of the methanol formed over the first bed to $CO + H_2$ over the second high temperature bed.

The experimental results shown in Table 3.3.5 (GHSV = 18,375 l/kg cat/hr) confirm the concept of using a double-bed catalyst system, with each of the catalyst beds at different temperatures to optimize the chemical syntheses occurring over each. It was noted that at high space velocity, very high productivities to isobutanol can be obtained. In fact, the overall productivity of the C_4-C_6 2-methyl iso-alcohols is nearly 200 g/kg cat/hr. It was also noted that some 20% of the C_7 oxygenates formed over the double-bed catalysts at both gas velocities consisted of 2-methyl-1-hexanol.

The double-bed catalysts were also tested at GHSV = 12,000 l/kg cat/hr, and it was observed that the CO conversion levels and the product space time yields fell between those obtained at the lower and higher GHSV results shown in Tables 3.3.4 and 3.3.5. A comparison of the results obtained over the double-bed catalysts at the three reactant flow rates is shown in Table 3.3.6, where the CO conversion is expressed on the basis of CO_2-free products.

In these experiments, quantities of ketones and aldehydes were observable. In Tables 3.3.4-3.3.6, these products are grouped with the corresponding alcohol products. Methyl esters are also formed but are not included in the tables. Of particular interest is the observation that no significant increase in the formation of methane was observed over the double-bed configuration with respect to the single-bed Cu-based catalyst, although some increase in the formation of higher hydrocarbons was evident. However, at the lower H_2/CO molar ratio of 0.45, Table 3.3.7 gives an indication of the side products formed during alcohol synthesis over the single bed low temperature catalyst.

The 3 mol% $Cs/Cu/ZnO/Cr_2O_3$ catalyst was retested at 310°C and 7.6 MPa with $H_2/CO = 0.45$. The GHSV utilized was 5500 l/kg cat/hr instead of 5450 l/kg cat/hr. Nearly identical results were obtained, except the methanol space time yield was 250 g/kg catal/hr (compare with Table 3.3.7).

Table 3.3.4 Kinetic Runs over a 3% Cs Cu/ZnO/Cr$_2$O$_3$ Catalyst and a 4% Cs Zn/Cr$_2$O$_3$ Catalyst (first and second column, respectively). The results are compared with the performances obtained by coupling the two catalysts (third column) in a double-bed experiment (top bed = 3% Cs Cu/ZnO/Cr$_2$O$_3$, bottom bed = 4% Cs Zn/Cr$_2$O$_3$).

Operating conditions:

     3% Cs Cu/ZnO/Cr$_2$O$_3$:   T = 325°C, P = 7.6 MPa, H$_2$/CO = 0.75,
GHSV = 5450 l/kg cat/hr

     4% Cs Zn/Cr$_2$O$_3$:   T = 405°C, P = 7.6 MPa, H$_2$/CO = 0.75,
GHSV = 5450 l/kg cat/hr

     Double-bed run: T$_{TOP\ BED}$ = 325°C, T$_{BOTTOM\ BED}$ = 405°C, P = 7.6 MPa, H$_2$/CO = 0.75,
GHSV = 5450 l/kg cat tot/hr

	Cs/Cu/ZnO/Cr$_2$O$_3$ (g/Kg cat/hr)	Cs/Zn/Cr$_2$O$_3$ (g/Kg cat/hr)	Cs/Cu/ZnO/Cr$_2$O$_3$ + Cs/Zn/Cr$_2$O$_3$ (g/Kg cat/hr)
MeOH	268.0	52.8	56.5
EtOH	20.0	0.77	1.07
PrOH	38.8	3.82	6.52
BuOH	6.55	0.29	1.36
PentOH	2.8	0.17	1.15
2m-PrOH	52.08	39.54	76.79
2m-BuOH	10.93	4.26	16.22
2m-PentOH	4.816	2.44	8.88
2-BuOH	4.50	1.84	1.02
3m-2-BuOH	5.00	0.46	2.77
3-PentOH	4.18	0.38	2.33
2m-3-PentOH	7.40	2.93	10.5
C$_{7+}$ oxygenates	47.80	51.8	55.4
CH$_4$	11.05	2.82	10.56
C2+ hydrocarbons	8.17	10.89	13.23
% CO conversion	30.64%	12.03%	18.70%

Table 3.3.5 Kinetic Runs over a 3% Cs Cu/ZnO/Cr$_2$O$_3$ Catalyst and a 4% Cs Zn/Cr$_2$O$_3$ Catalyst (first and second column, respectively). The results are compared with the performances obtained by coupling the two catalysts (third column) in a double-bed experiment (top bed = 3% Cs Cu/ZnO/Cr$_2$O$_3$, bottom bed = 4% Cs Zn/Cr$_2$O$_3$).

Operating conditions:

   3% Cs Cu/ZnO/Cr$_2$O$_3$:   T = 325°C, P = 7.6 MPa, H$_2$/CO = 0.75,
GHSV = 18375 l/kg cat/hr

   4% Cs Zn/Cr$_2$O$_3$:   T = 405°C, P = 7.6 MPa, H$_2$/CO = 0.75,
GHSV = 18375 l/kg cat/hr

   Double-bed run: T$_{TOP\ BED}$ = 325°C, T$_{BOTTOM\ BED}$ = 405°C, P = 7.6 MPa, H$_2$/CO = 0.75,
GHSV = 18375 l/kg cat tot/hr

	Cs/Cu/ZnO/Cr$_2$O$_3$ (g/Kg cat/hr)	Cs/Zn/Cr$_2$O$_3$ (g/Kg cat/hr)	Cs/Cu/ZnO/Cr$_2$O$_3$ + Cs/Zn/Cr$_2$O$_3$ (g/Kg cat/hr)
MeOH	1200.0	173.4	178.80
EtOH	68.70	2.75	7.05
PrOH	83.20	11.49	23.54
BuOH	15.23	0.95	4.18
PentOH	9.61	0.62	3.09
2m-PrOH	65.60	74.13	138.82
2m-BuOH	21.04	8.35	32.96
2m-PentOH	14.4	5.28	21.71
2-BuOH	9.68	2.5	5.17
3m-2-BuOH	10.17	0.94	7.22
3-PentOH	10.24	1.21	7.71
2m-3-PentOH	16.02	5.54	23.14
C$_{7+}$ oxygenates	67.50	78.0	105.5
CH$_4$	10.4	4.14	12.06
C2+ hydrocarbons	6.00	15.79	24.02
% CO conversion	14.65%	6.30%	11.71%

Table 3.3.6 Productivities and CO Conversions Observed for High Alcohol Synthesis with $H_2CO = 0.75$ Synthesis Gas at 7.6 MPa over the Double Bed 3 mol% $Cs/Cu/ZnO/Cr_2O_3$ and 4 mol% $Cs/ZnO/Cr_2O_3$ Catalysts under the Following Operating Conditions:

Top Bed: 3 mol% $Cs/Cu/ZnO/Cr_2O_3$ (1 g), 325°C

Bottom Bed: 4 mol% $Cs/ZnO/Cr_2O_3$ (1 g), 405°C.

The productivities of aldehydes and ketones have been added to those of the primary and secondary alcohols, respectively.

	GHSV = 5,450 l(STP)/kg cat/h (g/kg cat/h)	GHSV = 12,000 l(STP)/kg cat/h (g/kg cat/h)	GHSV = 18,375 l/(STP)/kg cat/h (g/kg cat/h)
MeOH	56.5	114.3	178.8
EtOH	1.1	3.9	7.0
PrOH	6.5	18.7	23.5
BuOH	1.3	3.3	4.2
PentOH	1.1	2.3	3.1
HexOH	1.3	1.9	2.3
2m-PrOH	76.8	114.6	138.8
2m-BuOH	16.2	27.1	32.9
2m-PentOH	8.9	16.0	21.7
2m-HexOH	7.5	17.4	24.0
2-BuOH	1.0	4.4	5.2
3m-2-BuOH	2.8	6.9	7.2
3-PentOH	2.3	6.8	7.7
2m-3-PentOH	10.5	19.7	23.1
MF	6.1	8.9	11.3
MAC	2.1	2.0	1.7
DME	2.9	4.4	4.8
C_{7+} oxygenates	46.9	135.5	81.5
CH_4	10.5	12.4	12.0
C_2-C_4 hydrocarbons	17.0	25.6	28.0
% CO conv.(CO2 free)	12.0%	9.4%	6.6%

76

Table 3.3.7 Product Distribution Observed over the 3 mol% Cs/Cu/ZnO/Cr$_2$O$_3$ Catalyst with H$_2$/CO = 0.45 Synthesis Gas at 310°C, 7.6 MPa, and with GHSV = 5,450 l(STP)/kg cat/hr. MeOH = methanol, EtOH = ethanol, PrOH = 1-propanol, BuOH = 1-butanol, PentOH = 1-pentanol, HexOH = 1-hexanol, 2m-PrOH = 2-methyl-1-propanol, 2m-BuOH = 2-methyl-1-butanol, 2m-PentOH = 2-methyl-1-pentanol, 2m-HexOH = 2-methyl-1-hexanol, 2-PrOH = 2-propanol, 2-BuOH = 2-butanol, 3m-2-BuOH = 3-methyl-2-butanol, 3-PentOH = 3-pentanol, 2m-3-PentOH = 2-methyl-3-pentanol, MF = methyl formate, MAC = methyl acetate, MPR = methyl propionate, MiBu = methyl isobutyrate, and MBU = methyl butyrate.

Species	Productivity (g/kg cat/h)	Species	Productivity (g/kg cat/h)
Primary Alcohols:		Methyl Esters:	
MeOH	231.0	MF	8.3
EtOH	22.3	MAC	7.4
PrOH	28.6	MBR	5.6
BuOH	6.1	MiBU	6.7
PentOH	1.3	MBU	2.8
HexOH	1.0		
2m-PrOH	28.0	Hydrocarbons:	
2m-BuOH	5.0	Methane	5.1
2m-PentOH	1.5	Ethene	0.02
2m-HexOH	1.5	Ethane	5.9
		Propene	0.1
Secondary Alcohols:		Propane	1.8
		Buta(e)nes	1.7
2-PrOH	0.1	Penta(e)nes	0.6
2-BuOH	1.5	Hexa(e)nes	0.6
3m-2-BuOH	2.9		
3-PentOH	2.1		
2m-3-PentOH	1.8	Others:	
		DME	1.8
Aldehydes:		C$_{7+}$ oxygenates	22.5
Acethaldehyde	0.7		
Propanaldehyde	1.1		
Isobutanaldehyde	0.9	CO$_2$	638.2
Ketones:			
Acetone	0.2	H$_2$O	3.4
2-Butanone	1.5		
3m-2-Butanone	1.7		
3-Pentanone	1.9	% CO conversion	20.2%
2m-3-Pentanone	3.0		

The 4 mol% Cs/ZnO/Cr$_2$O$_3$ catalyst was tested with GHSV = 12,000 l/kg cat/hr while all other reaction conditions were maintained constant for this high temperature catalyst (see Tables 3.3.4 and 3.3.5). The observed product space time yields are given in Table 3.3.8, in which the total CO conversion corresponds to 7.0%. Again, it is notable that the productivity of the linear C$_2$-C$_6$ alcohols was much lower over the high temperature Cu-free catalyst than over the Cu-based catalysts (see Tables 3.3.4, 3.3.5, and 3.3.7). As expected, the space time yields of methanol and isobutanol are between those at higher and lower GSVS, which are given in Tables 3.3.4 and 3.3.5.

Table 3.3.8 Space Time Yields (g/kg catal/hr) of Higher Alcohols and Other Products over the 4 mol% Cs/ZnO/Cr$_2$O$_3$ Catalyst at 405°C and 7.6 MPa from H$_2$/CO = 0.75 Synthesis Gas with GHSV = 12,000 l/kg catal/hr. The small quantities of aldehydes and ketones formed over this catalyst have been added to the productivities reported for the parent alcohols.

Product*	12,000 l/kg catal/hr
MeOH	132.8
EtOH	2.1
PrOH	8.7
BuOH	0.8
PentOH	0.5
HexOH	0.2
2m-PrOH	69.1
2m-BuOH	7.9
2m-PentOH	7.0
2m-HexOH	0.7
2-BuOH	1.2
3m-2-BuOH	0.9
3-PentOH	0.7
2m-3-PentOH	5.4
Methylformate	1.2
Methylacetate	0.8
DME	4.5
C$_{7+}$ Oxygenates	79.1
CH$_4$	3.9
C$_2$-C$_4$ HC	15.0
%CO Conv.$_{(CO2-free)}$	4.9

*m = methyl. CO$_2$ and H$_2$O are also formed but are not listed.

Cu/ZrO₂ Catalysts

Zirconia-based catalysts are being investigated for their potential as alcohol synthesis catalysts. A series of CuO/ZrO_2 catalysts having different Cu/Zr molar ratios were prepared by aqueous coprecipitation at constant pH and temperature, as described in the previous quarterly progress report.

Initial testing of zirconia-supported copper catalysts for alcohol synthesis from H_2/CO synthesis gas employed a $CuO/ZrO_2 = 10/90$ mol% catalyst. The catalyst was calcined at 350°C for 3 hr, was X-ray amorphous, and had an initial surface area of 149 m²/g. After the catalyst (2 g mixed with Pyrex beads for dilution) was loaded into the reactor, it was reduced in flowing 2 vol% H_2/N_2 at 330°C for 4 hr at ambient pressure.

This unpromoted Cu/ZrO_2 catalyst was tested under both methanol synthesis conditions for comparison with the Cu/ZnO catalyst ($H_2/CO = 2.33$) and higher alcohol synthesis conditions ($H_2/CO = 0.45$). The levels of CO conversion were rather low, and the space time yields of the products observed are given in Table 3.3.9. It is clear that methanol and dimethylether were the dominant products formed over this catalyst under the reaction conditions employed. At the higher temperatures, small quantities of higher alcohols were also formed. Comparison of the first and last tests that utilized the same reaction conditions indicated that the catalyst had become more active and more selective toward alcohols during the testing program.

A second catalytic test utilizing a fresh portion of the $CuO/ZrO_2 = 10/90$ mol% catalyst (2.0 g) calcined at 350°C was initiated to determine the reproducibility of the activity and selectivity observed in the first test with this catalyst. The influence of carbon dioxide and of steam in the reactant mixture on the catalytic activity of the Cu/ZrO_2 catalyst will be determined during the next quarter of research and will be reported in the next quarterly progress report.

Overall 4QFY95 Objectives

Future plans for Task 3 will focus on the following areas:

(i)   Continue studies of increasing the conversion of H_2/CO to higher alcohols by promotion of the $C_1 \rightarrow C_2$ carbon chain growth step over Cs-promoted $Cu/ZnO/Cr_2O_3$ and MoS_2 catalysts,

(ii)   Enhance the $C_2 \rightarrow C_3 \rightarrow C_4$ carbon chain growth steps over $Cs/Cu/ZnO/Cr_2O_3$ catalysts, and

(iii)   Prepare and test high surface area Cu/ZrO_2 catalysts, both Cs-doped and undoped, that are candidates for the synthesis of C_1-C_5 alcohols, in particular branched products such as isobutanol.

Table 3.3.9 The Space Time Yields (g/kg catal/hr) of the Products Formed over the 10 mol% Cu/ZrO_2 Catalyst. Testing was carried out at 7.6 MPa with $H_2/CO = 0.45$ and 2.33 and with GHSV = 5500 and 6120 l/kg catal/hr. The %CO converted to products is also given for each test.

GHSV H_2/CO °C Product	6120 2.33 250	6120 2.33 310	5500 0.45 310	5500 0.45 330	5500 0.45 350	6120 2.33 250
MeOH	24.1	50.3	150.0	117.5	82.5	40.4
DME	5.3	70.0	18.0	32.2	43.4	0.4
H_2O		7.6	1.5	2.6	4.2	0.7
MF		0.9			0.8	
EtOH			0.8	0.6	1.0	
PrOH		0.4		3.7	3.3	2.5
i-BuOH				1.7	1.5	
%CO Conv.	1.4	4.8	3.4	3.0	2.7	1.9

3.3.3 Study of Reaction Conditions and Promotion of Group VIII Metals for Isobutanol Synthesis (University of Delaware)

Introduction

The basicity of a dopant compound is thought to be an important variable that can be utilized to beneficially tune the surface properties of promoted catalysts for higher alcohol synthesis. With this in mind, we compared LiOH as a dopant with our previous results on a $LiNO_3$-doped catalyst. The results demonstrated were again that excess alkali-doping did not lead to an enhancement in higher alcohol productivity. In contrast, those results on the effect of pressure and GHSV on higher alcohol synthesis are quite consistent with the literature. Increasing GHSV leads to enhancement of methanol production and suppression of higher alcohol formation. Higher GHSV, that is, lower residence time, decreases the time required for the slow chain propagation step on the surface, thus leading to less higher alcohols. Reaction pressure has similar effects on catalytic performance. Higher pressure shifts the equilibrium toward methanol production. Interesting results were observed in the study of the Group VIII metal promoted catalysts: while most of the metals show little effect on catalytic activity and selectivity, cobalt exhibits significant promotion on activity and stability of the catalysts, which reveals the unique and important role of the minimal amount of cobalt in our catalysts.

Experimental

The LiOH-promoted catalyst was prepared by incipient-wetness impregnation of F6KOHN with a LiOH solution. As reported before, F6KOHN was prepared by KOH precipitation of the mixed-nitrate solution at 60°C (composition: Zr/Cu = 2, Mn/Cu = 0.5, Zn/Cu = 0.5, CoO = 0.2 wt%), calcined at 400°C under nitrogen. The catalyst used in the experiments varying GHSV

and pressure was F6KOHNLi, which was prepared as above except that it was doped with LiNO$_3$. The catalyst precursor for studying Group VIII metal promotion was AF6KOHN, prepared as F6KOHN except that no cobalt was included. The Group VIII metal-promoted catalyst were denoted as MAF6KOHN, where M = Co, Rh, Ir, Fe, Ni, or Pd. The Group VIII metals were impregnated on the catalyst precursor by incipient-wetness method, at a 0.2/wt % level. The solutions used for the impregnations were: an aqueous nitrate solution of cobalt, nickel, or iron; an aqueous ammonium solution of PdCl$_2$; and a CH$_2$Cl$_2$ solution of Rh(CO)$_2$ acac (acetylacetonate) or Ir(CO)$_2$acac, respectively. The alkali-doped or metal-promoted catalysts were dried at 100-130°C overnight (no further calcination) before they were loaded into the reactor.

The standard reaction test procedure used in this study was: catalyst reduction at 260°C with 5%H$_2$/N$_2$ for 24 hours; reaction conditions of 950-1000 psi, CO/H$_2$ = 1, T = 350, 400, 425°C (~ 20 hr at each temperature), and GHSV = 2900/hr. For GHSV and pressure effects tests, the catalyst was run at 350°C, GHSV = 6700/h, and P = 1000 psi for 20 hours first, then at 400°C, GHSV = 6700/hr, and P = 1000 psi for 20 hours. The pressure was then increased to 1400 psi and the catalyst was run for about 20 hours while temperature and GHSV were maintained; finally, the temperature was raised to 425°C and the reaction was carried out for another 20 hours while P = 1400 psi and GHSV = 6700/hr. The reaction data for 600 psi were collected from another set of experiments with fresh catalyst. For all reaction tests, liquid product was released and collected from a condenser (-10°C) after each reaction period, and then it was analyzed by GC.

The compositions and preparation methods of the catalysts reported here are summarized in Table 3.3.10.

Table 3.3.10 Compositions and Preparation Methods of the Catalysts

Catalysts	Compositions	Preparations
F6KOHNLi	Mn/Cu = 0.5, Zn/Cu = 0.5, Zr/Cu = 2, CoO = 0.2 wt%, 4 wt% LiNO$_3$ doping	Coprecipitation by dropping KOH solution to nitrate solution. Final pH = 12, nitrogen-calcined and LiNO$_3$ doped.
F6KOHNLiOH	Same as above except LiNO$_3$ replaced by 4 wt% LiOH doping	Same as above except LiOH doping
F6KOHN	Same as F6KOHNLi except no doping	Same as F6KOHNLi except no doping
AF6KOOHN	Same as above but no cobalt was included	Same as above except no cobalt was included
RhAF6KOHN	Same as above but doped with 0.2 wt% Rh	AF6KOHN doped with Rh
IrAF6KOHN	Same as AF6KOHN but doped with 0.2 wt% Ir	AF6KOHN doped with Ir
FeAF6KOHN	Same as AF6KOHN but doped with 0.2 wt% Fe	AF6KOHN doped with Fe
CoAF6KOHN	Same as AF6KOHN but doped with 0.2 wt% Co	AF6KOHN doped with Co
NiAF6KOHN	Same as AF6KOHN but doped with 0.2 wt% Ni	AF6KOHN doped with Ni
PdAF6KOHN	Same as AF6KOHN but doped with 0.2 wt% Pd	AF6KOHN doped with Pd

Results and Discussion

LiOH Doping vs. LiNO3 Doping

Since the alkali doping affects the acidity (basicity) of the catalyst surface, we expect that the composition of the alkali metal precursor could have some effect on performance of the catalysts. For this reason we tested a catalyst doped with LiOH solution, instead of $LiNO_3$ solution, as was used in the other Li-doped catalysts. The comparison of LiOH- and $LiNO_3$-doped catalysts is given in Table 3.3.11.

The time-on-stream plot in Figure 3.3.3 shows that the LiOH-doped catalyst behaves like the other doped or undoped F6KOHN catalysts, that is, relatively stable activity and selectivity, high CO_2 selectivity, and relatively low hydrocarbon selectivity.

Table 3.3.11 Liquid Product Selectivity (wt%) on $LiNO_3$- and LiOH-Doped Catalysts (@1000 psi, CO/H_2 = 1, GHSV = 2900/h)

Catalyst	T°C	MeOH	EtOH	nPrOH	iBuOH	Other	yield (g/g/h)
$LiNO_3$-doped	350	61.4	1.8	2.4	17.7	16.7	0.050
F6KOHN	400	25.3	4.5	5.9	22.9	41.4	0.078
	425	13.6	5.5	14.3	13.0	53.6	0.105
LiOH-doped	350	68.6	1.6	2.4	13.6	13.8	0.048
F6KOHN	400	24.3	5.5	8.0	19.0	43.2	0.082
	425	13.2	5.6	13.2	11.2	56.8	0.109

As with previous experiments, we found that doping with excess alkali produces little or no beneficial effect on our catalyst and may even be detrimental to higher alcohol synthesis, independent of the alkali precursor's composition.

Effects of GHSV and Reaction Pressure

Gas hourly space velocity (GHSV) and reaction pressure are two important variables for higher alcohol synthesis reaction. They could affect pathways of surface reactions and the thermodynamic equilibrium of the system, and have therefore been examined extensively in the higher alcohol synthesis literature. It was reported that relatively low GHSV is helpful for higher alcohol production since the relatively long residence time would allow more surface species to undergo chain growth to higher alcohols. The chain propagation step is always needed for any proposed mechanism for higher alcohol synthesis from CO hydrogenation. The effect of pressure is mostly addressed through thermodynamic equilibrium calculations. Higher pressure is more favorable for methanol formation than for the formation of higher alcohols. Hence, high pressure increases total alcohol productivity and probably higher alcohol productivity in terms of space time yield, but it does not enhance alcohol selectivity. In order to evaluate the effects of these factors on our catalysts, we tested them on catalyst F6KOHNLi. The experimental results are summarized in Table 3.3.12.

Table 3.3.12 Effects of Pressure and GHSV on the Alcohol Selectivity (wt%) and Yield of F6KOHNLi (@CO/H$_2$ = 1)

P (psi)	GHSV (l/h)	T°C	MeOH	EtOH	nPrOH	iBuOH	Other	Yield (g/g/h)
1000	2900	350	61.4	1.8	2.4	17.7	16.7	0.050
1000	2900	400	25.3	4.5	5.9	22.9	41.4	0.078
1000	2900	425	13.6	5.5	14.3	13.0	53.6	0.105
1000	6700	350	79.8	0.0	2.1	9.2	8.9	0.067
1000	6700	400	37.2	2.5	4.3	17.5	38.5	0.105
1400	6700	400	38.4	6.0	12.7	11.5	31.4	0.177
1400	6700	425	22.5	8.0	19.0	8.3	42.2	0.183
600	6700	350	70.4	0.0	1.7	12.9	15.0	0.025
600	6700	400	33.4	2.5	4.0	20.2	40.0	0.050
600	6700	425	20.6	4.3	8.4	15.2	51.4	0.050

When GHSV increases from 2900/hr to 6700/hr, methanol selectivity increases from 61.4 to 79.8% at 350°C and from 25.3 to 37.2% at 400°C; isobutanol selectivity decreases at the same time. These shifts in selectivity are not favorable for higher alcohol synthesis. However, a major advantage seen here is that the liquid yield is enhanced significantly with the increased GHSV. While isobutanol selectivity is not reduced excessively by more than doubling the GHSV, isobutanol yield is slightly enhanced, for example, from 17.9 to 18.3 mg/g/hr at 400°C. Therefore, some benefits in yield may accrue if we properly manage the GHSV in a certain range.

Another factor that is closely related to GHSV is the reaction pressure, which can alter the performance of the catalysts by changing the residence time of reactants on the surface. Table 3.3.11 provides the experimental results of the pressure effects on our catalysts.

With increasing reaction pressure from 1000 psi to 1400 psi, the higher alcohol selectivity patterns on the catalyst change significantly. Isobutanol selectivity is reduced, for example, at 400°C, from 17.5 to 11.5 wt%, while n-propanol selectivity is increased from 4.3 to 12.7%. Therefore, increased pressure favors n-propanol formation, but suppresses isobutanol selectivity. The clear advantage of applying higher pressure to the reaction is the great enhancement in total liquid productivity; for example, the productivity of the catalyst is almost doubled when pressure is raised from 1000 to 1400 psi at 400°C. When we consider the effect of pressure on the basis of isobutanol productivity (space time yield) instead of selectivity, we see the advantage of higher pressure. For example, increasing the pressure from 1000 to 1400 psi leads to enhancement of isobutanol yield from 18.4 to 20.4 mg/g/hr at 400°C, while isobutanol selectivity decreases significantly.

When the same catalyst was tested under a lower pressure of 600 psi, not only was a dramatically decreased liquid yield observed, but also little enhancement of isobutanol selectivity was realized. It seems that relatively high pressure is an essential requirement for efficient isobutanol production.

From these experimental results, it is reasonable to expect that a proper combination of high pressure and high GHSV could lead to high isobutanol yield, although low GHSV and moderate pressure are favored for higher isobutanol selectivity.

Time-on-stream plots in Figures 3.3.4 and 3.3.5 show stable performance of the catalyst, F6KOHNLi, under various GHSVs and pressures. From Figure 3.3.4 we can see another important advantage of applying higher pressure to the reaction. When the pressure was increased from 1000 to 1400 psi, not only were the CO/H_2 conversions increased, but also CO_2 and hydrocarbon selectivities were suppressed. This also points to the advantage of applying higher pressure, since we are seeking as low a hydrocarbon selectivity as possible.

Unfortunately, since we could not achieve pressures higher than 1500 psi (limited by CO gas tank pressure), it is impossible to take full advantage of these pressures/GHSV variables to optimize the performance of our catalysts for the best isobutanol yield.

Importance of Cobalt in Catalysts

A minor amount of cobalt in higher alcohol synthesis catalysts is considered a critical compositional factor. Cobalt's effect is discussed mechanistically as a chain growth promoter in the literature and in our previous work. However, questions such as the way global performance of a catalyst changes if other similar transition metals are used to replace the cobalt have not been carefully examined. The balance of this report will address this question using our most recent experimental results.

A series of catalysts was designed, prepared and examined to evaluate the effect of cobalt and other Group VIII transition metal promoters on the performance of these catalysts. The catalyst precursor, denoted as AF6KOHN, was made with exactly the same composition and preparation procedure as F6KOHN, except that cobalt was not included. With this as a starting material, various transition metals were impregnated onto the precursor using the incipient wetness method. The derived catalysts are coded as MAF6KOHN, where M = Co, Rh, Ir, Fe, Ni, or Pd, respectively. General performance of these catalysts is summarized in Table 3.3.13, and the time on-stream plots of them are provided in Figures 3.3.7-3.3.13.

Excluding the cobalt component from the catalyst increases the activity of the catalyst at low temperature (350°C), but higher temperature performance of the catalyst is also suppressed significantly. See CO conversion and liquid yield of the catalysts F6KOHN and AF6KOHN in Table 3.3.13. The poor high-temperature performance of the "no cobalt" catalyst is seen even more clearly when the time-on-stream plots of F6KOHN (cobalt coprecipitated) and AF6KOHN (no cobalt) are compared in Figures 3.3.6 and 3.3.7. Although the higher alcohol selectivity did not severely decline by excluding cobalt from the catalyst, the decreased total liquid yield, isobutanol selectivity, CO and H_2 conversions, and increase in hydrocarbon selectivity with increasing reaction temperature clearly show the important role played by cobalt at higher reaction temperature. Since higher alcohols were best produced at relatively high temperature, these results indicate that the minor amount of cobalt component in the catalyst is critical to maintaining high isobutanol yields.

84

The behavior of the cobalt-doped catalyst, CoAFKOHN, confirmed the role played by cobalt in the catalyst, since it exhibited an activity pattern similar to that of the cobalt coprecipitated catalyst, F6KOHN (see Figures 3.3.6 and 3.3.8). Both catalysts, F6KOHN and CoAF6KOHN, exhibited increased CO conversion and liquid yield with increasing reaction temperature. However, the isobutanol selectivity on CoAF6KOHN was not as high as on F6KOHN (Table 3.3.13), which could be due to poorer cobalt dispersion on the doped catalyst.

Attempts to modify the performance of catalyst AF6KOHN by doping it with Rh or Ir proved ineffective. The Rh- or Ir-doped catalysts were slightly less active and less selective compared with the unpromoted catalyst, AF6KOHN, and their general performance was very similar to the unpromoted catalyst, AF6KOHN, (see Table 3.3.13 and Figures 3.3.9 and 3.3.10). However, the transition metal precursors used and the treatment of the catalysts after doping of the precursor could be responsible for the ineffective promotion of the catalysts by Rh and Ir. The catalysts were prepared by incipient wetness impregnation of AF6KOHN with $Rh(CO)_2acac/CH_2Cl_2$ or $Ir(CO)_2acac/CH_2Cl_2$. No further pretreatment was carried out except to dry the materials at 100°C before reduction and reaction. This treatment might not be vigorous enough to produce sufficient interaction of the promoter with oxide surface. Therefore, further experiments are needed to examine the effect of calcination on the doped catalysts.

Ni or Pd promotion of the catalysts also did not improve the alcohol selectivity and productivity. Like the Rh- or Ir-promoted catalysts, Ni- or Pd-promoted catalysts have shown performance similar to the unpromoted catalyst AF6KOHN, that is, low isobutanol selectivity and decreased activity with increasing temperatures (see Table 3.3.12 and Figures 3.3.11 and 3.3.12). An exceptional result is observed with the Fe-promoted catalyst, FeAF6KOHN. The minor amount of Fe doping results in high CO conversion and high liquid yield, even at low temperature (350°C); see Table 3.3.12 and Figure 3.3.13. Unfortunately, few alcohols are produced in the reaction. The liquid, which appears as two phases, contains water and other hydrocarbon components. Hence, Fe promotion does not seem worth further exploration.

The ineffective promotion by most of the Group VIII transition metals studied to date undoubtedly arises from a combination of factors such as the precursors of the promoters and thermotreatment after doping. A more thorough examination of these approaches will be studied and reported in the future. However, the effective promotion of the catalysts by cobalt is a conclusive result largely independent of these secondary factors.

Conclusions

Basic alkali dopant LiOH, like the other alkali dopants studied before, shows no promotion for higher alcohol synthesis. Pressure and GHSV can significantly affect catalyst activity and selectivity. While low GHSV and moderate pressure favor improved isobutanol selectivity, properly selected high GHSV and high pressure can have the advantage of increasing isobutanol yield. Cobalt is an important promoter for maintaining high activity and selectivity for higher alcohol synthesis. In contrast with cobalt, most of the other Group VIII transition metals are ineffective promoters of our catalysts by the methods of doping and calcination used to date.

Future Work

Future work will focus on further examinations of precipitation methods, post treatment of the catalyst precursor, and reduction of the copper level in the catalyst to avoid agglomeration and to improve space time yield.

Table 3.3.13 Comparison of Performance of Group VIII Metal Doped-Catalysts

Catalysts	T°C	CO Conv. %	Yield g/g/h	MeOH wt%	nPrOH wt%	iBuOH wt%	Other wt%
F6KOHN	350	9.30	0.060	69.2	1.1	14.8	14.3
	400	18.9	0.083	27.3	2.0	24.0	43.6
	425	23.4	0.086	13.3	5.6	19.3	54.4
AF6KOHN	350	15.7	0.121	60.6	0.0	15.0	24.4
	400	11.4	0.075	30.4	2.3	20.8	46.5
	425	10.0	0.043	18.1	5.1	17.9	58.9
RhAF6KOHN	350	10.4	0.118	69.5	0.0	10.5	20.0
	400	8.10	0.080	38.1	2.0	20.4	39.6
	425	5.50	0.048	26.3	4.3	19.0	50.4
IrAF6KOHN	350	12.3	0.110	65.4	1.0	10.9	22.7
	400	11.7	0.068	33.3	1.8	18.7	46.2
	425	8.70	0.050	21.0	3.9	16.8	58.3
FeAF6KOHN	350	39.6	0.118				
	400	45.1	0.148				
	425	35.0	0.100				
CoAF6KOHN	350	8.2	0.050	65.7	2.0	8.3	23.9
	400	12.4	0.081	21.0	9.9	14.2	55.0
	425	22.4	0.106	12.7	15.7	8.1	63.5
NiAF6KOHN	350	10.7	0.095	59.0	2.2	11.6	27.2
	400	12.7	0.071	28.0	4.9	17.8	49.3
	425	10.3	0.054	19.9	5.6	17.1	57.3
PdAF6KOHN	350	17.2	0.142	53.8	1.7	14.5	30.0
	400	13.0	0.103	25.7	4.1	17.4	52.7
	425	10.7	0.058	19.7	6.0	17.5	56.8

Figure 3.3.3 Reaction Performance of F6KOHNLiOH (350-425°C, 1000 psi, CO/H2 = 1)
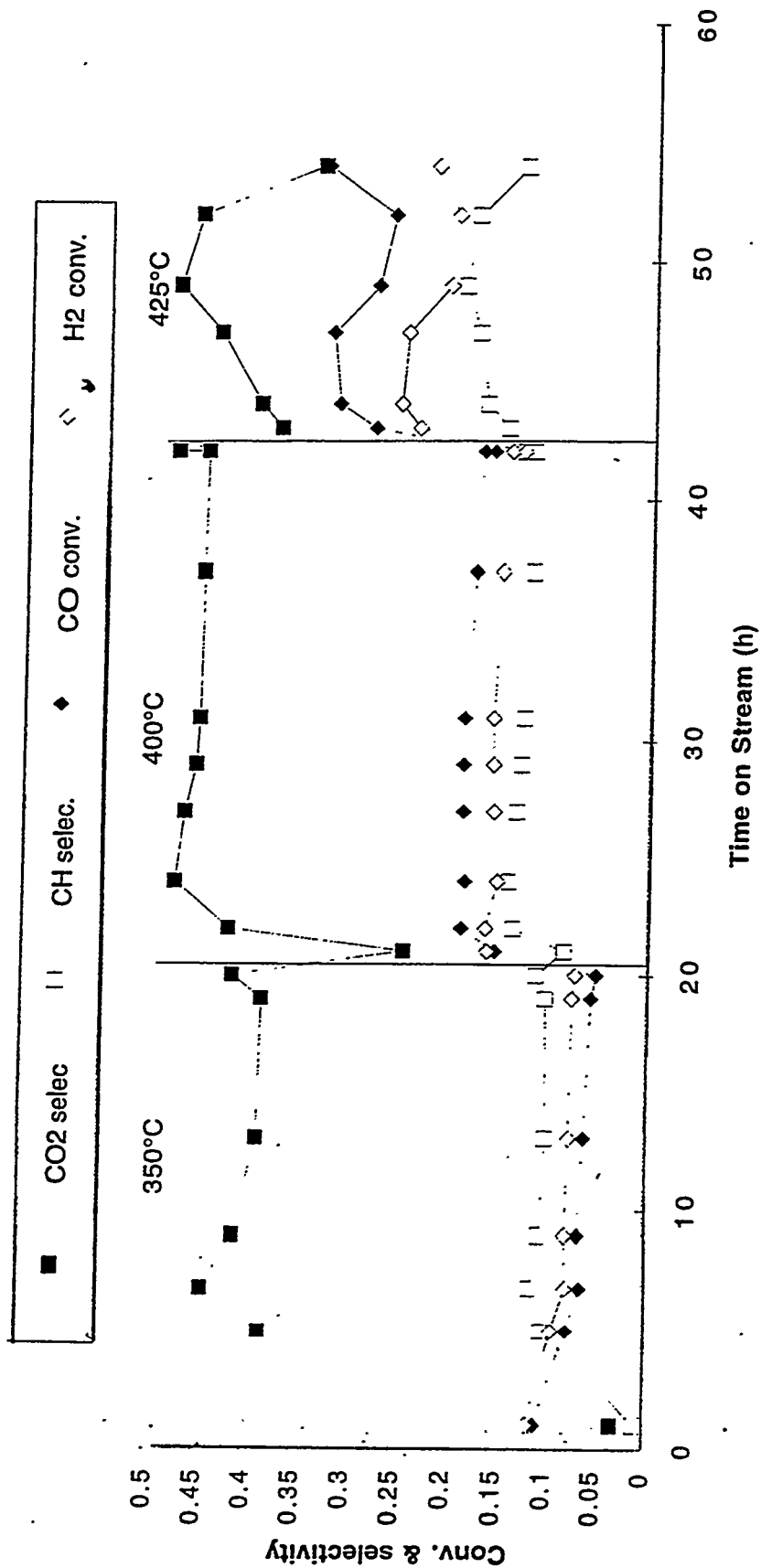
Figure 3.3.4 Effect of Pressure on the Performance of F6KOHNLi (GHSV = 6700/h, CO/H2 = 1)
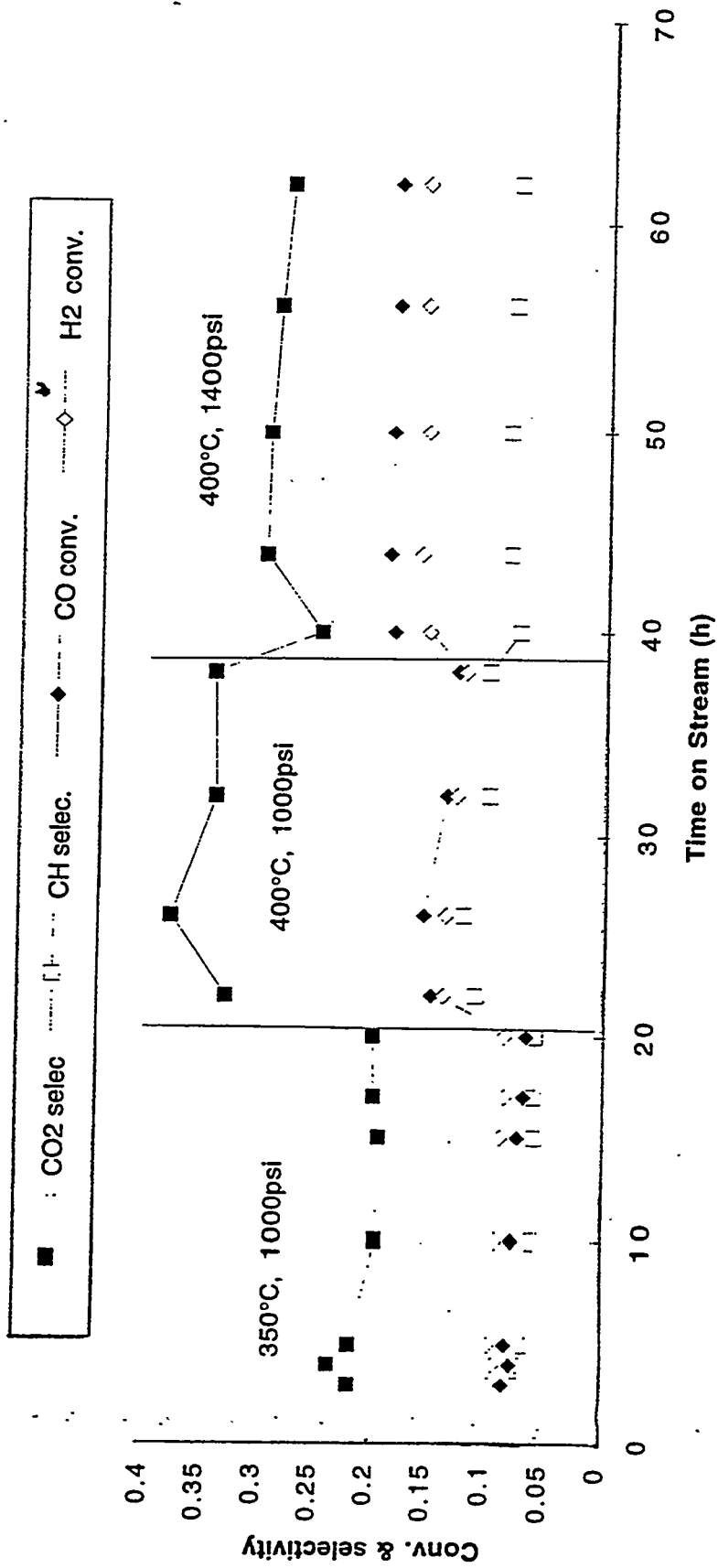
Figure 3.3.5 Reaction Performance of F6KOHNLi at Low Pressure (350-425°C, 600 psi, CO/H2 = 1)
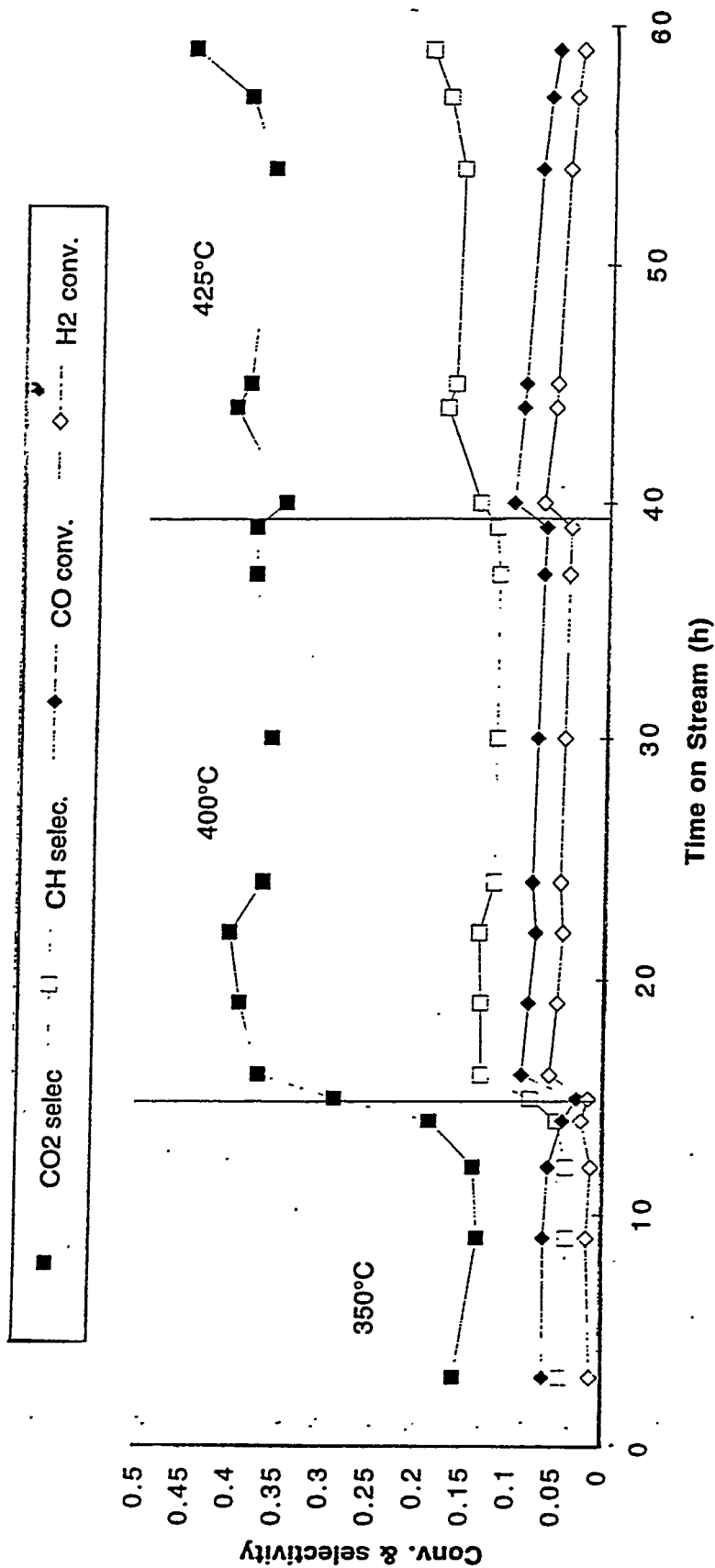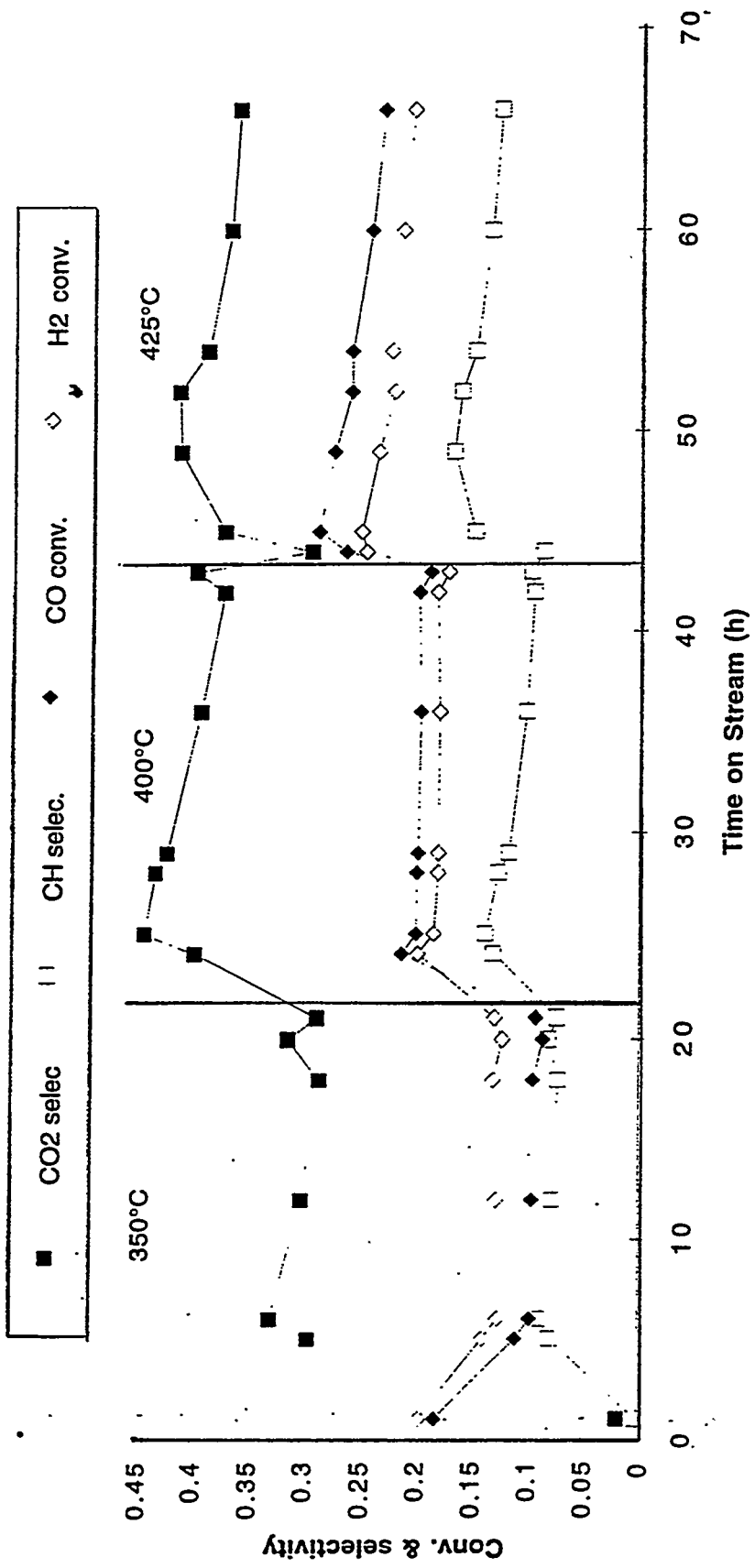

89

Figure 3.3.6 Reaction Performance of F6KOHN (350-425°C, 1000 psi, CO/H2 = 1)

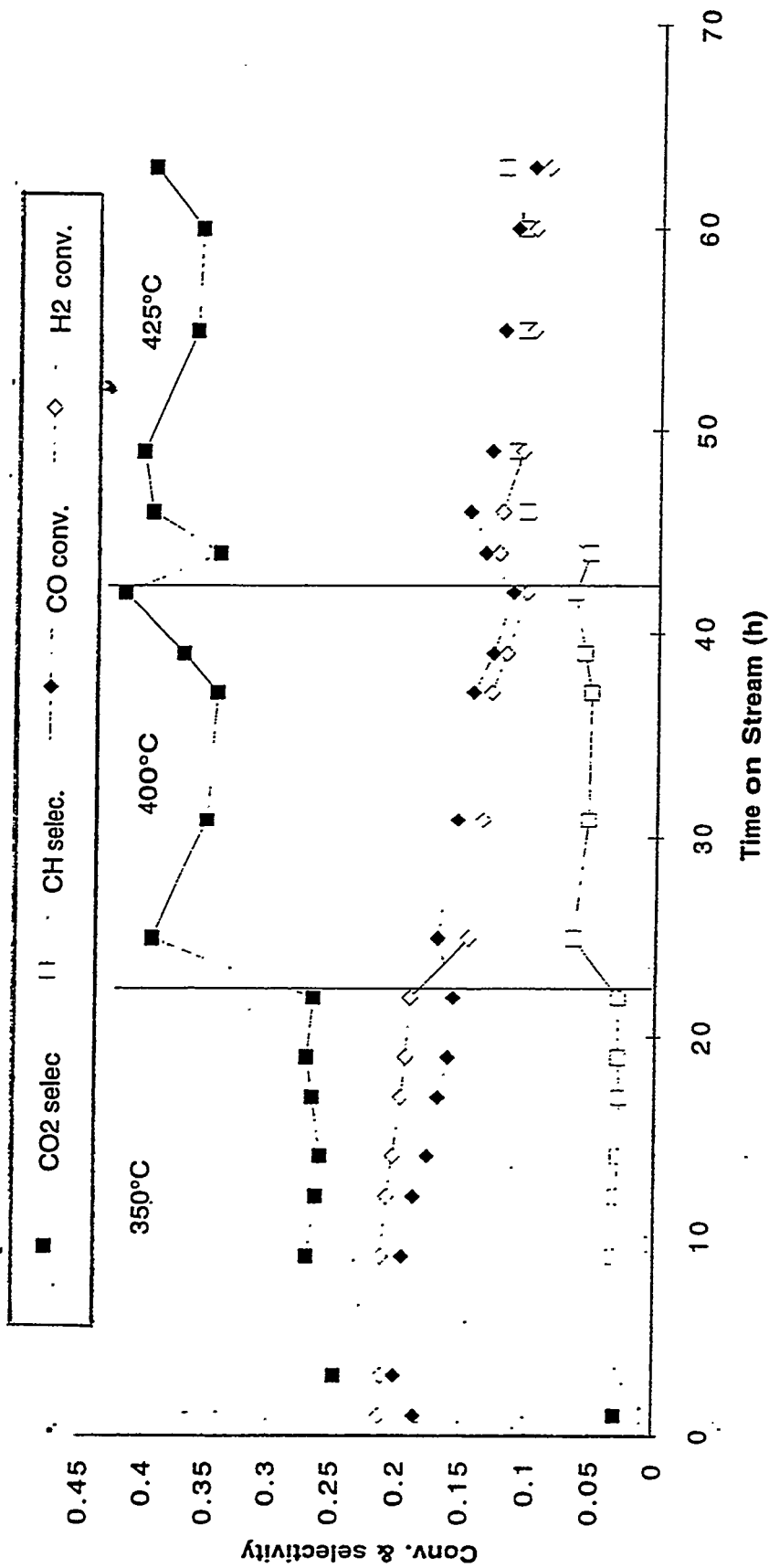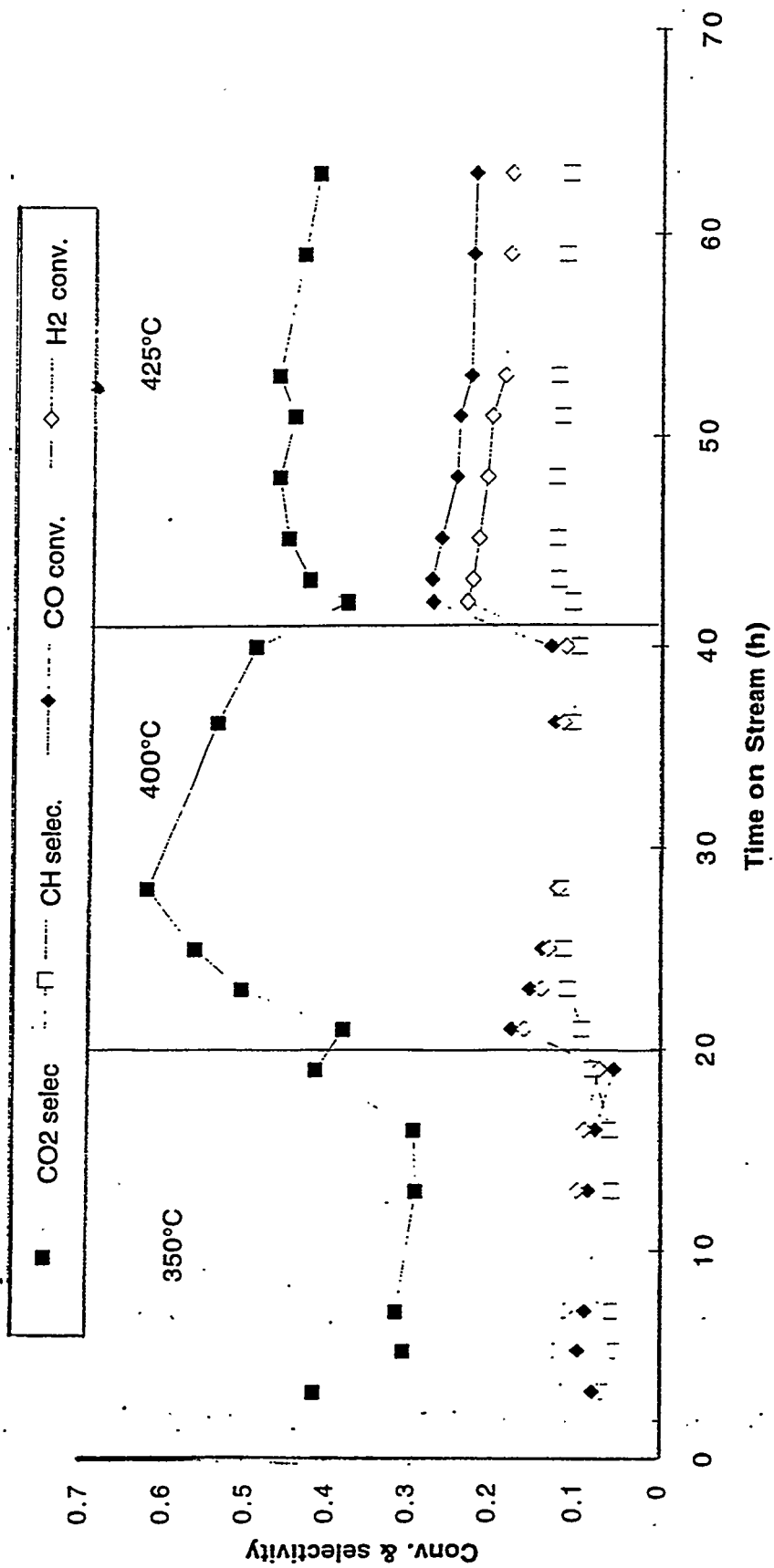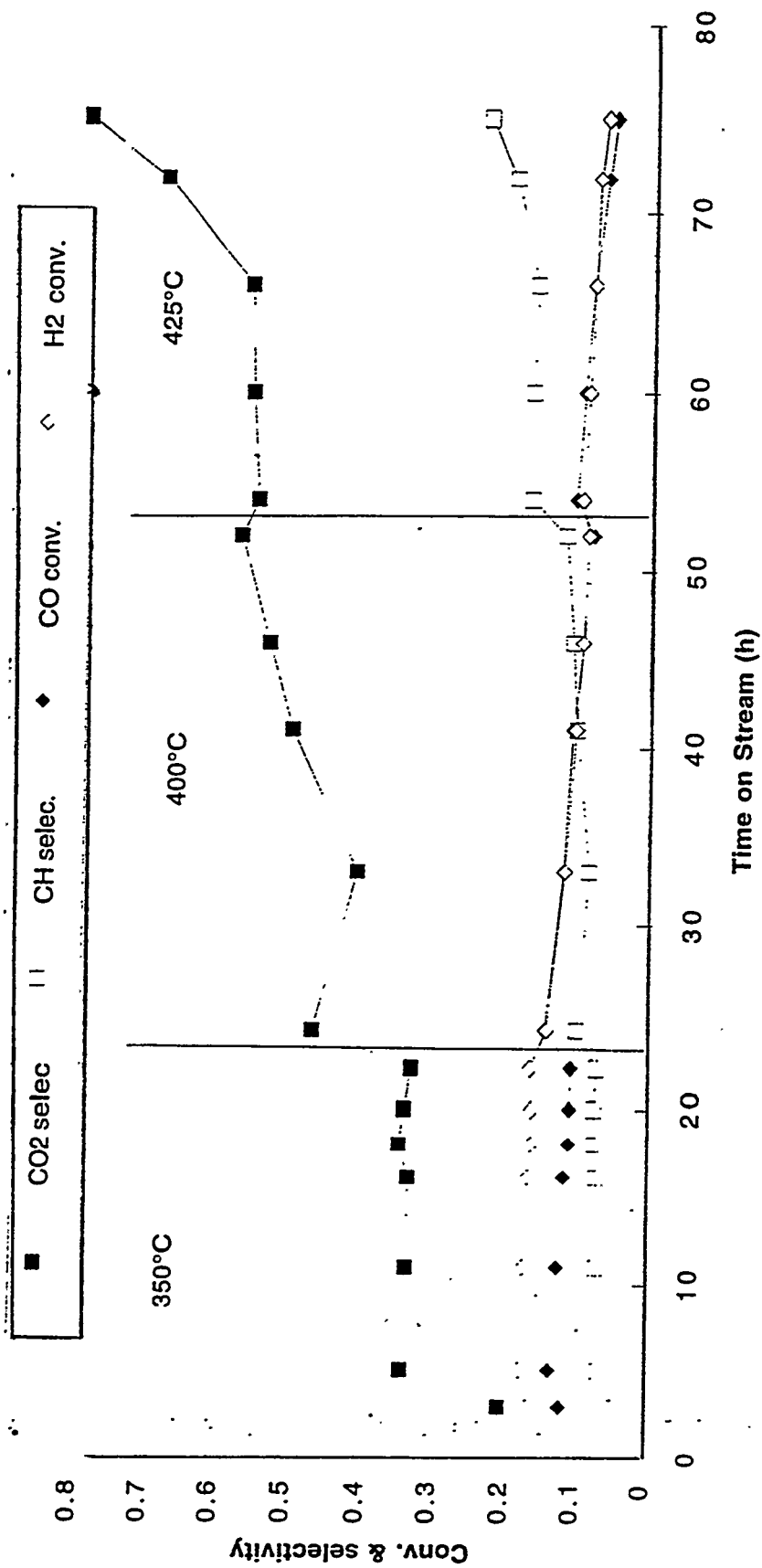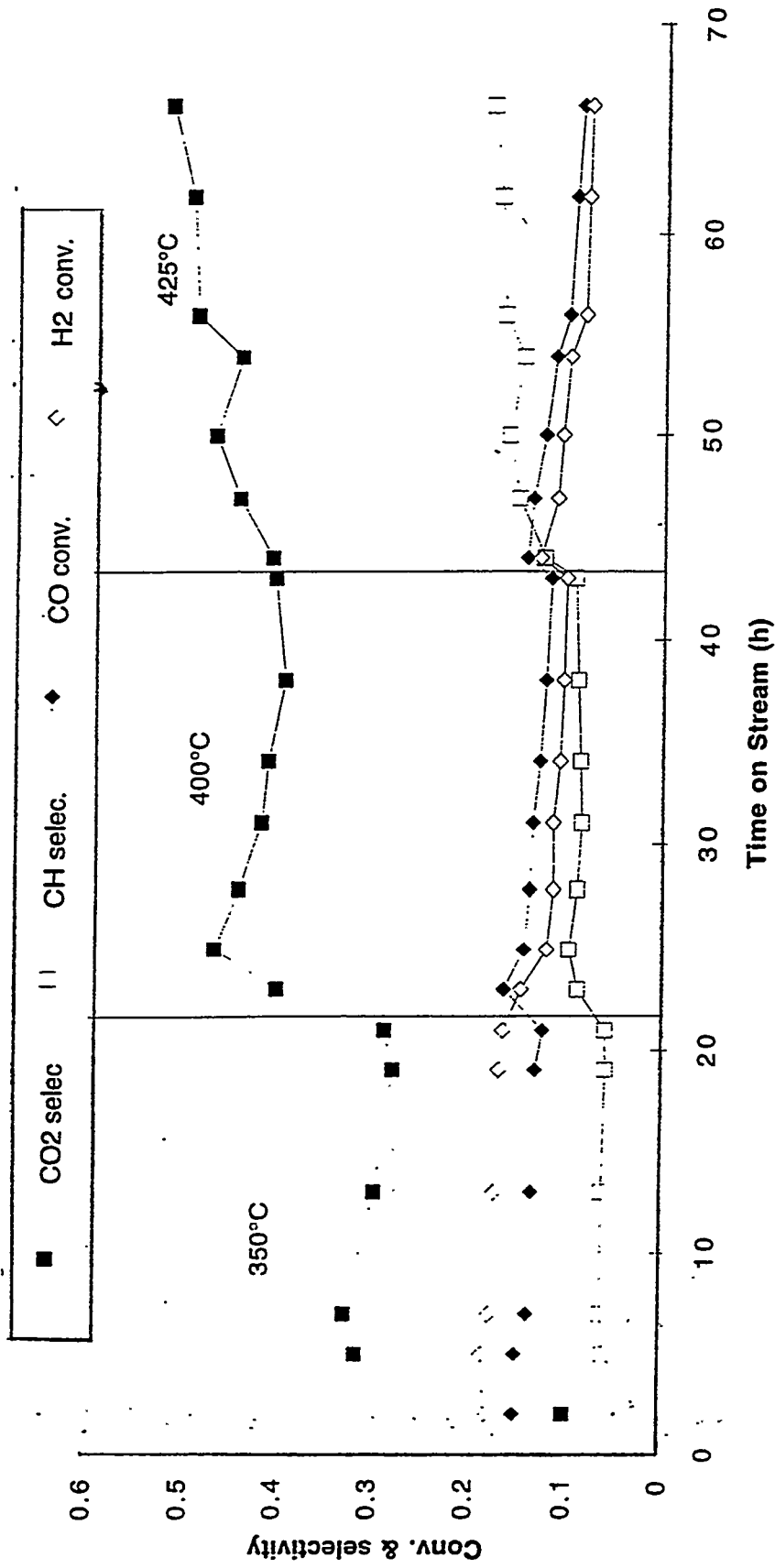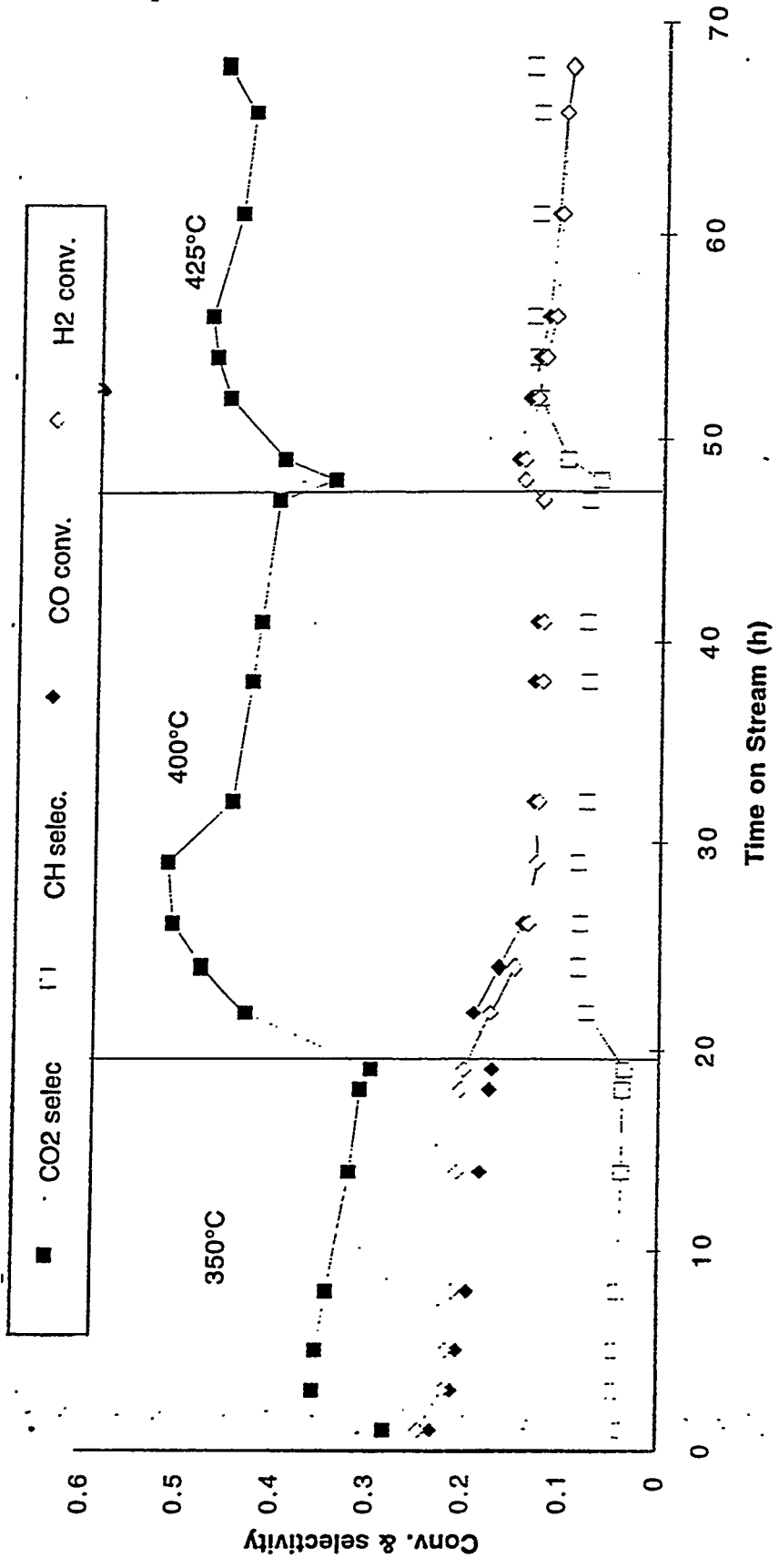**Figure 3.3.7 Reaction Performance of AF6KOHN (350-425°C, 1000 psi, CO/H2 = 1)**

Figure 3.3.8 Reaction Performance of CoAF6KOHN (350-425°C, 1000 psi, CO/H2 = 1)

Figure 3.3.9 Reaction of Performance of RhAF6KOHN (350-425°C, 1000 psi, CO/H2 = 1)

93

Figure 3.3.10 Reaction Performance of IrAF6KOHN (350-425°C, 1000 psi, CO/H2 = 1)

Figure 3.3.11 Reaction Performance of PdAF6KOHN (350-425°C, 1000 psi, CO/H2 = 1)

Figure 3.3.12 Reaction Performance of NiAF6KOHN (350-425°C, 1000 psi, CO/H2 = 1)
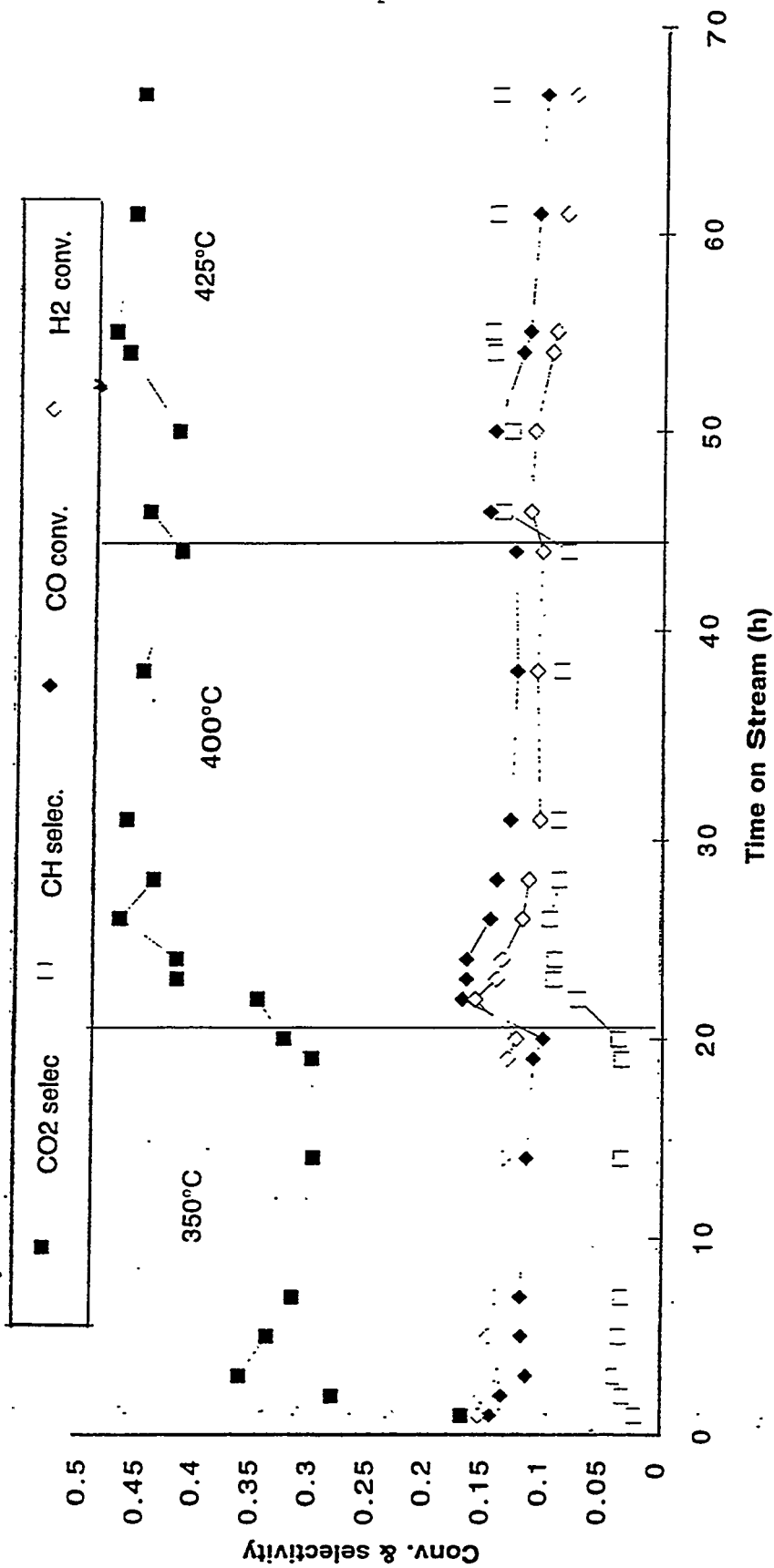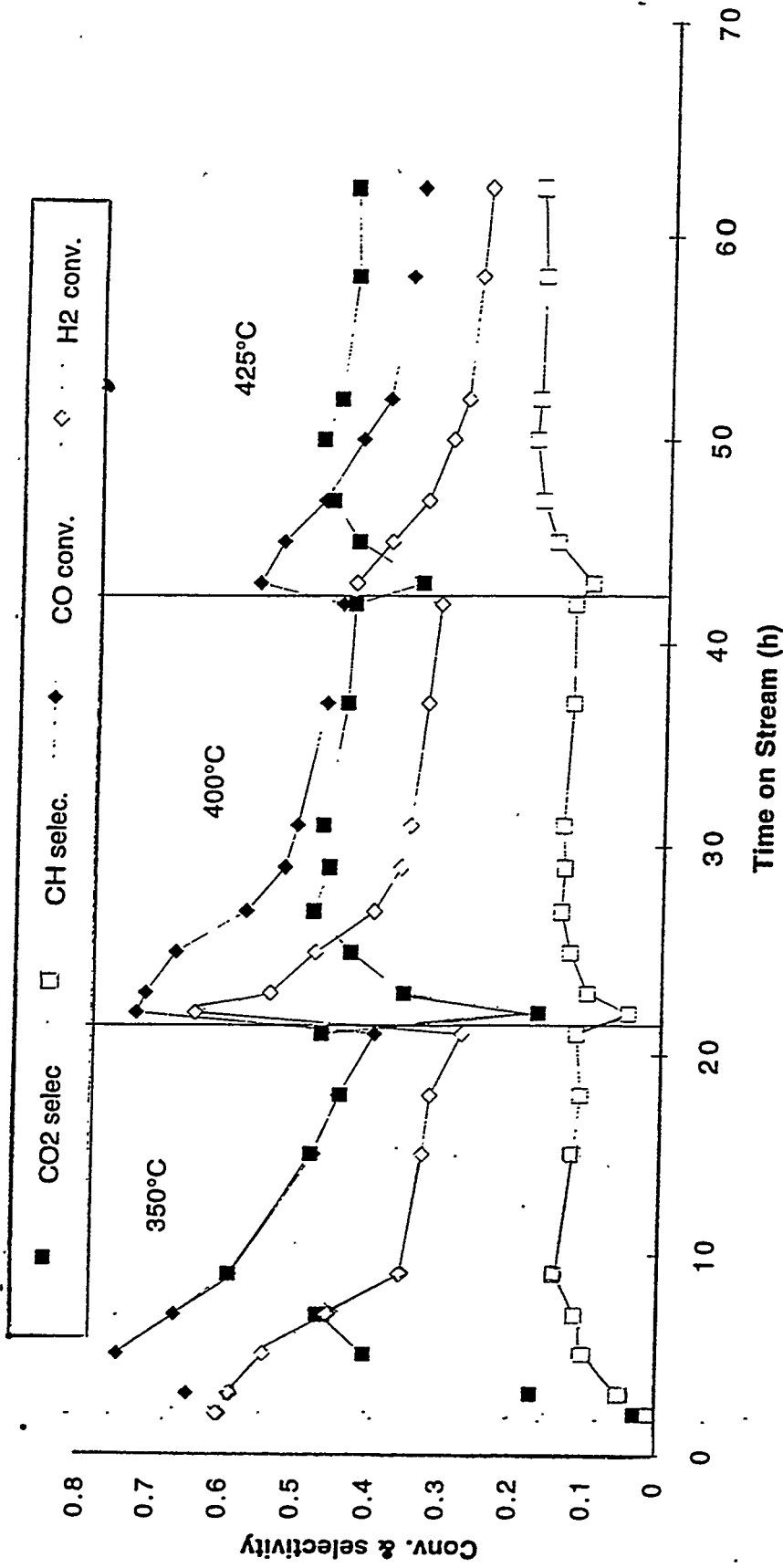
Figure 3.3.13 Reaction Performance of FeAF6KOHN (350-425°C, 1000 psi, CO/H2 = 1)

TASK 4: PROGRAM SUPPORT

Bechtel began work late in the quarter on the program support items specified in the last quarterly report. Some of their preliminary results are covered in the June monthly report. The work will be written up in more comprehensive fashion in the next quarterly report.

TASK 5: PROJECT MANAGEMENT

Reports and Presentations
A draft topical report was issued on the results of the Fischer-Tropsch II demonstration run recently completed. Comments have been received from DOE personnel on the report. The suggestions will be incorporated in the final report.

B. L. Bhatt presented a paper entitled "Productivity Improvements for Fischer-Tropsch Synthesis" at the 14th North American Meeting of the Catalysis Society. The paper, which was co-authored by Shell and DOE personnel, was well received.

Monthly reports for April, May, and June were prepared and submitted to DOE as scheduled. A draft Quarterly Report (No. 2) for the period January 1995 through March 1995 has been prepared.

Management Activities
The R&D subcontract with Eastman Chemical was finally organized and ratified by all parties. Congratulations to all for a Trojan effort!